THE BIOPHYSIOLOGY AND PATHOPHYSIOLOGY OF NERVE GROWTH FACTOR AT THE OCULAR SURFACE

By

Qiong Liu, M.D.

DISSERTATION

For the degree of

DOCTOR OF PHILOSOPHY

In

PHYSIOLOGICAL OPTICS AND VISION SCIENCE

(October, 2010)

Alison M. McDermott

William W. Miller

Debrah Otteson

Alan Burns

Dequan Li

Acknowledgements

This thesis could not be finished without the help and support of many people who are gratefully acknowledged here.

At the very first, I'm honored to express my deepest gratitude to my dedicated supervisor, Professor Alison M. McDermott, without whose guidance I could never have worked out this thesis. During the past five years she has offered me valuable ideas, suggestions and criticisms, with her profound knowledge in cornea physiology and immunology and rich research experience. Her patience and kindness are greatly appreciated. Whenever I was struggling, from the selection of specific research questions to minutest details of my experiments, from data analysis to the skills of scientific writing, Dr. McDermott was always there to help me. I have learnt a lot from her not only about dissertation writing and scientific presentations, but also professional ethics. I'm very much obliged for her efforts in helping me complete the dissertation.

I'm also extremely grateful to my previous supervisor, Dr. William L. Miller, whose patient and meticulous guidance and valuable suggestions were indispensable to the completion of this thesis. He helped me search for funding opportunities and even had discussions with me when he was much occupied with clinic and teaching. I could not have made it without his support and encouragement.

Dr. Debrah Otteson spared no effort in teaching me genetics and molecular biology. She has spent enormous time teaching me how to design primers, and trained me for grant writing. Those skills will continue to be useful in my future research career. Also the project could not be finished without her precious comments on my experiment.

I would also like to thank Dr. Alan Burns who helped me with immuno-histochemistry, imaging and gave me valuable comments and suggestions on my research project. He also provided me GFP-actin mice which were very useful for my project.

I would also like to thank Dr. Dequan Li for being my committee member and he gave me useful suggestions on my dissertation and instructions on efficient data presentation.

What's more, I wish to extend my thanks to the University of Houston, College of Optometry for providing me the opportunity to work and study in such a fantastic institute. I owe special thanks to Dr. Laura Frishman, Dr. Earl Smith and Michele Murphy for their help in keeping me on track in the program.

In addition, I would like to thank Debjani Gagen for her help with optimizing the protocols for isolation of monocytic lineage cells and immunohistochemistry, Dr. Huaizhu Wu (Baylor college of Medicine) for flow cytometry and Dr. Weimin Xiao for ELISA and Bioinformatics anlysis. The protocol for isolation of corneal cells for flow cytometry was provided by Dr. Hamrah Pedram (Massachusetts Eye and Ear Infirmary).

Special thanks to Dr. Michael Twa, Dr. Nimesh Patel and Dr. Sam Hanlon for performing the *in vivo* imaging of mouse corneas. Dr. Yingsheng Hu also helped me with statistics of the data.

Thanks are also due to my labmates and classmates, who never failed to give me great encouragement and suggestions. Special thanks should go to Rachel Redfern, Rose Reins, Zhou Wan, Ling Huang, Hasna Baidouri, Satya Kolar, and Joseph Manarang for their brainstorming with me when I failed coming up with ideas. I'm also indebted to other graduate students in the institute, Jing Wang, Xunda Luo, Minhua Wang, Johanna Tukler and Deepika Sridha for their encouraging me when I had problems with my experiment and writing this dissertation.

At last but not least, I would like to thank my family for their support all the way from the very beginning of my postgraduate study. I am thankful to all my family members for their thoughtfulness and encouragement.

Table of Contents

List of Publications

Q. Liu, A.M. McDermott, and W.L. Miller, *Elevated nerve growth factor in dry eye associated with established contact lens wear.* Eye Contact Lens, 2009. 35(5): p. 232-7.

List of Figures

List of Tables

List of Abbreviations

µg	microgram
µm	micrometer
BDNF	brain-derived neurotrophic factor
BMDC	bone marrow-derived cell
C	Celsius
CGRP	calcitonin gene-related peptide
CO2	carbon dioxide
CY5	cyanine 5 dye
DAG	diacylglycerol
DAPI	4',6-diamidino-2-phenylindole
EDTA	ethylenediamine tetraacetic acid
ELISA	Enzyme-linked immunosorbent assay
FITC	fluorescein isothiocyanate
FSC	forward scatter
hr	hour
IgG	immunoglobulin G
IL	interleukin
IP3	inositol triphosphate
IRAK	IL-1 receptor associated kinase
JNK	c-jun N-terminal kinase
KDa	kilodaltons
kg	kilogram
LASIK	laser-assisted in situ keratomileusis
M	molar
MAPK	mitogen-activated protein kinase
MCP	monocyte chemotactic protein
min	minute
MKKK	MAPK kinase kinase
ml	milliliters
mM	millimolar
MMP	matrix metalloproteinase
mOsm	milliosmolar
MUC	mucin
Na-K ATPase	sodium-potassium andenosine triphosphatase
NFκB	nuclear factor kappa-light-chain-enhancer of activated B cells
NGF	nerve growth factor
NHC	normal human conjunctival epithelial cells

nm	nanometer
NRAGE	neurotrophin receptor interacting melanoma-associated antigen
NRIF	neurotrophin receptor-interacting factor
NT	neurotrophin
PBS	phosphate buffered saline
PC12	Pheochromocytoma cell line
PCR	polymerase chain reaction
PDK	phosphoinositide-dependent kinase
PE	phycoerythrin
PI	propidium iodide
PI3K	phosphatidyl-inositol 3-kinase
PKB	protein kinase B
PRK	photorefractive keratectomy
RNA	ribonucleic acid
RT	room temperature
sec	second
Shc	Src homology 2-containing protein
SMAD	SMA- and MAD-related protein homolog
SSC	side scatter
SV40	simian virus 40
tp	total protein
TB	trypan blue
Tc	cytotoxic T cell
TGF	transforming growth factor
Th	helper T cell
TNF	tumor necrosis factor
TRAF	TNF receptor-associated factor
VEGF	vascular endothelial growth factor
VKC	Vernal Keratoconjunctivitis

Abstract

Purpose: Nerve growth factor (NGF) has been considered as a pleiotrophic factor that is expressed in the nervous, immune and structural tissues of the body, and affects nerve growth, regulates immune responses and influences the survival and functions of structural cells. However, the role of NGF at the ocular surface is less well understood compared with it effects in most other systems of the body. Therefore the purposes of the present study were: (1) To investigate the concentration of NGF in normal human tear film and determine if it is correlated with TGF-β1 in dry eye associated with established contact lens wear. (2) To investigate if exogenous NGF alters the expression of cytokines and growth factors by corneal and conjunctival epithelial cells, and affects cell viability in a dry eye culture model. (3) To determine the effect of NGF on migration and differentiation of murine monocytic lineage cells *in vivo* and *in vitro*.

Methods: (1) The concentration of NGF in the tear film of normal subjects and established contact lens wearers was measured by enzyme-linked immunosorbent assay (ELISA). The correlation of NGF levels to ocular surface dry eye index (OSDI), Schirmer test, corneal sensitivity and corneal innervation was determined. Tear film TGF-β1 was also measured by ELISA to test if its levels also correlated with NGF. (2) SV40 transformed human corneal epithelial cells (SV40-HCEC), primary cultured HCEC (P-HCEC) or a conjunctival cell line (IOBA-NHC) were treated for 24 or 48 hrs with serum-free growth-media of varying osmolality alone or also containing NGF (10 ng/ml

or 100 ng/ml). Culture media was collected and RNA was extracted and real time reverse transcription polymerase chain reaction (RT-PCR) was performed to detect mRNA expression of IL-13, IL-16, IL-1α, MCP-1, TLR4, 9, HLA-DR, TGF-β1 and 2. ELISA was performed to quantitate TGF-β1 and 2 levels in culture media and cell lysate. TrkA expression was assessed with real-time RT-PCR and flow cytometry. Cell viability was assessed by trypan blue exclusion test and MTT assay. (3) Murine monocytic lineage cells were isolated from peripheral blood, spleen and peritoneal cavity by a density gradient and negative selection with immunomagnetic beads against lymphocyte markers (B220/CD4/CD8). Purity was assessed by flow cytometry. Monocyte migration after 3hrs of treatment using various concentrations of NGF (1~200ng/ml) was tested with a blind-well migration chamber. The expression of surface markers (CD11c, CD11b) was evaluated by flow cytometry. For *in vivo* studies, intrastromal injection of NGF (1μg/ml, 2μl) was performed and then expression of CD11c, CD115 and CD11b were assessed by immunohistochemistry. The percentage of CD11c, Ly6C, CD115 positive cells in the epithelium and in the stroma was determined with flow cytometry 4 hours after NGF injection. The concentration of MCP-1 in the cornea was measured by ELISA.

Results: (1) There was a statistically significant decrease of corneal sensitivity in contact lens wearers compared with normal controls. The nerve density in the subepithelial plexus of contact lens wearers with dry eye was 538.8 ± 39.3 μm/image (3.959 ± 0.28 pm/ μm^2), and 537.1 ± 30.9 μm/image (3.947 ± 0.27 pm/ μm^2) in those without dry eye. Both of these values were significantly ($p = 0.032$) lower than in the normal controls (4.412 ± 0.21 pm/ μm^2). The concentration of tear NGF was increased in

contact lens wearers with dry eye, and was significantly greater ($p = 0.048$) compared with contact lens wearers without dry eye. TGF-β1 increased one fold in contact lens associated dry eye, and correlated with NGF levels. (2) IL-1α, IL-13, IL-16, MCP-1, and TLR4 mRNA expression was up-regulated by hyperosmolar stress and this increase was abrogated by NGF. TLR9 expression was not significantly changed by hyperosmolar stress or NGF treatment. HLA-DR decreased with hyperosmolar stress but did not change significantly with NGF. The expression of TGF-β mRNA and protein in all cell types was up-regulated by hyperosmolar stress 1.5 to 9 fold, and this was further enhanced in the presence of NGF. TrkA mRNA and protein were also up-regulated by NGF. Hyperosmolar stress induced approximately 35% conjunctival epithelial cell death but this was reduced to only 18% when NGF was present. (3) The purity of isolated monocytes was more than 90% as tested by flow cytometry. Blind-well chamber assays showed that NGF induced migration of monocytes in a concentration dependent fashion, with the highest concentration (200 ng/ml) being as effective as MCP-1 (5ng/ml). *In vitro*, NGF also increased expression of CD11c, CD11b, and MHCII on blood monocytes, suggesting that they differentiated into dendritic like cells. *In vivo* experiments showed that NGF induced migration of mouse monocytic lineage cells into the corneal stroma and this may be explained by increased MCP-1 secretion by stromal keratocytes.

Conclusion: (1) Tear film NGF levels were elevated in contact lens related dry eye, likely in response to anti-inflammatory factors such as TGF-β1. (2) The results for these studies imply that NGF may modulate ocular surface inflammation in dry eye by increasing TGF-β expression and by reducing epithelial cell death. Further these data

support a potential role for NGF in treating dry eye inflammation. (3) The specific studies showed that NGF induced migration of monocytes and promoted differentiation into a more mature antigen presenting cell phenotype. This suggests that NGF may facilitate corneal immunity through its effect on monocytes and monocyte-derived cells.

Chapter 1. Introduction: Literature Overview

I. Discovery and Definition of NGF

NGF was discovered by Rita Montalcini, Stanley Cohen and Viktor Hamburger in 1951.[1] Elmer Bueker, one of the postgraduate students working with Viktor Hamburger, grafted a small piece of murine sarcoma tissue into the body wall of a three day old chick embryo and then surprisingly observed that many sensory nerve fibers grew into the implanted tissue. He hypothesized that this could be explained by the invasive nature of the tumor that invaded the nearby tissue and enabled the nerve fibers to grow.[2] Rita Montalcini, however, did not agree with him and repeated Elmer's experiment: implanting mouse sarcoma tissue into chick embryos and then analyzing serial sections of silver stained embryos at 24 hr intervals.[1] She also observed hyperinnervation of the internal organs of the chick.[1] Based on this so called "mouse effect", she hypothesized that a factor that promoted nerve growth activity was released from the mouse sarcoma tissue.[1, 3] Following that, the "mouse effect" was further confirmed with snake venom and mouse salivary gland extract.[3] In 1960, the group was able to isolate a protein of 44,000 Da from salivary gland extract that had the ability to stimulate growth of sensory nerve fibers and neuronal cells *in vitro*, this protein was named nerve growth factor (NGF) because of its effects.[4]

The application of NGF was initially thought to be unpromising in clinical applications because it was isolated from malignant tissues and other unrelated origins such as snake venom. However in later studies NGF secretion was found in normal

tissues. By 1966, Montalcini and co-workers also discovered that daily injection of small amounts of antiserum to NGF (AS-NGF) to neonatal mice led to almost total disappearance of sympathetic ganglia (immunosympathectomy).[5] This dramatic effect started to interest other researchers and motivated them to study the origins and targets of NGF in the body.

Subsequently, Max *et al.* and Simson et al. found that NGF was produced by neurons and sympathoadrenal cells in normal animals and acted on these cells.[6-7] Later studies supported their discovery and found target-derived NGF activated receptors on neurons and neural crest derived cells, and stimulated proliferation, migration, axonal growth and apoptosis of these cells both in vivo and in vitro.[8-10] Because of their outstanding contribution to the discovery of NGF and other growth factors, Stanley Cohen and Rita Levi-Montalcini won the 1986 Nobel Prize in Physiology or Medicine.

Production of NGF by non-neuronal cells, including hematopoetic cells, fibroblasts, epithelial cells, and smooth muscle cells was discovered later and correspondingly the role of NGF has also been expanded.[11-13]. Burni et al. observed that NGF treatment increased the number of mast cells *in vivo* and *in vitro*, as well as stimulating histamine release.[14] In 1995, Lambiase *et al.* reported that NGF concentration increased in the plasma of vernal keratoconjunctivitis (VKC) patients and concluded that NGF was secreted from and promoted differentiation of T helper (Th)2 cells.[15] Subsequently, other immune cells, such as cytotoxic T (Tc) and B cells were

also found to be a source for and target of NGF.[16] These findings suggest that NGF is also involved in the allergic and chronic inflammatory responses of the body.

Currently NGF is described as a target-derived pleiotropic factor that acts on neurons, immune cells and structural cells through specific receptors.[17] The function of NGF includes promotion of tissue repair, regulation of cytokine and hormone production, and maintenance of homeostasis.[18] NGF promotes neuron and axonal growth and survival, induces allergic responses and is associated with wound healing and inflammation within different systems.[19]

II. Structural properties of NGF

NGF is the most studied member of a structurally and functionally similar family of neurotrophins (NTs). Other family members include Brain Derived Neurotrophic Factor (BDNF) and Neurotrophins (NT) 3, 4, 5 and 6. The active form of human NGF is composed of a dimer of two β subunits and therefore is also named βNGF. Structurally, each subunit is a glycoprotein of 118 amino acids and with a molecular weight of 30kDa (Figure 1.1 A).[3] Human βNGF is capable of non-convalently binding to other subunits: α2, ɣ 2, and forms a high molecular weight protein.[20] All subunits are composed of two pairs of anti-parallel β–strands. The α subunit is a structural unit and is inactive; and the γ2 subunit is a highly active protease that is involved in the maturation of NGF from its pro- form.[20] The loci and functions of the subunits are summarized in Table 1.1.

The sequence of NGF is highly conservative across different species. Based on the most recent data from University of California, Santa Cruz (UCSC) genome database,

the identity between human and mouse NGF DNA sequence is 86% (Figure1.1 B).

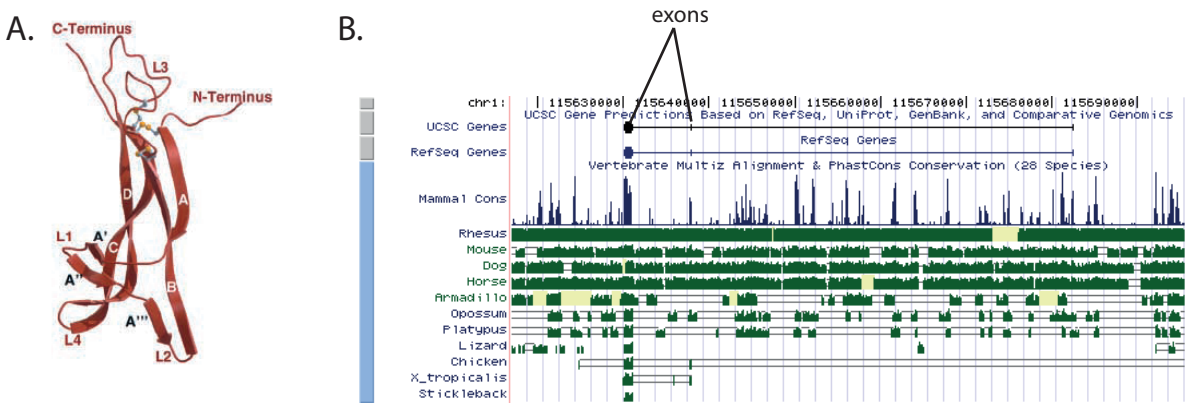

Figure 1.1 Structure and gene loci of human βNGF.
A. Ribbon diagram depicting the structure of the βNGF monomer.[21] Grey and yellow region on top of the diagram shows the csteine-knot motif for stabilizing the structure. L1-L4 shows the loop regions and A~D indicates structural segments that are determined by X-ray crystallography. B. Comparison among βNGF gene sequence of human, mouse and other species. The information is from the UCSC genome database and was last updated on 2008/12.[22] Green fragments show the identical regions. Exons are indicated on the reference gene and were conserved among different species.

Table 1.1 Summary of human NGF gene loci and functions.

Subunit	Gene locus	OMIM	Function
α	19q13.3 Nerve growth factor, alpha subunit	162020	No measurable enzymatic activity; necessary for the formation of the stable hexameric complex
β	1p13.1 Nerve growth factor, beta subunit	162030	Growth-promoting activity
γ	19q13.3 Nerve growth factor, gamma polypeptide	162040	Arginylesterase activity; cleaves pro-beta-NGF at 2 or more sites to generate active growth factor

The gene which codes for the human NGF β subunit contains 3 exons and 2 introns.[23] This gene codes for a large polypeptide, which binds with the α and γ subunits and forms a large complex of 34kDa called preproNGF.[24] Later, the signal peptide of the β subunit is removed and forms an intermediate product named proNGF.[25] Recent studies have shown that pro-NGF also has intrinsic neurotrophic activity, but this was only about one fifth of that of mature NGF.[26] At the N terminus of the β subunit, a conformational change is initiated by a convertase called furin which cleaves N-linked glycosylation of the proNGF and trims the oligosaccharide chains which are required for transportation of proNGF from the endoplasmic reticulum to the *trans* Golgi.[27] Then, the enzyme activity of the γ subunit cleaves arg.glyCOOH at the C terminus which generates a protein with low biological activity. ProNGF has a longer half life than NGF and is considered the storage form of NGF in cells.[28] After cleavage by the serine protease plasmin and the matrix metalloproteinase (MMP) 7, the βNGF subunit matures and the protein is secreted into the extracellular fluid.[29]

Compared to the human, murine NGF is secreted in two forms: 2.5S and 7S, both of which are functionally active.[30] The 7S NGF, similar to the human preform,

contains α2, β2, and γ2 subunits, and only the β subunit has biological function. The 2.5S NGF is a 26kDa protein, usually a dimer of 2 monomers of 13kDa, and is a degradation product of the β subunit of the 7S form with some functional sites exposed and therefore is more potent.[31] The mouse βNGF used in the dissertation is a dimer degraded from 7S NGF *in vitro* and has the same biological activity as βNGF.[32]

III. NGF and down-stream signaling pathways

NGF mainly binds to two distinct cell surface receptors, the tropomyosin tyrosine kinase (TrkA) and the p75 pan-neurotrophin receptor (p75).[33-34] NGF specifically binds to TrkA, with a slow binding and dissociation speed, therefore it is considered the "high affinity" NGF receptor.[35] In comparison, p75 binds all members of the NT family with equal affinity and all have a fast binding and dissociation speed therefore it is considered the "low affinity" receptor.[35] The tyrosine kinase-mediated signaling pathway downstream of TrkA is thought to have a major role in promoting survival and differentiation of neurons and other cells.[36] For the p75 receptor, both in vivo and in vitro studies have shown that ligand binding induces neuronal apoptosis.[35, 37]

III A. TrkA receptor and signaling pathways

The TrkA receptor belongs to a family of transmembrane glycoproteins with intrinsic receptor tyrosine kinase activity, with other family members being TrkB and TrkC. The human TrkA receptor is a 140 kDa transmembrane protein encoded by a proto-oncogene located on chromosome 1 and is highly specific for NGF.[34] Each trk receptor has an extracellular domain and an intracellular domain. The extracellular domain of the trk receptor contains two subsets of cell adhesion motifs: 1) three leucine-rich motifs (LRM) surrounded by two cysteine clusters at the amino terminal; 2) two consecutive immunoglobulin-like C2 domains. The intracellular domain is the tyrosine kinase domain and a short carboxyl terminus.[38]

Studies have shown that NGF can also bind to TrkB and TrkC, but with lower affinity than for TrkA.[39] Other neurotrophins that activate trkB are: BDNF, NT-4, and (with low affinity) NT-3.[40-42] TrkC is activated by NT-3.[43]

TrkA is selective for NGF and the peptide binds to the immunoglobulin-like C2 domains in the extracellular portion of the receptor.[38] After ligand binding, two monomeric TrkA receptor peptides dimerize and the tyrosine kinase in the intracellular domain is auto-phosphorylated to activate the signal transduction cascade illustrated in Figure 1.2. Most of the reported studies about the cascade were carried out in PC12 cells, a cell line derived from a pheochromocytoma of the rat adrenal medulla.[44] The signaling cascade for TrkA mainly includes:

(1) Activated TrkA receptor kinase phosphorylates and activates phospholipase Cγ, which subsequently cleaves phosphatidyl inositol 4,5 bisphosphate into diacylglycerol (DAG) and inositol triphosphate (IP_3).[45-47] IP_3 acts on the ER to induce calcium release.[45, 48] With the increased calcium concentration in the cytoplasm, DAG activates protein kinase C (PKC) which then activates the mitogen-activated protein kinase (MAPK) pathway, including MAPK kinase kinase (MKKK1 to 6), c-jun N-terminal kinase (JNK), p38 and extracellular signal-regulated kinases (ERK).[49-51] Activation of the MAPK pathway regulates transcription and promotes neuronal survival and differentiation.[52]

(2) Activated TrkA receptor kinase phosphorylates phosphatidyl-inositol 3-kinase (PI3K).[53] Activated PI3K then induces phophatidyl inositol 3,4 production and recruits phosphoinositide-dependent kinase (PDK) 1 to the inner leaflet of the cell membrane and then activates protein kinase B (PKB).[54-55] Activated PKB affects gene transcription by activation of Rac and the MAPK pathway or activates atypical protein kinase C (PKC) without involvement of MAPK pathway.[56-57]

(3) Activated TrkA receptor phosphorylates Src homology 2-containing protein (Shc), which binds to an adaptor protein called growth factor receptor bound protein-2 (Grb-2) and activates son of sevenless (Sos).[45, 58] The activated Sos recruits Ras to the cell membrane leading to activation of Ras.[59] Sos-Ras may then activate the Raf kinase or Rap-1 leading to phosphorylation of Raf.[60-61] Activated Raf subsequently activates the MAPK pathway and transcription factors involved in promoting cell proliferation and survival.[62]

(4) Activated TrkA activates SMA- and MAD-Related protein homolog (SMAD) 3, a protein that modulates signals of TGF-β.[63] SMAD3 forms a heteromeric complex with SMAD4 and then translocates into the nucleoplasm where it affects the transcription of TGF-β.[63]

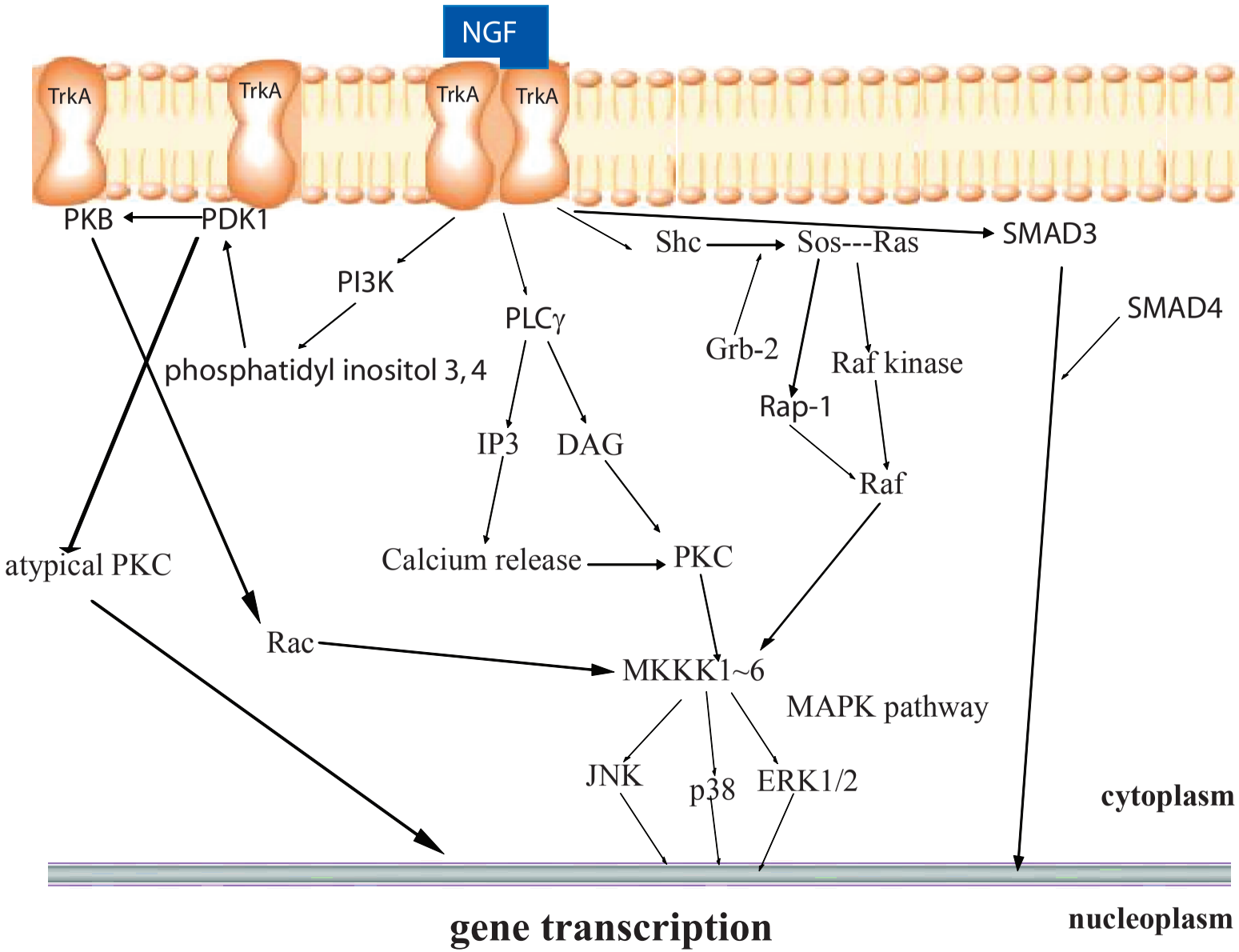
NGF
TrkA
TrkA
TrkA
TrkA
PKB
PDK1
PI3K
phosphatidyl inositol 3, 4
PLCγ
IP3
DAG
Shc
Sos---Ras
Grb-2
Rap-1
Raf kinase
Raf
SMAD3
SMAD4
atypical PKC
Calcium release
PKC
Rac
MKKK1~6
MAPK pathway
JNK
p38
ERK1/2
cytoplasm
gene transcription
nucleoplasm

Figure 1.2 Signal transduction pathways following activation of the TrkA receptor.

NGF dimer binds with TrkA and induces its dimerization. The receptor-dimer is autophosphorylated and activates gene transcription through MAPK pathway or atypical PKC. The abbreviations are defined in the abbreviation list. The figure is modified from Freund *et al.*, 2004.[18]

III B. p75 and signaling pathway

The p75 receptor is involved in development and apoptosis of neurons.[64] It was also reported that the p75 receptor may facilitate the binding specificity and increase the affinity of NGF for TrkA.[65] The role of p75 activation in immune and structural cells is unclear.

The p75 receptor is a 399 amino acid, 75kDa transmembrane protein, and is encoded by a gene located on human chromosome 17.[66] It is a member of the tumor necrosis factor-α (TNF-α) receptor family which all contain an extracellular domain, an transmembrane domain and an intracellular domain.[67] Similar to other members of the family, the extracellular domain of the p75 receptor has four repetitive cysteines rich domains and does not have an Ig domain.[68] The transmembrane domain of the p75 receptor is unique in that it passes the membrane once only whereas other TNF-α receptor family membranes have multiple transmembrane domains. Unlike TrkA, the intracellular domain of p75 receptor is composed of 155 amino acids which do not have catalytic activity. Both pro-neurotrophins and mature NTs can bind with high specificity to the p75 receptor.[29] Following binding with its ligands, two p75 receptors bind with each other and form homodimers. Activation of p75 has mainly been associated with apoptosis, cell cycle arrest and promoting cell survival through the main pathways illustrated in Figure 1.3. The downstream signaling pathways of the p75 receptor mainly include:

(1) Activated p75 receptor recruits adaptor proteins including neurotrophin receptor-interacting factor (NRIF) to the cytoplasmic domain of the receptor.[69] NRIF activates the MAPK pathway through activation of small G proteins such as Rac1 and p21Ras, PKA, increased ceramide synthesis or direct activation of JNK.[70-72] Activated JNK then directly phosphorylates Bad, p53 or Bax, induces release of Cytochrome c from mitochondria and activates caspases, particularly caspase 3 and 9.[71, 73] p53 may also be activated by another adaptor protein called neurotrophin receptor interacting melanoma-associated antigen (NRAGE).[64, 70]

(2) Activated p75 receptor recruits TNF receptor-associated factor (TRAF) 6 and then activates IL-1 receptor associated kinase (IRAK) and atypical PKC, or activates PI3K and then Akt/PKB, or recruits receptor interacting protein-2 to the cell membrane and leads to activation of the NFκB pathway which includes IκB, p50/p52 and IKKB. The NFκB pathway then blocks apoptosis by binding with MKK7 and preventing JNK activation, and activating apoptosis inhibitors.[68, 74-75] In this way, activated p75 may also be involved in promoting cell survival.

(3) Activated p75 receptor recruits and activates Schwann cell factor (SC)-1 which migrates into the nucleus and leads to cell cycle arrest.[64]

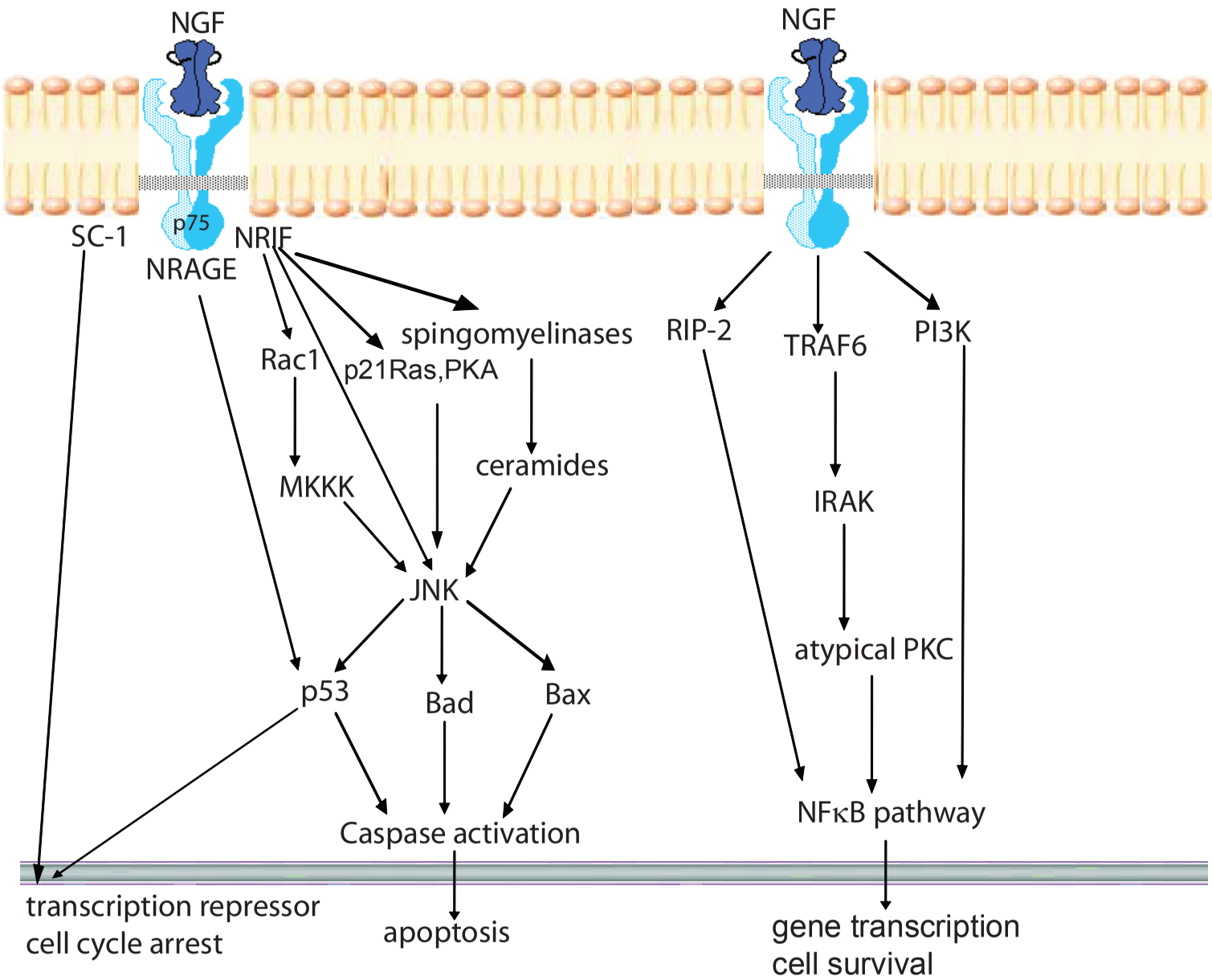
NGF
NGF
p75
SC-1
NRAGE
NRIF
Rac1
p21Ras,PKA
spingomyelinases
ceramides
MKKK
JNK
p53
Bad
Bax
Caspase activation
transcription repressor
cell cycle arrest
apoptosis
RIP-2
TRAF6
PI3K
IRAK
atypical PKC
NFκB pathway
gene transcription
cell survival

Figure 1.3 Signal transduction pathways of the p75 receptor.

Similar to trkA, NGF dimer binds with p75 (blue) and induces its dimerization and activation. The activated receptor then affects cell cycle arrest, induces apoptosis and increases gene transcription associated with cell survival. The abbreviations are defined in the abbreviation list. The figure is modified from Freund *et al.*, 2004.[18]

IV. NGF and nervous system

As mentioned earlier, NGF has been shown to promote survival of cultured sympathetic and sensory spinal neurons.[3] NGF is produced and secreted by sympathetic and sensory neurons in the target organs.[76] Following receptor binding, target derived NGF is captured by receptor-mediated endocytosis and transported through axons to neuronal cell bodies to affect neuronal survival, growth and apoptosis. Sources and effect of NGF in the nervous system include:

(1) During development, NGF is expressed in target regions of sensory nerves and guides growing axons to their final target. Montalcini et al. demonstrated that NGF was essential for maintaining viability of nociceptive, sensory and sympathetic neurons.[3] In trkA or NGF mutant animals, these neurons are not able to differentiate.[77-79] Later studies indicated that NGF dependent sensory nerves are most abundant in skin and heart than other organs and NGF depletion results in abnormal sensory nerve development.[80-81]

(2) In the adult central and peripheral nervous system, NGF can be synthesized by many neurons and glial cells. NGF from this source may act on the NGF secreting cells (autocrine) and on neighboring cells (paracrine), as well as distant neurons through axonal transport. Transgenic mice that over-express NGF in the somata of trigeminal sensory neurons show abnormal growth of sympathetic nerve fiber into the skin.[82] NGF also up-regulates production of neurotransmitters such as CGRP and substance P from neurons and enhances axonal transportation of the μ opioid receptor, which

regulates inflammatory pain.[83] NGF increased secretion of cytokines such as IL-6 and IL-10 from the neurons and regulates neurological inflammation.[83] In axons, NGF has been shown to induce alterations in the cytoskeleton and subsequently lead to accumulation of mitchondria, but does not have any effect on other organelles and vesicles, suggesting that NGF may increase the growth cones which require a large energy supply.[84]

(3) In neurological disorders such as Alzheimer's disease and diabetic neuropathy, defects in expression of NGF and receptors were found in different stages, indicating that NGF may be involved in the occurrence of these disorders.[85-86] Exogenous NGF in different animal models can attenuate the degeneration of neurons and improve neurological dysfunction at the end stage of neural diseases such as Alzheheimer's disease.[87-88] Binding of the p75 receptor with its β-amyloid agonist can induce apoptosis of neurons in the brain and may contribute to the pathophysiology of Alzheimer's disease.[87]

V. NGF and inflammatory responses

NGF and its receptors can also be produced by structural cells (defined as cells that mainly function to maintain the structure of the body, such as epithelial cells, fibroblasts, etc) including bronchial epithelial cells, cutaneous fibroblasts, retinal pigment epithelial cells, vascular endothelial cells and immune cells such as mast cells, macrophages and eosinophils.[3, 13, 89-93] Similar to the nervous system, NGF acts by autocrine and paracrine signaling on these cells.[77] NGF may act as a mediator between

the nervous and inflammatory system coordinating their response to various stimuli. The possible sources and effect of NGF on different types of structural cells and immune cells are summarized in Table 1.2 and Table 1.3. Generally, NGF has been shown to induce proliferation, activation and recruitment of immune cells, especially mast cells and eosinophils.[3, 19, 94-95] To date, the exact role of this neurotrophin on monocytes/macrophages/dendritic cells (referred to collectively as monocytic lineage cells in this dissertation) remains largely unknown. Results of studies indicate that NGF acts on monocytes as an immunoregulatory factor because exposure of resting monocyte cultures to exogenous NGF induced differentiation into macrophage phenotype or dendritic cells, enhanced macrophage phagocytosis and migration, and increased antimicrobial activity by promoting oxidative burst.[96-99]

NGF synthesis in structural cells and immune cells is increased in inflammatory conditions both *in vivo* and *in vitro*. When immune cells were treated with pro-inflammatory factors such as interleukin (IL)-1β, TNF-α, and IL-4 or lipopolysacharide (LPS) *in vivo*, secretion of NGF from nearby structural cells and immune cells was significantly increased; and the increased NGF was able to induce subsequent increases in other factors such as TGF- α and enhance tissue repair.[100-103] In vivo, serum NGF is up-regulated in several autoimmune, inflammatory and fibrotic disorders such as systemic lupus erythematosus, scleroderma, rheumatoid arthritis, and in allergic diseases such as asthma, rhinoconjunctivitis and vernal keratoconjunctivitis (VKC).[18, 104-107]

Among the different types of immune cells, the effect of NGF on monocytic lineage cells are not as clear as the other cell types such as mast cells and eosinophils.[95] Monocytic lineage cells are produced in the bone marrow under the influence of IL-4 and granulocyte-monocyte colony stimulating factor (GM-CSF), and infiltrate tissues through the circulation and differentiate into dendritic cells or macrophages.[108-110] Different stages of monocytic lineage cell development/maturation can be identified by the combination of surface markers as summarized in Appendix II. The differentiation process will be further discussed in Chapter 5. Monocytic lineage cells can phagocytose pathogens and function as antigen presenting cell in different tissues.[108] Monocytic lineage cells can also secrete several cytokines and growth factors (tumor necrosis factor, and NGF).[111-112] In addition, monocytic lineage cells contribute to the wound healing responses of tissues after injury.[113] Both human and mouse peripheral blood monocytes express NGF and trkA/p75 messenger RNAs and biologically active proteins, and produce NGF upon immunological stimulation, [95, 114-116] indicating that NGF may be involved in these immune responses. Recently NGF has been shown to up-regulate expression of adhesion molecules such as CXCR4 and CD11c therefore enhance the migration of monocytes.[97, 114] NGF also induced migration of macrophages *in vitro*.[98] However, to date there is no direct evidence if NGF has the same effect on monocytes in the peripheral blood or spleen.

Table 1.2 Summary of the sources and effects of NGF on structural cells.

Source	Effect
Fibroblast	Contraction, proliferation, differentiation, migration, collagen synthesis
Epithelial cells	Proliferation, migration, differentiation, regulating adherent molecule expression
Endothelial cells	Proliferation
Smooth muscle	Contraction, proliferation, migration

Table 1.3 Summary of the sources and effect of NGF on immune/inflammatory Cells.

Source	Effect
Mast cell	Activation, survival, migration,increasing mediator secretion
B/T lymphocyte	Differentiation, proliferation, Th2 cell differentiation, cytokine production, increase IgG and IgE production
Eosinophil	Proliferation, activation, survival, cell degranulation
Neutrophil	Chemotaxis, proliferation, activation, survival
Basophil	Activation, cytokine production
Monocytes	Differentiation, proliferation, survival
Macrophage	Activation, differentiation, proliferation, survival, phagocytosis
Dendritic cell	Maturation, differentiation, proliferation, survival, phagocytosis, increased antigen presenting ability

VI. NGF at the ocular surface

VI A. Localization

NGF, TrkA and p75 are widely expressed at the ocular surface.[117-126] Previous immunohistochemical studies have shown NGF, TrkA and p75 immunostaining in cornea, limbus, conjunctival epithelial cells, conjunctival goblet cells, fibroblasts originating from keratocytes, and corneal endothelial cells.[117-122] In the cornea and limbus, both NGF and TrkA are expressed in all layers of corneal epithelial cells, especially basal epithelial cells.[120, 122] The p75 receptor, however, is only found in the basal epithelial cells.[120, 122] Neither NGF not its receptors were found in normal corneal stroma.[122] Lacrimal gland acinar and duct epithelial cells also express NGF and the two main receptors, and may contribute to the secreted NGF in the tear film.[117] In the latter, normal NGF concentration is in the range of 550pg/ml to 1200pg/ml, and is necessary for maintaining normal corneal innervation.[123-126]

VI B. Function

Similar to skin, NGF and its receptor expression is important for maintaining normal corneal nerve density and corneal sensation. TrkA null mice have an abnormal distribution of corneal innervation and may develop keratoconus.[127-128] Lambiase et al. showed that NGF ointment significantly increased the recovery of corneal sensation in severe neurodegenerative corneal ulcer patients.[129] In animal models of refractive surgeries, NGF also accelerated the recovery of corneal sensitivity and corneal innervation which was disrupted by the surgical procedure.[130]

Another important function of NGF in corneal wound healing responses is to promote epithelial and stromal recovery, as well as modulate stromal-epithelial interactions. *In vitro*, NGF induces corneal epithelial cell proliferation and differentiation.[131] Topical application of NGF enhanced epithelial recovery in animals following an experimental epithelial injury, viral keratitis, and in patients with autoimmune corneal ulcers which did not respond to any other cytokines or growth factors.[129, 132-134] In the stroma, NGF regulates the differentiation of keratocytes into myo-fibroblasts which contract and lead to wound closure.[118] NGF topical application also delays the onset of stromal remodeling that often results in anterior stroma opacification, although the mechanism remains unclear.[129]

VI C.Association with diseases

NGF, Trk and p75 expression is affected by chronic allergic and inflammatory diseases of the ocular surface.[107] Increased expression of NGF and receptors was found in patients with Sjogren's syndrome, an autoimmune disease in which immune cells attack exocrine cells in the lacrimal gland and salivary gland.[123] Moreover in VKC patients, a strong correlation was found between high serum NGF and increased IgE level and mast cell number, indicating NGF secretion may be induced by the allergic responses of the ocular surface.[135] Consistent with that, immunohistochemical studies showed that NGF and its receptors were increased in inflamed juvenile conjunctival nevus, a disease characterized by eosinophil infiltration and increased IgE.[136] NGF may affect ocular surface inflammation in many ways. Recently Aloe et al. reported that NGF decreased toll-like receptor (TLR) 4, the receptor for LPS, in corneal epithelial cells

in vitro.[137] The decreased TLR4 may subsequently induce down-regulation of cytokines such as IL-1ß and IFN-γ at the ocular surface.[137]

VI D.Therapeutic application

Clinically, NGF has been used in treating patients with corneal and skin ulcers and Alzheimer's diseases and has been reported to induce healing of structural cells and neurons.[132, 138] One possible side effect of topical NGF application is angiogenesis, which was observed by Lambiase et al. in their clinical trials.[129] This might be explained by NGF facilitating production of VEGF, as shown in other tissues of the body.[139] NGF also increases the secretion of mucin from goblet cells and may be beneficial to dry eye.[121] Recently NGF was tested in several animal studies and clinical trials for enhancing wound healing, increasing recovery of corneal sensation and alleviating symptoms in dry eye.[129-130, 132-133, 140] However, the mechanisms remain unclear.

VII. Monocytic lineage cells in the cornea

Bone marrow-derived cells (BMDCs) (2.2~3.5 percent of all stromal cells, depending on the location) of the monocyte lineage were found in the normal human and mouse cornea (Figure 1.4).[141-142] Both in human and mouse, the main cell type in the epithelium is dendritic cells (Langerhans cells).[141, 143] In the stroma, the BMDCs are mainly distributed in the anterior stroma of the central and paracentral regions as well as all stromal layers of the peripheral cornea and play a role in the innate and adaptive immune responses.[142] In addition, BMDCs transplanted from enhanced GFP

transgenic mice were detected as enhanced GFP-positive cells in normal corneal stroma, suggesting that leukocytes observed in the corneal stroma are derived from the bone marrow.[144] BMDCs are presumed to migrate centripetally into the corneal stroma from limbal and conjunctival vessels, because the normal cornea is avascular. However, the mechanism that accounts for the distribution of BMDCs in the normal human corneal stroma is still unknown. Huang et al. reported that large numbers of monocytic lineage cells migrated into the mouse corneal stroma within 12 to 24 hrs following an epithelial injury.[145] Further, Ebihara et al. found that the recruitment of BMDCs can be induced by chemokines such as macrophage chemotractant protein (MCP)-1 secreted from cultured fibroblasts derived from keratocytes *in vitro*.[146] However, to date the chemokines that affect the migration of the monocytic lineage cells in the cornea *in vivo* remain unclear.

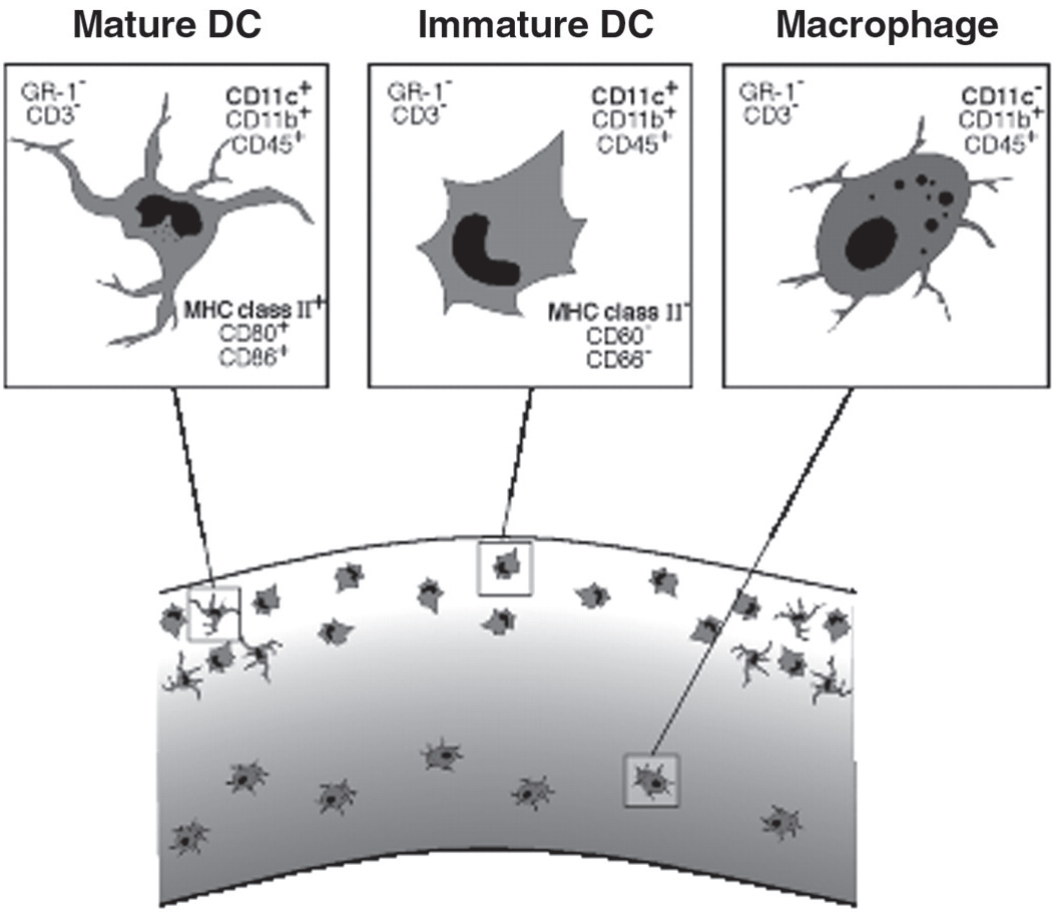

Figure 1.4 Monocytic lineage cells are found in the normal corneal stroma.
The figure was taken from the article by Hamrah *et al.*, 2003.[142] Dendritc cells are mainly found in the anterior stroma, whereas macrophages are mainly found in the posterior stroma.

Chapter 2. Thesis Hypothesis and Rationale

Nerve growth factor is a pleiotropic factor that affects the nervous system, the immune system and structural cells. It functions as a mediator that regulates the balance between the three systems. NGF is involved in inflammatory processes such as recruitment of inflammatory cells, and regulates cytokine and growth factor production in different organs of the body such as bronchus, brain and skin.

At the ocular surface, NGF is increased with a vaiety of disorders including allergy, dry eye, keratoconus, diabetic keratitis, and congenital corneal ulcer. Increased NGF is probably secreted by corneal epithelial cells or keratocytes in response to various stimuli, although its mechanism and function in these diseases remains unclear. NGF has been shown to enhance the recovery of corneal innervation as well as corneal epithelial cells after injuries in animal models. According to the literature, it is hypothesized that increased NGF may be induced by injuries to corneal nerves and inflammatory stimuli to corneal epithelial cells and keratocytes. The increased NGF may in turn enhance recovery of corneal innervation and affect local inflammatory and immune responses. Based on the effect of NGF on inflammatory responses in other organs, NGF may affect the expression of inflammation associated molecules, such as TGF-β, and chemotactic proteins, such as MCP-1. NGF may also affect the influx and differentiation of immune cells, such as monocytic lineage cells, in the cornea with or without inflammatory stimuli. NGF has also been shown to increase the viability of corneal and conjunctival epithelial cells *in vitro* possibly through the TrkA receptor which has been identified on the

membranes of corneal and limbal epithelial cells. However it remains unclear if NGF will also promote cell survival in response to hyperosmolar stress.

Currently, NGF and mimetics are being studied for future clinical therapy for dry eye and corneal ulcers, but their therapeutic effect is not well understood. The present studies provide information about the corneal inflammatory and immune response and addresses the role of NGF in these processes. Through these studies, we will understand some of the possible effects of NGF on corneal immunity and will also collect further evidence about whether NGF can be used in clinical therapy.

Specifically it is hypothesized that:

Specific Aim 1: To test if tear film NGF is increased in dry eye subjects associated with established contact lens wear and is correlated with decreased corneal innervation and increased TGF-β.

Increased levels of NGF can be induced by nerve injuries or inflammatory responses in other systems of the body. At the ocular surface, increased NGF has been reported in several neurodegenerative and inflammatory disorders; however the mechanism of the increase is not clear. Established contact lens wearers with clinical symptoms of dry eye had decreased nerve sensation and increased inflammatory responses, characterized by increased levels of inflammatory cytokines and growth factors. Therefore contact lens related dry eye is a suitable model for studying the factors at the ocular surface that affect NGF secretion *in vivo*. In this specific aim, tear film NGF

concentration was measured in normal subjects and contact lens wearers to test if it correlated with decreased corneal innervation or tear film inflammatory TGF-β levels.

Specific Aim 2: To test if NGF affects production of inflammation-associated molecules by cultured corneal and conjunctival epithelial cells in a dry eye culture model.

To investigate the role of NGF on inflammatory responses of ocular surface cells *in vitro*, the effect of exogenous NGF on corneal and conjunctival epithelial cells was studied in this specific aim. Hyperosmolar stress was used to mimic the dry eye environment, in which increased NGF was reported previously. Here the effect of NGF on the epithelial cell survival and expression of inflammation associated molecules produced by these cells was tested.

Specific Aim 3: NGF induces migration and differentiation of monocytic lineage cells *in vitro* and *in vivo*.

Here three sub-aims were addressed:

3A. To test the effect of NGF on migration of monocytic lineage cells isolated from peripheral blood, spleen and peritoneal lavage fluid.

3B. To test if NGF induces differentiation of monocytic lineage cells into dendritic cells and macrophages.

3C. To determine if the observed migration effect is a direct effect of NGF on monocytic lineage cells or if it is acting through macrophage chemotractant protein (MCP)-1.

Another possible role of NGF at the ocular surface is to affect immune cells and regulate immune responses. Recent studies have reported that the normal mouse cornea has a significant amount of monocytic lineage cells. The factors that affect the distribution of those cells are not clear. According to the effect of NGF in other systems of the body, NGF could induce the migration and differentiation of monocytic lineage cells. However, it is unclear if NGF has the same effect at the ocular surface. In this specific aim the effect of NGF on migration and differentiation of monocytic lineage cells was studied *in vitro and in vivo*.

The proposed effects of NGF are listed in Figure 2.1.

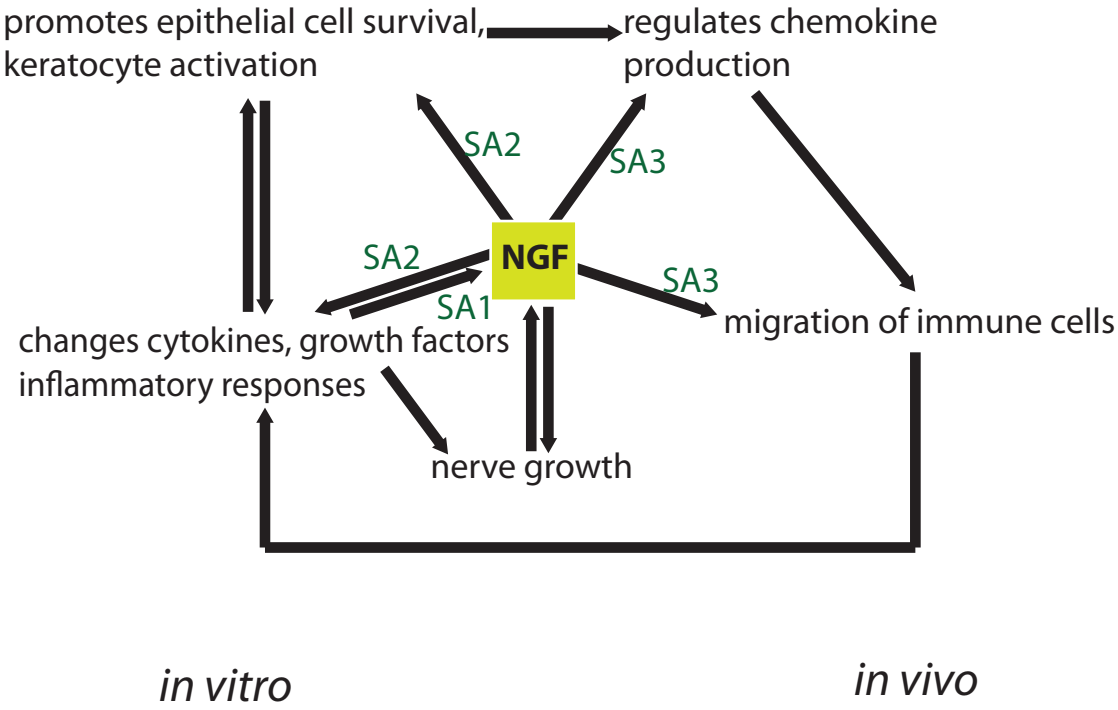

Figure 2.1 Summary of overall hypothesis and rationale of the dissertation.
The possible role(s) of NGF at the ocular surface on epithelial cells, immune cells and nerves were studied using both in vitro and in vivo models. SA: specific aim.

Chapter 3. Elevated Nerve Growth Factor In Dry Eye Associated With Established Contact Lens Wear (published data)

I. Introduction

Nerve Growth Factor (NGF) is normally in low concentrations in the tear film and may originate from lacrimal gland, corneal and conjunctival epithelial cells or goblet cells.[147-149] Also, recent studies have shown that corneal stromal keratocytes can produce NGF in vitro.[150] NGF has been observed to promote nerve regeneration and increase proliferation, differentiation and migration of corneal epithelial cells.[151] Tear film NGF levels can increase significantly in a number of conditions, such as refractive surgeries,[152-153] neurodegenerative corneal ulcer and keratoconus, possibly reflecting a compensatory response due to damaged corneal nerves in these disorders.[140, 154] NGF has been found to promote recovery of corneal sensation and increased corneal epithelium after surgery.[152, 155] NGF has also been shown to be up-regulated in inflammatory and immune conditions, such as vernal keratoconjunctivitis and allergic rhinoconjunctivitis, and dry eye although the underlying mechanism(s) is not clear.[156-158]

NGF is a pleiotropic factor that was discovered in 1951.[159] As a member of the neurotrophin gene family, it is well recognized for its role in promoting peripheral nerve growth and survival.[159] Previous studies have also found that NGF is increased in inflammatory conditions such as asthma,[160] and may be regulated by expression of several cytokines and growth factors involved in inflammation such as transforming

growth factor (TGF)-β1.[161] NGF may affect expression of inflammatory molecules such as toll-like receptor 4,[162] and human leukocyte antigen-DR on monocytes,[163] and regulate tissue fibrosis through TGF- β1.[164]

Established contact lens wearers are one group of patients in which superficial corneal nerve structures are damaged. According to Patel et al., nerve numbers in the subepithelial plexus were decreased, as visualized by *in vivo* confocal microscopy.[165] Corneal sensitivity was significantly decreased in those subjects and they did not observe any decrease in stromal nerves.[165] Dry eye is another frequent complication of established contact lens wear. According to previous reports, approximately 50% of the 35 million contact lens wearers in the United States have dry eye symptoms, and some 12% to 42% reported intense symptoms that affected the comfort of contact lens wear. [166-168] The cause of dry eye associated with contact lens wear remains unclear and both nerve damage and inflammation might be involved.

Based on the previous literature, it is hypothesized that tear film NGF is up-regulated in long-term contact lens wears due to the presence of nerve damage. Furthermore, in subjects with dry eye, it is expected that NGF levels will be even higher due to chronic inflammation. Tear levels of NGF have been studied in normal subjects and patients with dry eye,[158] however, to date, no published study has examined the concentration of NGF in contact lens wearers. Thus, the purpose in conducting the present study was to examine the corneal subepithelial nerve plexus in long-term contact lens wear with and without dry eye and correlate those findings to the tear levels of NGF

and TGF-β1, a known regulator of NGF production in other tissues of the body. This study will also look into the possibility of NGF as a novel medication that maybe used to address dry eye associated with contact lens wear.

II. Methods:

Established contact lens wearers (18 subjects, daily contact lens wear > 1 year) and 6 normal control subjects without contact lens wear history were recruited for the study (subject characteristics are summarized in Table 3.1). The mean age of normal subjects was 26.33 ± 2.58, and it was 28.22 ± 4.31 years for contact lens wearers (mean ± standard deviation). All participants gave informed consent and completed the Ocular Surface Disease Index (OSDI) questionnaire (Appendix IV).[169] The protocol was approved by the institutional review board (IRB) at the University of Houston. The majority of the subjects (16 of 18) were wearing silicone-hydrogel contact lenses. Two were wearing hydrogel daily disposable contact lenses. All subjects wore the contact lenses for more than 8 hours per day. Each subject was examined with biomicroscopy without sodium fluorescein to exclude other corneal pathology. Schirmer test without anesthesia was performed to assess tear production. Corneal sensitivity was measured with a Cochet-Bonnet aesthesiometer (0.08 mm filament, Luneau, Paris, France).[170] The results of the various tests are summarized in Table 3.2. A subject was diagnosed as dry eye with OSDI > 20 and schirmer test (without anesthesia) of less than 10mm wetting in 5 minutes. All subjects (normal and contact lens wearers) were measured at the same time of the day and all measurements were done in the same order.

Table 3.1 Summary of the general characteristics of the recruited subjects.

Subject	Age	Gender	OSDI	Contact Lens History
ZC	27	M	33.30	J&J daily disposible for 6 years; RGP 4 years
YL	30	M	25.00	J&J daily disposible for 2 years, 3D
SS	24	F	20.00	Acuvue advance
LL	25	F	25.00	Acuvue oasis, 1 year; acuvue advance, 1year
XY	25	F	22.50	Acuvue advance
LR	31	F	16.00	BL 2 week, 3years
TG	34	M	20.80	Y
MA	31	M	11.20	Y
LH	24	M	6.25	N
SD	27	F	6.70	Y
DS	27	F	4.60	Y
ZZ	27	F	27.50	N
LW	35	F	22.70	Y
EM	26	M	25.00	Y
GR	28	M	16.00	Y
QL	25	F	11.20	N
ML	35	F	20.00	N, 2 years after LASIK
XB	24	F	11.20	N
JH	30	M	25.00	Y
XT	30	M	11.20	N
JM	29	M	10.40	Y
JW	29	F	4.60	N
RB	26	F	4.60	N
CZ	29	F	13.00	PureVision monthly
DL	25	F	2.10	Acuvue Oasis and Acuvue advance, 10 years
NM	27	M	4.10	Acuvue
ES	24	M	2.10	Acuvue advance and BL; 10 years

Y: established contact lens wearers unable to provide information on the type of contact lens that they usually wore; N: subjects that had never worn contact lenses before; BL:Bausch and Lomb; J&J: Johnson & Johnson.

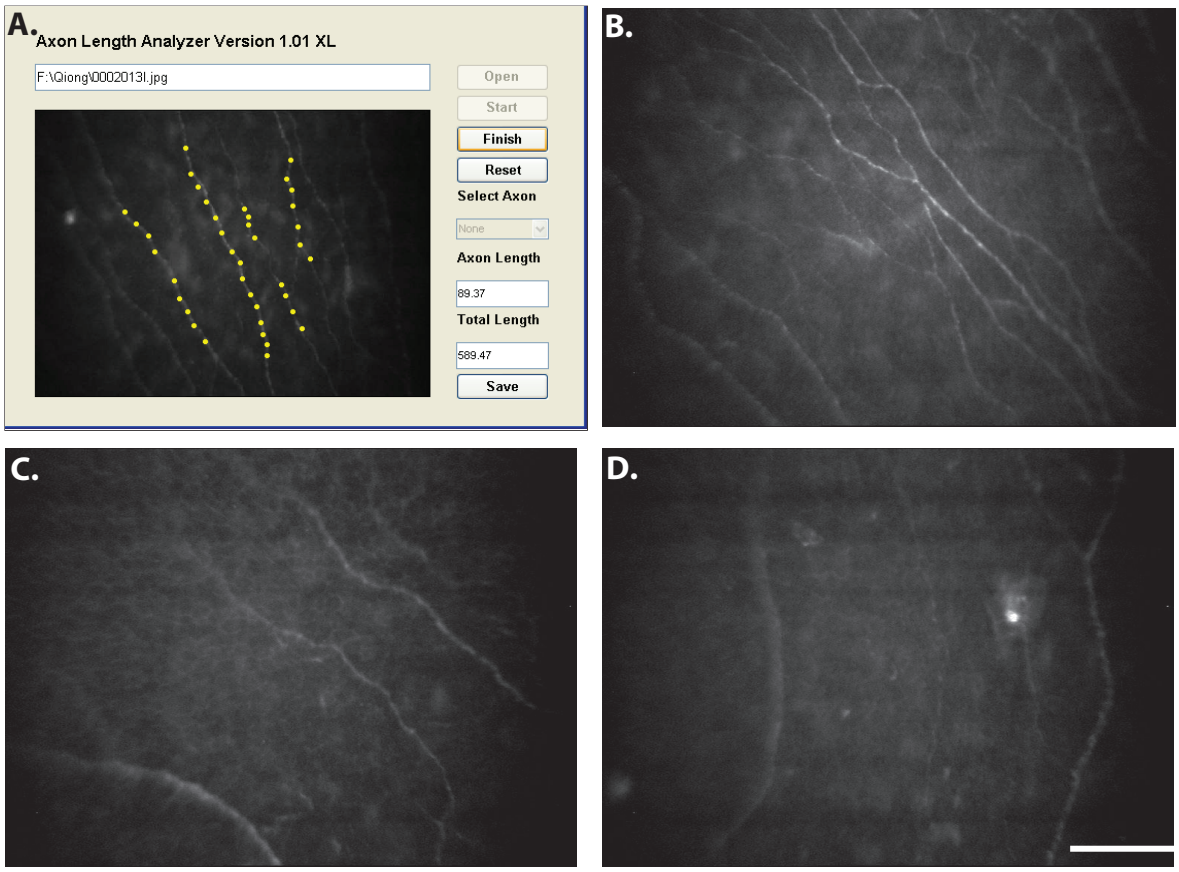
A.
Axon Length Analyzer Version 1.01 XL
F:\Qiong\0002013l.jpg
Open
Start
Finish
Reset
Select Axon
None
Axon Length
89.37
Total Length
589.47
Save
B.
C.
D.

Figure 3.1 Human corneal nerve measurements in the subepithelial plexus.

A. A Matlab program was used to measure the density of the subepithelial plexus. Yellow dots were placed manually at each of the turning points and the program automatically calculated the distance between each two continuous points and summed the data to give the length of each nerve when the button Finish was clicked. The total length of the yellow-dotted nerves was summed up by the programme. *In vivo* confocal microscopy images of subepithelial plexus in 3 subjects from 3 groups respectively. B. Normal control subject; C. Contact lens wearer without dry eye; D. Contact lens wearer with dry eye. Scale bar: 100 μm.

T_{90} was measured in order to objectively measure the tear turnover and assess the tear film of the subjects.[171] Tear-clearance, T_{90} (the time for 90% of fluorescein to be cleared from the tear film) was determined with a fluorophotometer (Fluorotron Master, Ocumetrics, Mountain View, California). Autofluorescence of the cornea was measured before application of dye, after which, 2µl of 5% high molecular weight fluorescein (FITC-Dextran; GreenPark Pharmacy, Houston, TX) was instilled into the inferior meniscus. Fluorescence measurements were taken every 2 minutes for 15 minutes and then every 5 minutes until the tear film fluorescence peak concentration returned back to baseline level. Data from the first 5 minutes were excluded because of fast decay due to the initial reflex tearing, which may occur after sodium fluorescein instillation. Peak fluorescence values at the ocular surface were then corrected for baseline readings. A four-parameter exponential curve was fitted as previously described and the time when 90% of the peak fluorescence was eliminated was recorded.[171]

In vivo confocal microscopy was then carried out to measure the subepithelial nerve plexus (ConfoScan3, Nidek, Technologies America, New Orleans, LA) in the center of the cornea. Topical anesthesia was induced using 0.5% proparacaine hydrochloride (Bausch & Lomb Pharmaceuticals Inc., Tampa FL, USA). A small bolus of Genteal gel (Novartis, St. Louis, MO, USA) was placed on the tip of the objective as an optical coupling media to the cornea. In this study, the subepithelial nerve plexus was defined as the nerve structures located between anterior stroma and basal epithelia, and where no keratocytes and basal epithelial cells were clearly visible. The image size of each frame was 435×312 µm² and the axial depth of images was 2.5 µm. The images

were exported in JPEG format with 768×576 pixels. Two measurements were taken for each eye, and 3 focused images of the subepithelial plexus were randomly selected from each measurement for analysis. The total length of "focused nerves" in each image was measured by a Matlab program as demonstrated in Figure 3.1A (the detailed programme is listed in Appendix III). Only the subepithelial nerves with identified beading structures and sharp edges were measured. Other nerves were considered out of focus. Two nerve parameters were measured: *Branching:* the number of nerve branching points in the focused nerves was counted manually. *Density:* the total length of focused nerves (μm) in the image was measured and divided by the area of the image.[172]

Fifteen to twenty minutes after *in vivo* confocal microscopy, 20 μl of basal tears were collected from the inferior meniscus of each subject (tear samples were pooled for both eyes of each patient) with a 0.5 μl glass capillary, and stored at -80 ºC until analysis. Total protein concentration was then quantitated with a Bradford assay. Tear samples (diluted 1: 10 in assay buffer) were analysed by ELISA to determine the levels of NGF (Chemicon International Inc., Temecula, CA). For measuring TGF-β1 by ELISA, the samples were diluted 1:12 in assay buffer then activated by incubating with 1M HCl for 10 minutes before testing as per the manufacturer's instructions (R&D Systems, Minneapolis, MN, USA). All samples were measured in duplicate.

Statistical analyses were performed with MiniTab software (Minitab 13.2, trial version) using one-way analysis of variance (ANOVA) to test the difference among contact lens wearers without dry eye, contact lens wearers with dry eye, and normal

control subjects.[173-174] Normality test was performed to see if the data were normally distributed. Post-hoc comparisons were made with a two sample student t-test. $P < 0.05$ was considered statistically significant.

III. Results

III A. General characteristics of subjects

A paired t-test was performed to test the difference between the two eyes of each subject. No statistically significant differences were observed for Schirmer test, T_{90}, corneal sensitivity, and nerves (p = 0.67, 0.33, 0.92, 0.82), therefore data from one eye of each subject was randomly picked for data analysis. The subjects were diagnosed as having dry eye if they had an OSDI score of more than 20 and Schirmer test without anesthesia of less than 10mm wetting/5 minutes. Based on these conditions, the subjects were divided into three groups as shown in Table 3.2.

Compared with the normal group, a statistically significant decrease in corneal sensitivity was observed with dry eye contact lens wearers (p = 0.02). But the difference was not statistically significant between dry eye and normal contact lens wearers (p = 0.47), and between normal control and normal contact lens wearers (p = 0.053). No statistically significant correlation was found between corneal sensitivity and other dry eye parameters.

Table 3.2 Summary of the dry eye tests in three groups of subjects.

	N	CL	CL&DES	One-WAY ANOVA
Subjects	6	10	8	
OSDI	8.17 ± 3.37	9.27 ± 6.42	23.37 ± 3.14	t (24) = 5.22, p = 0.002
Schirmer (mm)	15.03 ± 1.75	14.38 ± 2.34	9.72 ± 0.34*	t (24) = -7.361, p = 0.000
T_{90} (minutes)	23.39 ± 1.64	21.04 ± 3.86	26.03 ± 4.88	t (24) = 1.576, p = 0.145

The data are shown as mean ± standard deviation. N: normal; CL: contact lens wearers without dry eye; CL&DES: contact lens wearers with dry eye syndrome. * indicates statistical significance compared with normal group. ($p < 0.005$)

III B. Subepithelial nerve plexus characteristics

The density and branching of nerves were measured with a Matlab program and the repeatability was evaluated by measuring some of the same images twice on different days. A paired t test was then performed and no statistical significance was found ($p = 0.90$).

Data for the subepithelial nerve plexus are summarized in Figure 3.1 A. The subepithelial nerve plexus density was decreased significantly in contact lens wearers, compared to the normal group ($p = 0.009$), as shown in Figure 3.1 B~D. However, although reduced, no statistically significant difference in branching was found with one-way ANOVA. Subepithelial nerve density and branching was positively correlated (Pearson Correlation, $r = 0.72$, $p = 0.01$), as shown in Figure 3.1 B. And a positive correlation was found between corneal sensitivity and subepithelial nerve density (Pearson Correlation, $r = 0.57$, $p = 0.058$), as shown in Figure 3.1 C. The correlation was not statistically significant.

A.

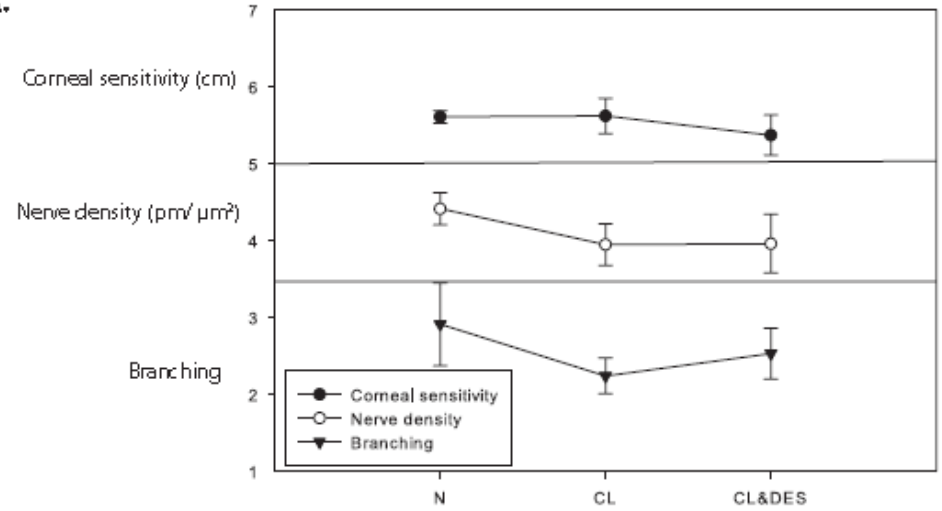
Corneal sensitivity (cm)
Nerve density (pm/ µm²)
Branching
Corneal sensitivity
Nerve density
Branching
N
CL
CL&DES

B.

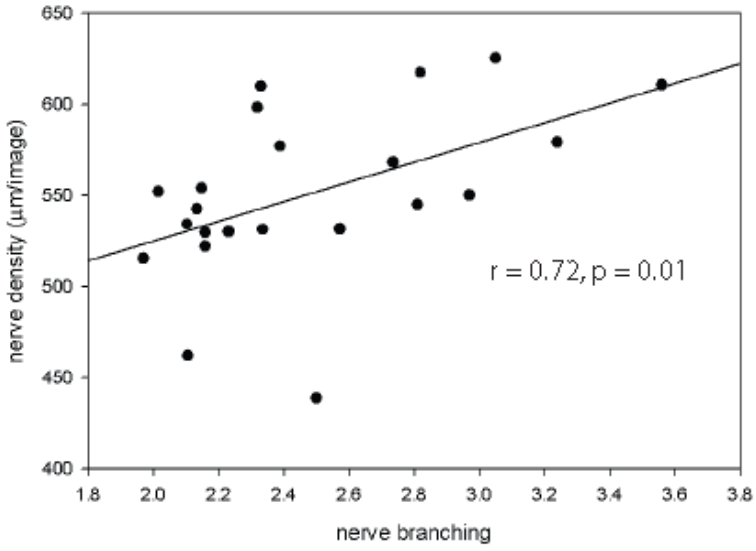
nerve density (µm/image)
nerve branching
r = 0.72, p = 0.01

C.

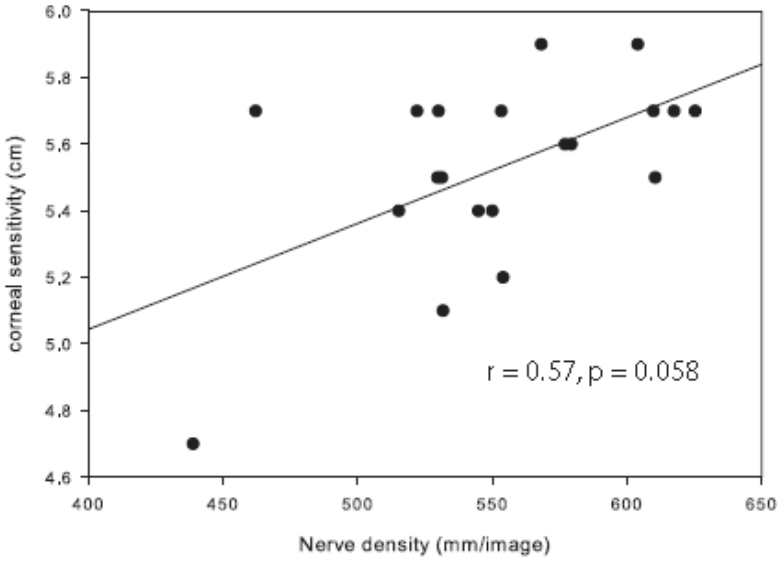
corneal sensitivity (cm)
Nerve density (mm/image)
r = 0.57, p = 0.058

Figure 3.2 The correlation between measurements of corneal sensitivity, corneal nerve density and branchings.

A. Corneal sensitivity, nerve density and branching of all subjects. N: normal; CL: contact lens wearers without dry eye; CL&DES: contact lens wearers with dry eye syndrome. B. Correlation between corneal nerve branching and nerve density in subepithelial plexus of all subjects. The correlation is statistically significant. C. Correlation between corneal nerve density and corneal sensitivity is not statistically significant.

III C. Tear NGF concentration

Tear NGF/mg total protein (tp) level was measured with ELISA as described in the methods. NGF concentration ranged between 149.4 pg/mg tp to 6080 pg/mg tp. The average NGF concentration for contact lens wearers with dry eye was significantly higher than contact lens wearers without dry eye ($p = 0.04$). However, as shown in Figure 3.3 no difference was found between normal subjects and contact lens wearers without dry eye ($p = 0.14$). No correlation was found between NGF concentration and subepithelial nerve plexus density or branching (data not shown).

III D. Tear TGF-β1 concentration

The concentration of TGF-β1 in the tear film was measured by ELISA after acid activation. The TGF-β1 concentration was higher in contact lens wearers with dry eye and was statistically significantly different from normal control and normal contact lens wearers ($p = 0.042$, 0.024, respectively, figure 3.4A). A statistically significant positive correlation was found between TGF-β1 and NGF, as shown in figure 3.4B (Pearson Correlation, $r = 0.59$, $p = 0.05$).

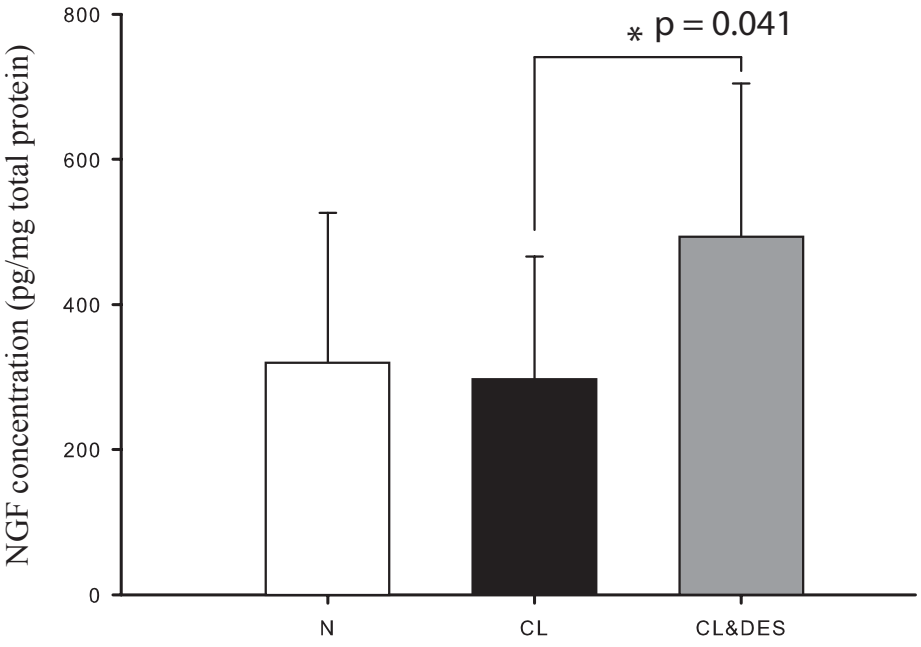

Figure 3.3 Tear NGF concentrations in all three groups of subjects. N: normal; CL: contact lens wearers without dry eye; CL&DES: contact lens wearers with dry eye syndrome. Data were plotted as mean ± standard deviation. * indicates statistically significance difference. (p = 0.041)

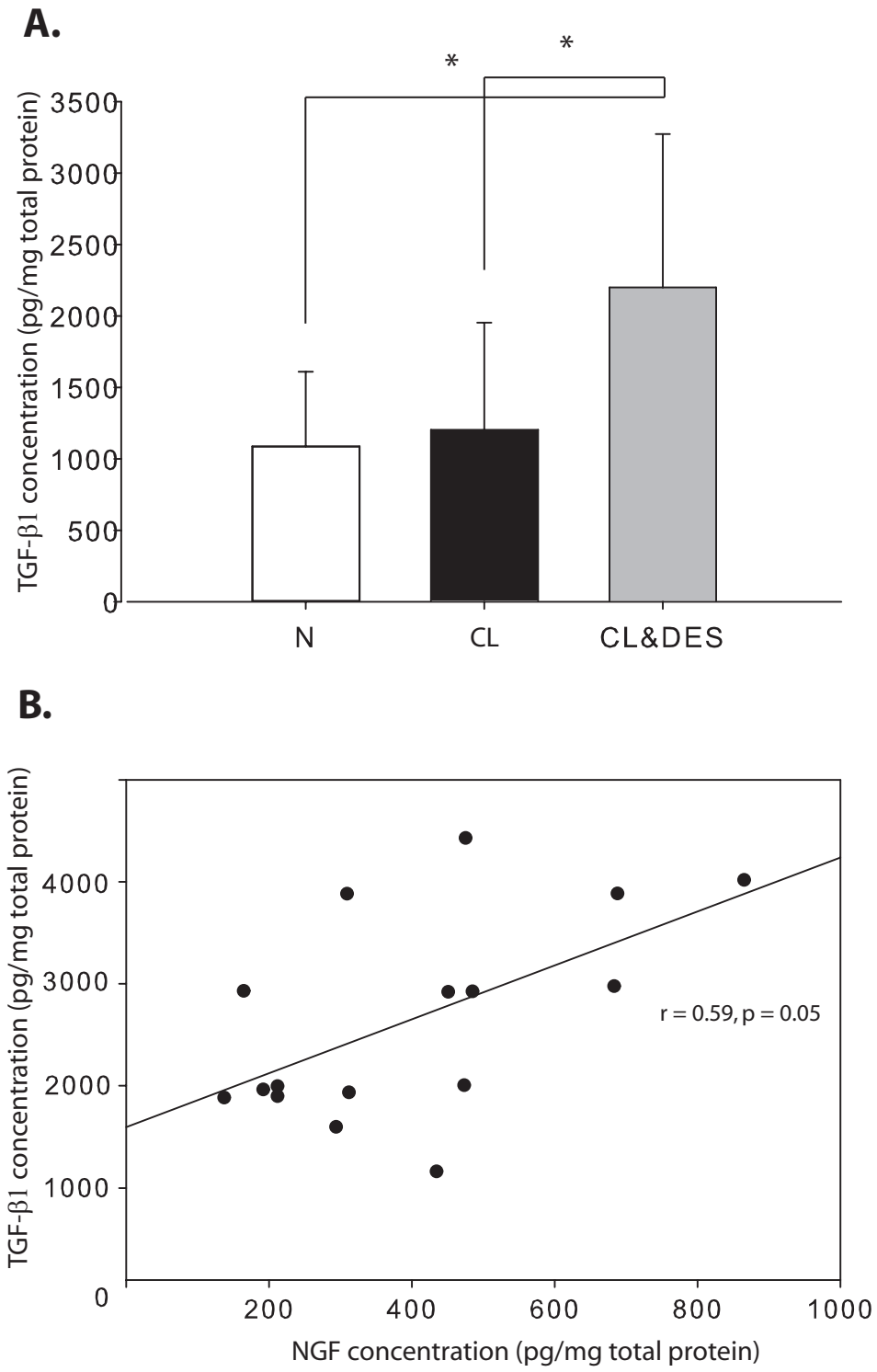
A.
*
*
TGF-β1 concentration (pg/mg total protein)
3500
3000
2500
2000
1500
1000
500
0
N
CL
CL&DES
B.
TGF-β1 concentration (pg/mg total protein)
4000
3000
2000
1000
0
r = 0.59, p = 0.05
200
400
600
800
1000
NGF concentration (pg/mg total protein)

Figure 3.4 Tear TGF-β1 concentrations in three groups of subjects.

A. Tear TGF-β1 concentration in normal subjects (N), contact lens wearers without dry eye (CL), and contact lens wearers with dry eye (CL&DES). B. Correlation between NGF concentration and TGF-β1 concentration. Data were plotted as mean ± standard deviation. (*) indicates statistically significance difference. ($p < 0.05$)

IV. Discussion

NGF concentration in the tear film is up-regulated in a number of diseases that cause nerve injury and inflammation at the ocular surface such as diabetic keratitis and congenital corneal ulcer. In the present study, tear film NGF concentration and its possible association with corneal innervation and tear TGF-β1 was studied in long-term contact lens wearers. The present study showed that NGF was increased in contact lens wearers with dry eye. However, while the levels of TGF-β1 correlated with those of NGF, there was no significant correlation between NGF concentration and subepithelial nerve density and branching.

Previous studies have shown that tear film NGF concentration was significantly up-regulated following nerve damage such as occurs with refractive surgeries, neurogenic corneal ulcer, diabetes mellitus and keratoconus.[140, 153, 175] In these disorders, NGF was found to promote survival of corneal nerves, and helped preserve normal corneal sensation. In the present study, subepithelial plexus nerves were altered, as indicated by decreased density and branching, in contact lens wearers without dry eye, but tear NGF concentrations were not increased compared to normal subjects. One possible reason for this is that in contact lens wearers the nerve damage is minor compared to that resulting from refractive surgeries and corneal ulceration, so the change in tear film NGF due to lens wear per se might not be so great.

However, the present study showed that in addition to decreased nerve density and branching, the concentration of tear film NGF was significantly up-regulated in

contact lens wearers with dry eye. This observation suggests that the elevated levels of NGF are related to the occurrence of dry eye rather than contact lens induced nerve damage. Notably the change in NGF was correlated with TGF- β1. The latter is an anti-inflammatory factor that can be used as a marker for monitoring chronic inflammation.[176] As mentioned in the introduction, TGF- β1 has been shown to up-regulate NGF,[164] which suggests that NGF can increase in response to chronic inflammation. Further, as noted earlier, NGF has also been shown to increase in chronic inflammatory diseases at the ocular surface.[156] Thus the observation of elevated level of tear NGF in contact lens wearers with dry eye, a known chronic inflammatory condition,[169] is consistent with the published literature.

In vivo confocal microscopy has been used previously to measure corneal innervation. The nerve density values in the present study were lower than previously reported. In the present study a density of 600.46 ± 21.25 μm /image was observed in normal subjects whereas Benítez-Del-Castillo et al. reported 787 ± 105 μm/image.[177]. However, compared with previous studies in which all nerves were counted, here only the focused nerves in the images were measured and those without sharp edges were not counted within the analysis. Using this new criterion the measurement values demonstrated lower standard deviations than previous studies. (21.25 μm /image with n = 6 in normal group, compared to 105 μm /image with n = 25 from Benítez-Del-Castillo et al.), and is a more precise measurement for subepithelial nerve density. The data obtained from measuring all nerves and focused nerves only several times on the same subjects

was also compared, and lower standard deviations were obtained again with the focused nerves only.

Although there was a statistically significant decrease in subepithelial nerve density, a parallel decrease in corneal sensitivity was not observed. This can be explained by the inherent limitations in the Cochet-Bonnet esthesiometer, since this instrument only measures the sensation from mechanical receptors, which represent only a minor portion of all the corneal receptors.[177] It is possible that contact lens wear may also affect thermal and chemical receptors in addition to mechanical, as shown by Simpson et al.[178]

In this study tear sample collection was performed about twenty minutes after the two confocal measurements were done. By that time the topical anesthesia effect of proparacaine should be almost gone. There might be some gel left that affects the concentration of NGF, but the concentrations obtained are similar to previous studies.[179] Another limitation of the study is the small sample size recruited in each study cohort.

In conclusion, the present study suggested that NGF was increased in dry eye related to long-term contact lens wear in response to chronic inflammation. Decreased nerve density in the subepithelial plexus did not induce the NGF increase as shown by the findings in contact lens wearers without dry eye.

Chapter 4. Nerve growth factor (NGF) Modulates Expression of Inflammation Associated Molecules in a Dry Eye Culture Model

I. Introduction

Previous studies have found that NGF is secreted by several structural cells such as epithelial cells and fibroblasts, and is involved in inflammatory processes.[180] NGF has been reported to affect proliferation, apoptosis and migration of structural cells, subsequently affecting inflammatory reactions on or induced by those cells.[181] This versatile growth factor has also been reported to up-regulate secretion of IL-10 and TGF-β and to down-regulate IL-1β and IL-6 in vitro, indicating that NGF can alter the microenvironment at inflammatory sites.[162-163, 182] In turn, cytokines modulate NGF secretion, for example IL-10 down-regulated and IL-1β up-regulated NGF secretion from cultured neuronal and glial cell lines.[183-184] Many of the effects of NGF are mediated via the high affinity tropomyosin-related kinase (Trk) A receptor, in which binding of NGF leads to activation of signaling pathways such as Mitogen-Activated Protein Kinase (MAPK), phosphatidyl inositol 3-kinase (PI3K) or SMADs.[163, 185-186] Other Trk receptors, such as TrkB and TrkC, have only low affinity for NGF. p75 belongs to the neurotrophin receptor superfamily and is less specific for NGF and it is mainly associated with NGF induced apoptosis via activation of Gi and Rho proteins.[187]

At the ocular surface, NGF and its receptors were found to be expressed by lacrimal gland acinar and duct cells, corneal and conjunctival epithelial cells, fibroblasts (derived from keratocytes after stromal injury or cultured keratocytes), goblet

cells and endothelial cells.[188-191] NGF is also present in the tear film and the concentration of NGF in the tear film and ocular surface increases after injury in human refractive surgery patients and animal wounding models. Further, NGF can stimulate corneal wound healing in rats but not dogs.[130, 189, 192] Notably NGF has been successfully used to treat neurodegenerative corneal ulcers in human patients, and was found to accelerate nerve growth and recovery of structural cells.[107, 129, 132, 193] Similar to other systems and tissues, NGF secretion from conjunctival epithelial cells was up-regulated by inflammatory cytokines such as IL-1β. A recent study showed that NGF decreased IL-10 secretion from conjunctival epithelial cells isolated from patients with vernal keratoconjunctivitis. However, no study has rigorously tested the effect of NGF on secretion of inflammatory cytokines by non-diseased ocular surface cells.[194-195]

Previously, we and others have reported that NGF levels in the tear film are increased in patients with contact lens related dry eye.[123-124] Lee et al. (2006) noted that treatment with 0.1% prednisolone eye drops reduced NGF levels in tears of patients with keratoconjunctivitis sicca (KCS) to levels comparable to those in normal subjects.[123] This was accompanied by improvements in symptoms, leading the authors to suggest a role for NGF in inflammatory processes in dry eye. However, in contrast to the detrimental effects of NGF implied by the study of Lee at al. (2006), topical administration of NGF and of an NGF mimetic have been used to relieve dry eye symptoms in animal models.[140, 196] The mechanism by which NGF relieves dry eye symptoms remains unclear. However, Lambiase et al. and Wang et al. showed that NGF treatment *in vitro* increases MUC5Ac production from cultured conjunctival goblet cells,

which may help restore the mucin component of the tear film.[121, 197] Additionally, Chang et al. reported that increased NGF secretion induced by IL-1β correlates with decreased caspase activation, suggesting that NGF may decrease corneal epithelial cell apoptosis.[194] Based on previous studies in other systems and tissues, here it is hypothesized that NGF may also affect cytokines and other inflammatory factors produced by ocular surface epithelial cells, and so help ameliorate inflammatory responses in dry eye.

To address this hypothesis, the effects of NGF were investigated in a hyperosmolar media culture model that mimics a dry eye environment. Hyperosmolality at the ocular surface is a key characteristic of dry eye. A previous study has shown an average tear film osmolality for dry eye patients of 343 ± 32 mOsm/kg, with the highest value of 440mOsm/kg.[198] Also it was reported that 3 months after LASIK, a time when dry eye is prominent, average tear osmolality can reach 481.27 ± 67.84 mOsm/kg, with the highest value of 648 mOsm/kg.[199] Based on these data, the cell lines were cultured with 400, 450 and 500 mOsm/kg culture media to mimic the dry eye environment to study the effect of NGF on dry eye inflammation at the ocular surface. Specifically the role of NGF in modulating the expression of inflammation associated molecules including TLR4, TLR9, HLA-DR, and TGF-β1, 2 and in modulating corneal and conjunctival epithelial cell viability in a hyperosmolar environment was determined.

II. Methods

II A. Cell culture:

Simian Virus 40-transformed human corneal epithelial cells (SV40-HCECs)[200] and normal human conjunctival epithelial cells (IOBA-NHC)[201] were cultured with SHEM media (Ham's F12 and DMEM 1:1, supplemented with 10ng/ml EGF, 0.1μg/ml cholera toxin, 0.5μg/ml bovine insulin) or NHC media (Ham's F12 and DMEM 1:1, supplemented with 2ng/ml EGF, 1μg/ml bovine insulin, 0.1μg/ml Cholera toxin, 5μg/ml hydrocortisone) with 10% fetal bovine serum, and gentamicin (30μg/ml). Primary cultured (P)-HCECs prepared as previously described were grown in EpiLife media with supplement (Cascade Biologics, Portland, OR).[202] All cells were maintained in a humidified atmosphere of 95% air/5% CO_2 at 37 °C. When confluent, cells were passed using standard 0.25% trypsin/0.2% EDTA methods. P-HCECs of passages 1 to 2, SV40-HCECs of passages 19-42, and IOBA-NHCs of passages 72-82 were used in the experiments.

Hyperosmolar media (400, 450, 500 mOsm/kg) were prepared according to a previous study, by adding appropriate amounts of 1M NaCl to the serum free culture media (starting osmolalities: SHEM 369 ± 0.8 mOsm/kg, NHC 309 ± 1.5 mOsm/kg, EpiLife 295.5 ± 2.1 mOsm/kg).[203] Osmolality was measured using a Vapro 5520 pressure osmometer (Wescor, Logan, UT). To examine the effects of hyperosmolar media and NGF on expression of various inflammation associated molecules, cells were seeded into 6 well plates with 3000 cells/well and were pre-incubated for 24 hrs in serum-free media before switching to serum-free hyperosmolar media with or without the addition of 10 or 100ng/ml human β-NGF (R&D systems, Minneapolis, MN). After 24 or

48 hrs incubation the culture supernatant and cell lysate were collected and stored at -80°C until analysis.

II B. Trypan Blue exclusion test and MTT assay

After incubating SV-40 HCECs, IOBA-NHCs and P-HCECs with culture media (control or 400, 450, 500 mOsm/kg) with and without the addition of NGF (10 ng/ml or 100 ng/ml), for 24 or 48 hrs, cell viability was determined by the trypan blue exclusion test. At the end of the treatment, culture supernatant was collected then centrifuged (600 g, 2 mins) to harvest any floating cells. Adherent cells were washed once with PBS and then detached with 0.25% trypsin/0.2% EDTA. Pellets from floating and attached cells were re-suspended in PBS then pooled. Trypan Blue (10µl at 0.4%) was added to 40 µl of the pooled cell suspension. After two minutes, the total number of dead cells (blue) and live cells (unstained) were counted with a hemocytometer. Cell death was calculated by dividing the number of dead cells by the total number of cells.

MTT assays were also performed to obtain objective quantitative information about cell viability under hyperosmolar stress. Cells were plated on 96-well plates at a density of 5×10^{3} cells in 100 µL media per well. After 24 hrs incubation with 10ng/ml or 100 ng/ml NGF with or without hyperosmolar media, cell viability was measured by the reduction of 3-(4,5-dimethylthiazol-2-yl)-2,5-diphenyltetrazolium bromide (MTT, Sigma-Aldrich, San Diego, CA). MTT solution (20 µL of 5 mg/mL) was added to each well and incubated at 37 ºC for 4 hrs. The supernatant was discarded and 100 µL DMSO was added to dissolve the formazan crystals. Absorbance at 570 nm with a reference

wavelength of 680nm was measured using a Fluostar plate reader (BMG LABTECH, Cary, NC).

II C. RNA extraction and Real-time RT-PCR

Total RNA was extracted from the cells using an RNeasy Kit (Qiagen, Valencia, CA) then analysed by two–step reverse transcription-polymerase chain reaction (RT-PCR). The RT step was carried out using a Thermoscript RT kit (Invitrogen, Carlsbad, CA) using 1 μg total RNA and 1 μl oligo(dT) primers. The quantitative real-time PCR step was performed using SYBR green master mix (Stratagene, La Jolla, CA). Gene-specific primers (25 pmol) were used to detect mRNA expression of the constitutively expressed GAPDH gene as the housekeeping gene and the test genes TLR4, TLR9, HLA-DR, TGF- β 1, 2, IL-1α, IL-13, IL-16, Monocyte chemotactic protein (MCP)-1, NGF and TrkA. The primer sequences used are listed in table 4.1. Primer validation information is listed in Appendix VI. PCR amplification was performed for 40 cycles of denaturation at 94 °C (50 sec), annealing 60 °C (1 min), and primer extension at 72 °C (1 min). Comparative mRNA expression levels relative to an untreated media only control were obtained with the MxPro 3000 software. Water and no reverse transcriptase samples were used as negative controls. All primers used in this experiment were optimized for use in the experiments and all products were sequenced using traditional fluorescence methods to confirm their identity.

Table 4.1 The primer sequences used in the present experiment.

	Sequence
GAPDH	forward 5'-GCCAAGGTCATCCATGACAAC-3', reverse 5'-GTCCACCACCCTGTTGCTGTA-3
TLR4	forward 5′ - AGCCACGCATTCACAGGG -3′ , reverse 5′ - CATGGCTGGGATCAGAGTCC -3′
TLR9	forward 5′ -ACTGTTCAGCCGGAGATGTTT -3′ , reverse 5′ -TCAGGGCCTTCAGCTGGTTTC -3
HLA-DR	forward: 5'-GGGCATTCCATAGCAGAGACA-3' reverse: 5'-TGGGACCATCTTCATCATCAA-3'
TGF-β1	forward 5'- TTCAAGCAGAGTACACACAGCATA -3', reverse 5'- ACTCCGGTGACATCAAAAGATAAC -3'
TGF-β2	forward 5'- AGACTTGAGTCACAACAGACCAAC -3', reverse 5'- TATATAAGCTCAGGACCCTGCTGT -3'
NGFB	forward 5'- TACTGTGGACCCCAGGCTGT -3', reverse 5'- TCTTATCCCCAACCCACACG -3'
NTRK1	forward 5'- CTGTGCTGGCTCCAGAGGAT -3', reverse 5'- AGGAGGTTGTGGCACTCAGC -3'
IL-13[204]	forward 5'- GCCCTGGAATCCCTGATCA -3', reverse 5'- GCTCAGCATCCTCTGGGTCTT -3'
IL-16[205]	forward 5'- AAGGGGCATCTCCAACATCATCAT -3', reverse 5'- CTCCTGCCAAGCTGAACCCAAGAC -3'
IL-1α[206]	forward 5'- TGGCTCATTTTCCCTCAAAAGTTG -3', reverse 5'- AGAAATCGTGAAATCCGAAGTCAAG -3'
MCP-1[207]	forward 5'- CGCCTCCAGCATGAAAGTCT -3', reverse 5'- ATGAAGGTGGCTGCTATG -3'

II D. Western-blot for TrkA

After culturing SV40-HCECs with NGF (100 ng/ml) for 10 min or 24 hrs, cells were harvested with a single detergent lysis buffer (20 mM Tris-HCl, pH 7.5, 150 mM NaCl, and 1% NP-40 with one tablet of protease inhibitor cocktail, Sigma-Aldrich). The protein concentration in each sample was measured by a Bradford assay. Protein (20 μg) was loaded into each lane of a 10% SDS-polyacrylamide minigel and subjected to one-dimensional electrophoresis. Subsequently, the separated proteins were blotted to a PVDF membrane at 100 V for 75 mins on ice. The membrane was then blocked with 5% non-fat milk in Tris buffered saline (TBS) for 1 hr at room temperature, rinsed three times with 0.1% Tween in TBS (TTBS), and reacted with a rabbit-antihuman TrkA antibody (1:500 in 5% dry milk/TTBS, Calbiochem, San Diego, CA) or a rabbit anti-human phosphorylated TrkA antibody (1:1000 in 2% BSA/TTBS, Calbiochem) overnight. The membranes were washed in TTBS three times for 10 min each, and then incubated with horseradish peroxidase-conjugated goat anti-rabbit IgG (Jackson Laboratories, West Grove, PA, 1:5000 in 5% dry milk/TTBS or 2% BSA/TTBS) for 1 hour at room temperature. After thorough washing, the immunoreactivity was visualised by ECL detection (Amersham, Piscataway, NJ) on a x-Ray film.

II E. Flow Cytometry

The expression of TrkA in SV40-HCECs was also examined by flow cytometry. After serum starvation for 24 hrs, SV40-HCECs were incubated with 500 mOsm/kg serum free media for 24 hrs. To determine TrkA expression, cells treated with NGF (100 ng/ml) were harvested and stained with antibodies against phosphorylated TrkA and total

TrkA. For phosphorylated TrkA, cells were washed with PBS once after 24 hrs incubation with 500 mOsm/kg media and then were treated for 10 mins with NGF (100 ng/ml). For total TrkA, cells were treated simultaneously with 500mOsm/kg and/or NGF (100 ng/ml) for 24 hrs.

At the end of the treatment, cells were detached from the culture plates by incubating in PBS containing 2% EDTA for 5 mins at 37 °C. The cells were then fixed with 1% paraformaldehyde for 30 mins at room temperature, and then permeabilized with 0.2% Triton-X for 5 mins. Cells were incubated with antibodies against total TrkA and phosphorylated TrkA for 30 mins at room temperature. The antibodies were labeled with a Zenon Alexa Fluor 488 rabbit IgG antibody labeling kit (Molecular Probes, Eugene, OR) 10 mins before use. Each of the steps mentioned above was followed by two washes with PBS for 5 mins. The cells were then re-suspended in 1ml of PBS and analyzed with a BD FACSCantoII flow cytometer (BD Parmingen, San Jose, CA) and Flowjo software (TreeStar, San Carlos, CA). For each sample, 10000 events were recorded.

II F. Inflammatory Cytokine Array

Secretion of various inflammatory cytokines by SV40-HCEC was screened with a human inflammatory cytokine array kit (R&D Systems) following the instructions from the manufacturer. Briefly, human cytokine array membranes coated with 36 specific cytokine antibodies were probed with cell culture supernatants from SV40-HCECs stimulated for 24 hrs with NGF (100 ng/ml) and hyperosmolar (500 mOsm/kg) stress.

The membranes were blocked by incubating with the blocking buffer from the kit for 1.5 hrs at room temperature and then samples were added and incubated for 1hr at room temperature. The biotinylated detection antibody cocktail was then added and incubated for 1 hr at room temperature to form an "antibody-sample-antibody sandwich". HRP-conjugated streptavidin was added and membranes visualized with chemiluminescence. Average signal density for each cytokine was determined by densitometry analysis using an Alpha Imager (Alpha Innotech, San Leandro, CA), and signals were normalized to the positive control (combination of multiple IgGs provided by the manufacturer) on the same membrane.

II G. Statistical Analysis

Experiments were repeated at least three times for each cell line unless otherwise stated. Data are presented as the mean $\pm$SD of independent representative experiments in the figures. Statistical analyses were performed by MiniTab software (MiniTab 14.0) using a one-way compared by one-way ANOVA. Post hoc analysis was performed using the Student's t -test with Bon- ferroni's correction for multiple comparisons to assess the effect of hyperosmolar stress. Two-sample t-test was used to assess the effect of NGF treatment compared to corresponding controls with the same osmolality. $P < 0.05$ was considered statistically significant. The difference in cell viability with NGF and/or hyperosmolar stress was assessed using χ^2 statistics with $p < 0.01$ considered statistically significant.

III. Results

III A. NGF promoted cell survival and proliferation

Hyperosmolar stress induced morphological alterations in both IOBA-NHC and SV40-HCECs (Figure 4.1). The cells were shrunken, and the cell-cell contacts were reduced, compared with the cells maintained in media of normal osmolality. Also at the end of the treatment, more floating cells were observed with hyperosmolar stress (data not shown). NGF alone did not induce any significant morphological changes in normal osmolar media. Compared with the 500 mOsm/kg treated control, in the cells treated with NGF and hyperosmolar media the shrinkage of the cytoplasm was less severe. No obvious differences were found between the IOBA-NHC and SV40-HCECs.

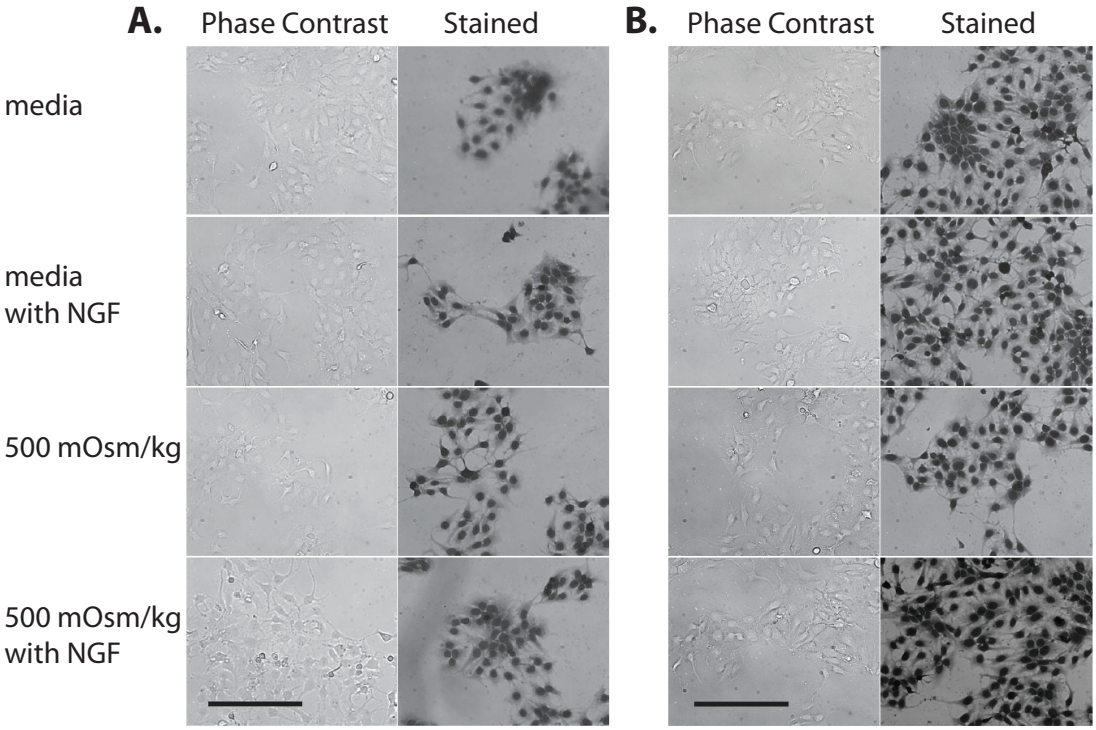
A.
Phase Contrast
Stained
B.
Phase Contrast
Stained
media
media
with NGF
500 mOsm/kg
500 mOsm/kg
with NGF

Figure 4.1 Effect of hyperosmolar media on cell morphology.

A. The left column shows phase contrast images of SV40-HCECs after 24 hrs exposure to hyperosmolar culture media (500mOsm/kg) in the absence and presence of 100 ng/ml NGF. The cells in the right column were stained with methylene blue. B. The morphology of IOBA-NHC after 24 hrs exposure to hyperosmolar culture media (500 mOsm/kg) in the absence and presence of 100 ng/ml NGF. Scale bars: 100 μm.

To determine if NGF had a protective effect against hyperosmolality induced cell death cell viability was tested using the trypan blue (TB) exclusion test and MTT assay. Data were normalized to the serum free media treated control of normal osmolality (Figure 4.2A and B). Floating cells were included for the two tests. When counted with a hemocytometer, the total number of IOBA-NHC was 1.81×10^6 in the control cultured with serum free media after 24 hrs. However, only 0.99×10^6 cells were found with 500 mOsm/kg media, indicating that about half of the cells were lost due to decreased proliferation or increased cell death under the hyperosmolar stress. The TB exclusion test indicated that the percentage of dead cells was significantly increased with 500 mOsm/kg (Figure 4.2A). When assessed by the MTT assay, the number of live IOBA-NHC with hyperosmolar stress was also decreased (Figure 4.2B). The changes observed with MTT assay were greater than with TB exclusion test. This can be likely explained by the fact that MTT assay is more sensitive than TB exclusion test. Both 10 ng/ml and 100 ng/ml NGF treatment promoted the viability of the IOBA-NHC exposed to 500 mOsm/kg stress compared to its corresponding controls (Figure 4.2A, B). By MTT assay 100ng/ml NGF was more effective (Figure 4.2B).

The TB exclusion test showed that the number of live SV40-HCECs with hyperosmolar stress was decreased by less than 10%, which was much less than with IOBA-NHC (data not shown). Similarly decreased cell viability was observed with MTT assay (Figure 4.1C). NGF also increased the percentage of viable SV40-HCECs in 500mOsm/kg compared to the hyperosmolar only control. The experiment was also repeated twice with P-HCECs, and the results confirmed a protective effect of NGF.

A.

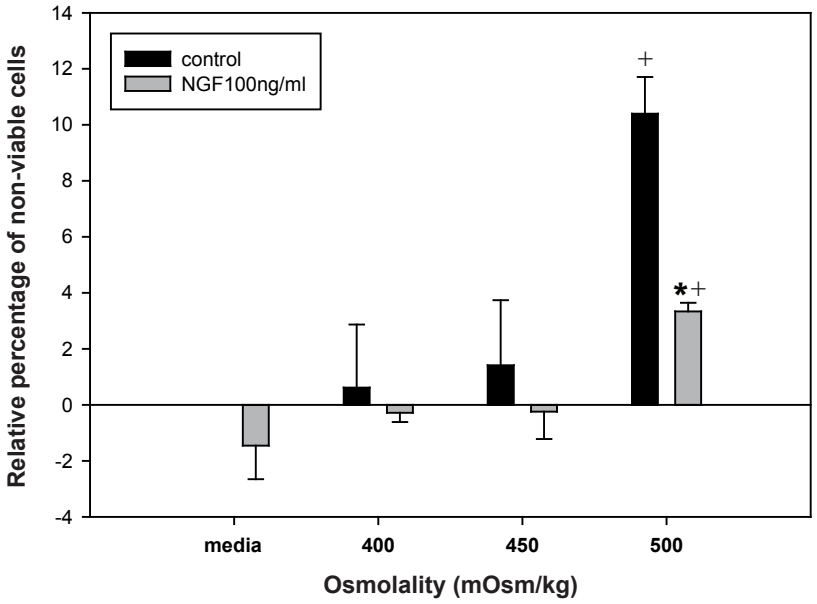
control
NGF100ng/ml
Relative percentage of non-viable cells
14
12
10
8
6
4
2
0
-2
-4
media
400
450
500
Osmolality (mOsm/kg)

B.

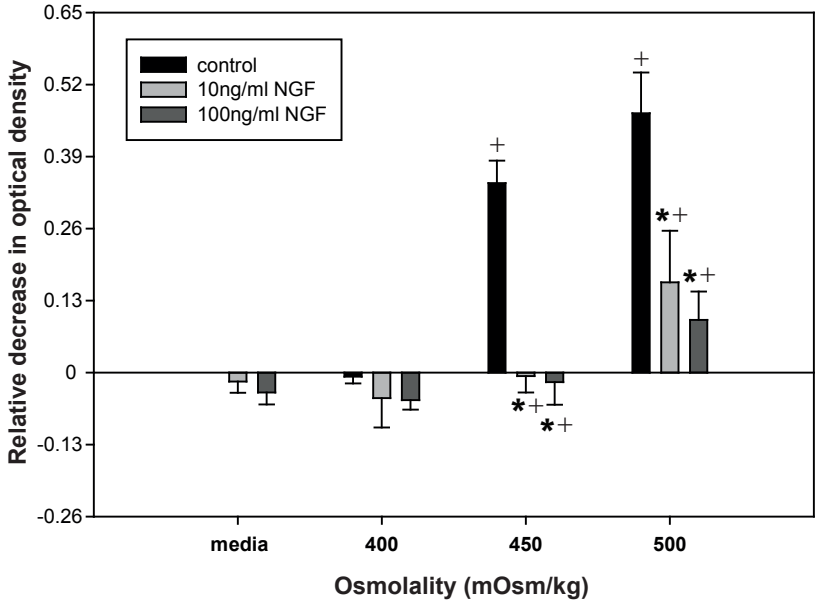
control
10ng/ml NGF
100ng/ml NGF
Relative decrease in optical density
0.65
0.52
0.39
0.26
0.13
0
-0.13
-0.26
media
400
450
500
Osmolality (mOsm/kg)

C.

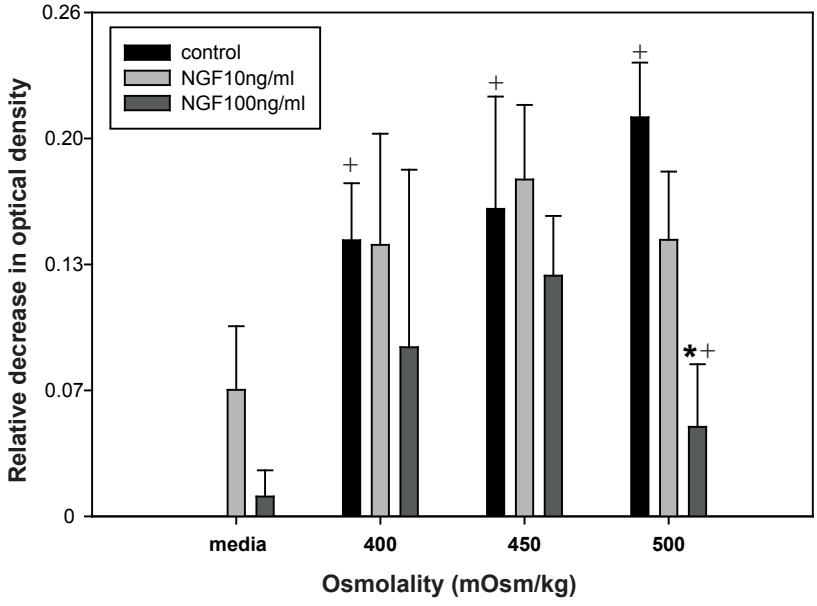
control
NGF10ng/ml
NGF100ng/ml
Relative decrease in optical density
0.26
0.20
0.13
0.07
0
media
400
450
500
Osmolality (mOsm/kg)

Figure 4.2 Protective effect of NGF against hyperosmolar stress induced cell death.

Cell viability in response to hyperosmolar media with and without NGF were tested with IOBA-NHC cells (n = 3) using the trypan blue exclusion test (A) and MTT assay (B) or with SV40-HCECs using MTT assay (C). + indicates statistical significance compared with the normal osmolality control; * indicates statistical significance compared with the control at the same osmolality (χ^2 test, $p < 0.01$).

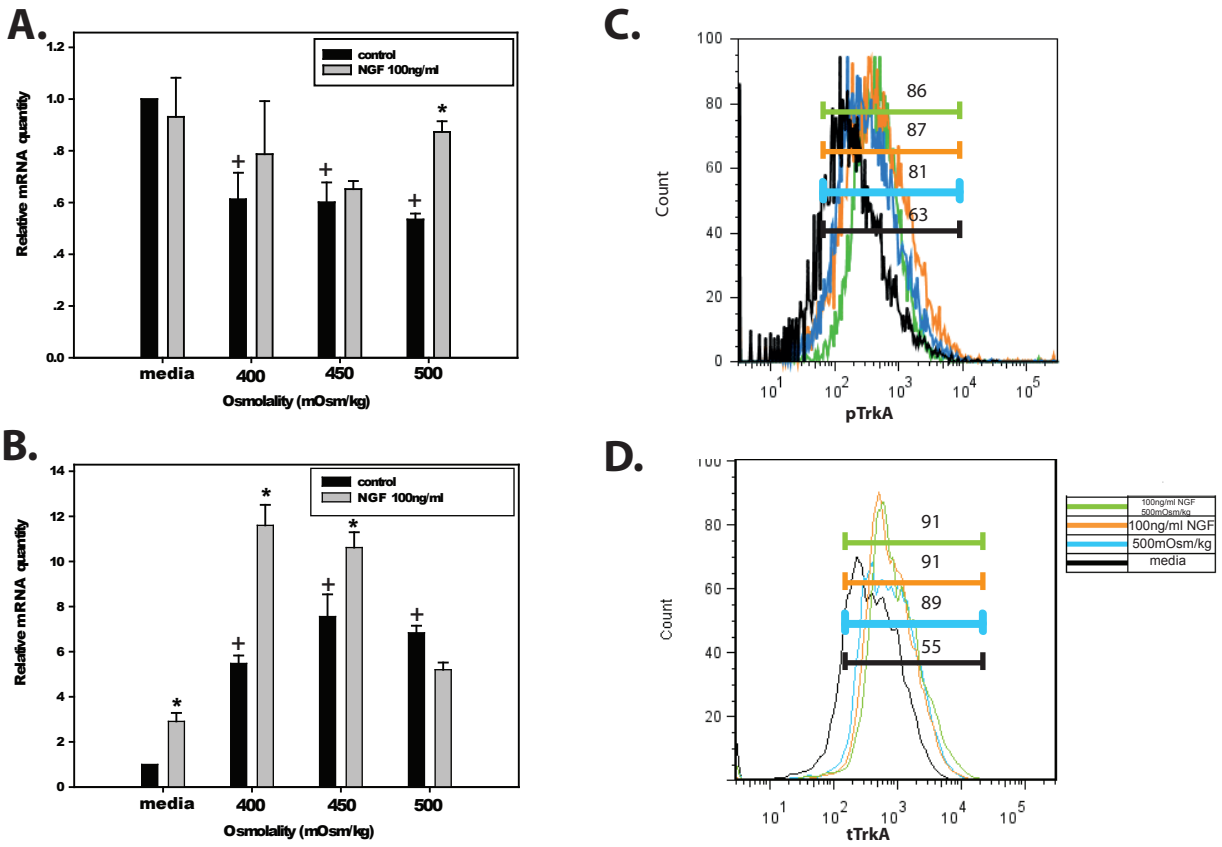
A.
control
NGF 100ng/ml
Relative mRNA quantity
media
400
450
500
Osmolality (mOsm/kg)
B.
control
NGF 100ng/ml
Relative mRNA quantity
media
400
450
500
Osmolality (mOsm/kg)
C.
Count
86
87
81
63
pTrkA
D.
Count
91
91
89
55
tTrkA
100ng/ml NGF
500mOsm/kg
media

Figure 4.3 Effect of NGF on expression of TrkA by SV40-HCECs.

NGF (A) and TrkA (B) mRNA expression by SV40-HCECs (n = 3) after being exposed to NGF (100 ng/ml) and hyperosmolar stress for 24hrs. * indicates a statistically significant difference compared to controls of the same osmolality (ANOVA and posthoc t-test with Bonferreni correction). + indicates statistical significance compared with the normal osmolality control (post hoc t-test, $p < 0.05$). C, D. Flow cytometry analysis of phosphorylated TrkA (pTrkA) (C) and total-TrkA (tTrkA) (D) when treated with hyperosmolar stress for 24 hrs. For pTrkA, NGF was added for 10 mins after pretreating the cells with 500 mOsm/kg for 24 hrs. For assessment of tTrkA, the cells were simultaneously treated with NGF and 500 mOsm/kg for 24 hrs. The experiments were repeated 3-5 times and data shown are representative of one experiment. The numbers on the plots show the percentage of the gated cells in the total cell population.

III B. Hyperosmolar stress and NGF up-regulate the expression of TrkA

It has been reported that NGF application can increase the production of NGF through a positive feedback mechanism.[208] In this experiment, NGF mRNA was expressed at base line by all cell types tested, but decreased significantly with hyperosmolar stress as shown for SV40-HCEC in Figure 4.3A. NGF treatment slightly increased NGF mRNA expression, although the effect was only statistically significant with 500 mOsm/kg. A previous study suggested that effects of NGF on promoting cell survival were mainly induced by activation of TrkA,[19] therefore the expression and phosphorylation of TrkA was studied. Hyperosmolar stress increased SV40-HCEC TrkA mRNA expression which peaked at 450 mOsm/kg (Figure 4.3B). NGF treatment also up-regulated TrkA expression compared with untreated cells and significantly enhanced the effect of 400 and 450mOsm/kg hyperosmolar media (Figure 4.3B). Comparable results were found with P-HCECs and IOBA-NHC (data not shown).

Flow cytometry was used to measure changes in phosphorylated TrkA and total TrkA in SV40-HCECs. Phosphorylated TrkA was increased after 10 mins culture with NGF (Figure 4.3C). When the cells were pre-treated with 500 mOsm/kg media for 24 hrs, phosphorylated TrkA was also increased compared with the normal osmolar control. However, 10 mins culture with NGF in the cells pre-treated with hyperosmolar stress did not change pTrkA compared with the hyperosmolar control. As shown in panel C, total TrkA was increased with hyperosmolar stress and/or NGF, but the combination of the two did not further enhance the effect. This is consistent with the RT-PCR result presented for 500mOsm/kg in Figure 4.3B. The results were also confirmed by western blot, using the same antibodies (data not shown).

III C. Effect of NGF on inflammatory molecule expression

To test the effect of NGF on the inflammatory responses in our model, the expression of inflammatory cytokines following NGF treatment was screened with an inflammatory cytokine array (Appendix V). Compared with the normal control, SV40-HCEC secretion of IL-1α, IL-13 was increased by more than 0.5 fold with exposure to 500 mOsm/kg (Figure 4.4). IFN-γ, IL-6, MCP-1, TNF-α, SDF-1, RANTES increased to less than 1.5 fold. NGF alone more than doubled IFN-γ and TNF-α, but only slightly increased or decreased the rest of the cytokines. Compared with hyperosmolar media alone, the additional presence of NGF increased the secretion of IL-1α, MCP-1, but decreased that of IL-8, IL-6, IL-16, IL-13, TNF-α, SDF-1, RANTES. The mRNA expression of IL-1α, IL-16, IL-13, PAI-1, MCP-1 was determined by real-time RT-PCR because those cytokines were altered the most in the inflammatory cytokine array. The trend in IL-1α, IL-13, MCP-1 mRNA expression was similar to that observed with the protein array (Figure 4.4), suggesting that hyperosmolar stress and NGF may affect production of those cytokines at the mRNA level. IL-16 mRNA expression, however, was increased with hyperosmolar stress and the combination of hyperosmolar media and NGF, while the protein array data, indicated that it was decreased with NGF and/or hyperosmolar stress compared with the normal osmolar control.

A.

Summary of inflammatory cytokine array (n=1)

	media	media 100ng/ml NGF	500mOsm/kg	500mOsm/kg 100ng/ml NGF
positive control	1	1	1	1
IFN-γ	0.23	0.43 (1.9)	0.31 (1.3)	0.32 (1.4)
Gro-α/CXCL-1	0.70	0.63 (0.9)	0.44 (0.6)	0.48 (0.7)
GM-CSF/CSF-2	0.34	0.23 (0.7)	0.30 (0.9)	0.42 (1.2)
CD40L/CD154	0.30	0.21 (0.7)	0.41 (1.4)	0.37 (1.2)
IL-8	0.30	-0.04 (-0.1)	0.20 (0.7)	0.16 (0.5)
IL-6	0.61	0.54 (0.9)	0.69 (1.1)	0.55 (0.9)
IL-1r	0.26	0.27 (1.0)	0.48 (1.8)	0.31 (1.2)
IL-1α	0.18	0.25 (1.4)	0.28 (1.5)	0.36 (2.0)
IL-16	0.23	0.14 (0.6)	0.16 (0.7)	0.05 (0.2)
IL-13	0.39	0.40 (1.0)	0.59 (1.5)	0.26 (0.7)
PAI-1	0.20	0.19 (1.0)	0.16 (0.8)	0.39 (2.0)
MCP-1	0.61	0.65 (1.1)	0.65 (1.1)	0.87 (1.4)
sTREM-1	0.09	0.07 (0.8)	0.08 (0.9)	-0.05 (-0.6)
TNF-α	0.09	0.18 (2.0)	0.13 (1.4)	-0.19 (-2.1)
SDF-1	0.08	0.10 (1.3)	0.11 (1.4)	-0.28 (-3.5)
RANTES	0.11	0.16 (1.5)	0.18 (1.6)	0.02
negative control	0	0	0	0

B.

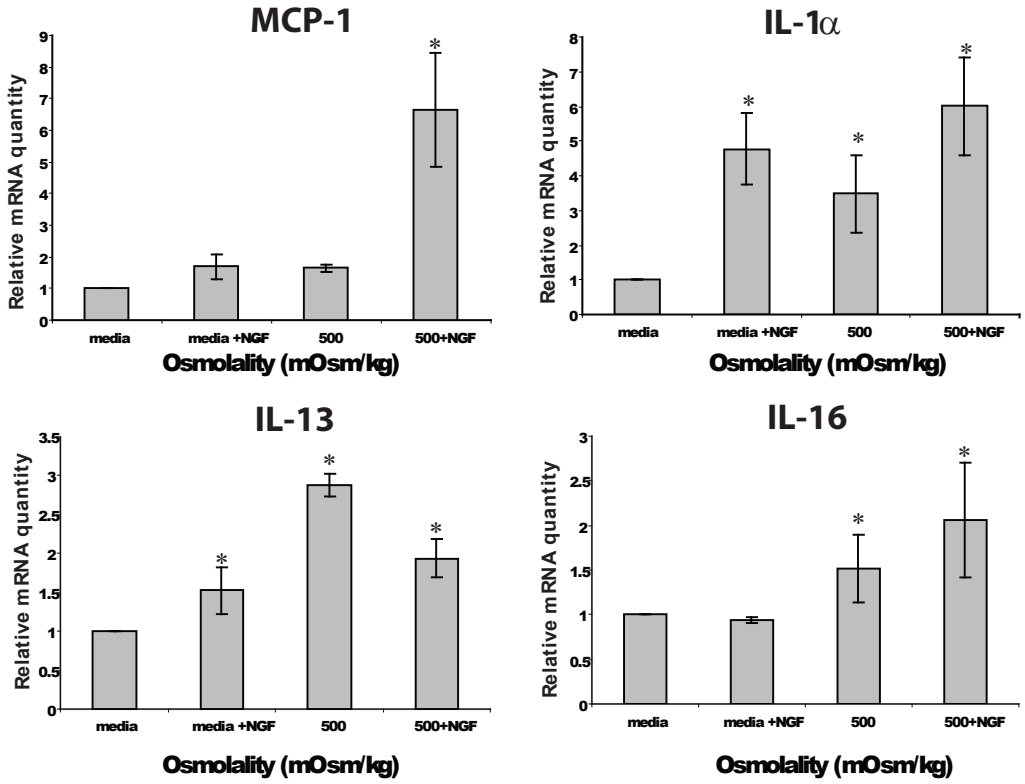

Figure 4.4 Effect of NGF on expression of inflammatory cytokines.

A. Summary of the inflammatory cytokine array findings for protein secreted into the culture media. SV40-HCECs were treated with hypersomolar (500 mOsm/kg) media and/or NGF (100 ng/ml) for 24hrs. The data shown are the averages of three densitometry measurements from one experiment. Readings from negative controls were first subtracted from the actual readings from positive controls and each cytokine, and then the readings from each cytokine was normalized to the positive controls. Numbers in parentheses are the fold changes compared with the media control. B. Expression of MCP-1, IL-13, IL-1α, and IL-16 mRNA by SV40-HCECs after 24 hrs exposure to hyperosmolar stress (500 mOsm/kg) with or without 100ng/ml NGF (n = 3). * Indicates a statistically significant difference compared to cells exposed to culture media of normal osmolality ($p<0.05$, ANOVA and posthoc t-test with Bonferoni correction).

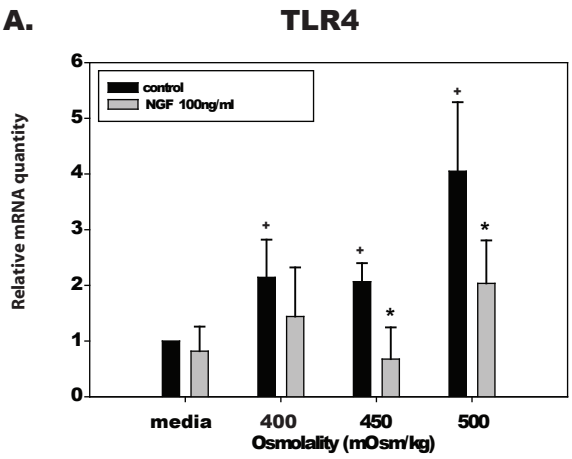
A.
TLR4
control
NGF 100ng/ml
Relative mRNA quantity
0
1
2
3
4
5
6
media
400
450
500
Osmolality (mOsm/kg)

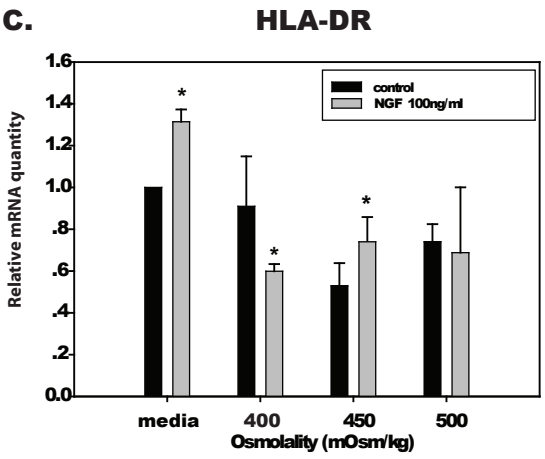
C.
HLA-DR
control
NGF 100ng/ml
Relative mRNA quantity
0.0
.2
.4
.6
.8
1.0
1.2
1.4
1.6
media
400
450
500
Osmolality (mOsm/kg)

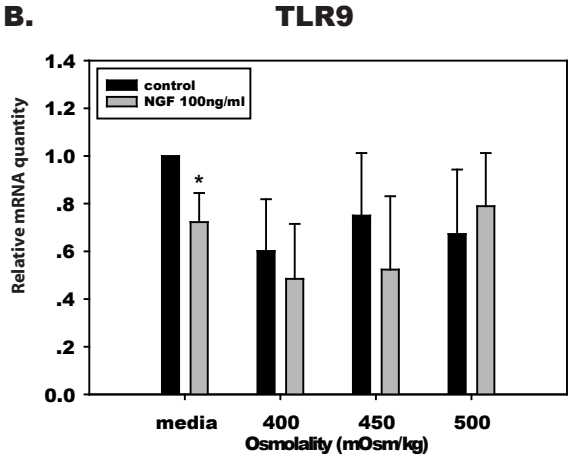
B.
TLR9
control
NGF 100ng/ml
Relative mRNA quantity
0.0
.2
.4
.6
.8
1.0
1.2
1.4
media
400
450
500
Osmolality (mOsm/kg)

Figure 4.5 Effect of NGF on mRNA expression of other inflammatory molecules. TLR4 (A), TLR9 (B) and HLA-DR (C) mRNA expression by SV40-HCECs were determined after exposure to hyperosmolar stress and/or 100ng/ml NGF for 24hrs. * indicates statistical significance compared with the control at the same osmolality (t-test, $p < 0.05$). + indicates statistical significance compared with the normal osmolality control (post hoc t-test, $p < 0.05$).

Expression of other inflammation associated molecules was also investigated in all cell lines by RT-PCR. TLR4 mRNA expression was significantly up-regulated in SV40-HCECs ($p = 0.032$, $t = 4.27$, $df = 3$, oneway ANOVA) in response to hyperosmolar stress compared to cells exposed to media of normal osmolality. NGF alone had no effect on TLR4 expression, but significantly decreased expression induced by 450 mOsm/kg and 500 mOsm/kg media. (Figure 4.5A). TLR9 (Figure 4.5B) and HLA-DR (Figure 4.5C) mRNA were down-regulated in response to hyperosmolar stress, but the effect was not statistically significant ($p = 0.29$ for TLR9, $p = 0.42$ for HLA-DR, oneway ANOVA). NGF did not have any effect on TLR9 or HLA-DR with media of different osmolality.

III D. TGF-β1 and 2 secretion was stimulated by hyperosmolar stress and NGF

Previously TGF-β was found to be up-regulated or down-regulated in response to NGF in other cells such as vessel endothelial cells and keratocytes,[118, 209-210], and was increased with dry eye. Therefore, the effect of 24 hrs incubation with NGF and hyperosmolar media on expression of TGF- β1 and β2 was assessed. Real-time RT-PCR showed that exposure of SV40-HCECs to hyperosmolar stress resulted in significantly increased mRNA expression of TGF- β1 and β2 (Figure 4.6A and 4.6C respectively). Similarly, the concentrations of TGF- β1 and β2 secreted into the culture media were increased (Figure 4.6B, 4.6D). In normal osmolar media, 100 ng/ml NGF alone did not induce any significant change in mRNA expression of either TGF- β1 or β2 and only induced a slight increase in TGF- β2 protein concentration compared to untreated controls. However on, exposure to 10 ng/ml of NGF, both TGF- β1 and β2 protein secretion were increased. When the cells were treated with hyperosmolar media and 100

ng/ml NGF together, there was no significant difference in TGF- β1 mRNA or protein secretion with 400 mOsm/kg compared to hyperosmolar media alone. However, at higher osmolalities, there was a small, but statistically significant, increase in TGF-β1 mRNA and protein expression in the additional presence of NGF ($p = 0.039$ for mRNA, $p = 0.022$ for protein, oneway ANOVA). For TGF-β2, 100 ng/ml NGF did not significantly change mRNA expression at any osmolality but protein secretion was above that stimulated by hyperosmolality media alone ($p = 0.192$ for mRNA, $p = 0.032$ for protein, oneway ANOVA). Subsequently it was observed that 10ng/ml of NGF, was more effective than 100ng/ml and induced a significant increase in both TGF- β1 and β2 secretion in all conditions. The experiments were repeated twice with P-HCECs from different donors, for which similar changes were found (data not shown).

In IOBA-NHC, TGF- β1 was similarly altered by both NGF, with 10ng/ml more effective than 100ng/ml (data not shown). TGF- β2 mRNA expression was significantly up-regulated with hyperosmolar stress ($p = 0.012$, $t = 6.324$, $df = 3$, oneway ANOVA), and slightly increased more with NGF in some conditions, although the effect was not statistically significant (Figure 4.7A). Interestingly, the concentration of TGF- β2 in the culture supernatant with and without hyperosmolar stress or NGF was too low to be detected by the ELISA kit. To test if TGF- β2 was being synthesized but not secreted, ELISA was performed on IOBA-NHC lysates (Figure 4.7B). The level of TGF-β2 in IOBA-NHC lysates increased with hyperosmolar stress ($p = 0.036$, $t = 5.28$, $df = 3$, oneway ANOVA). Both 10 ng/ml and 100 ng/ml of NGF increased the concentrations of

TGF-β2 in IOBA-NHC lysates with normal and 400 mOsm/kg media, but decreased the concentrations with 450 and 500 mOsm/kg media.

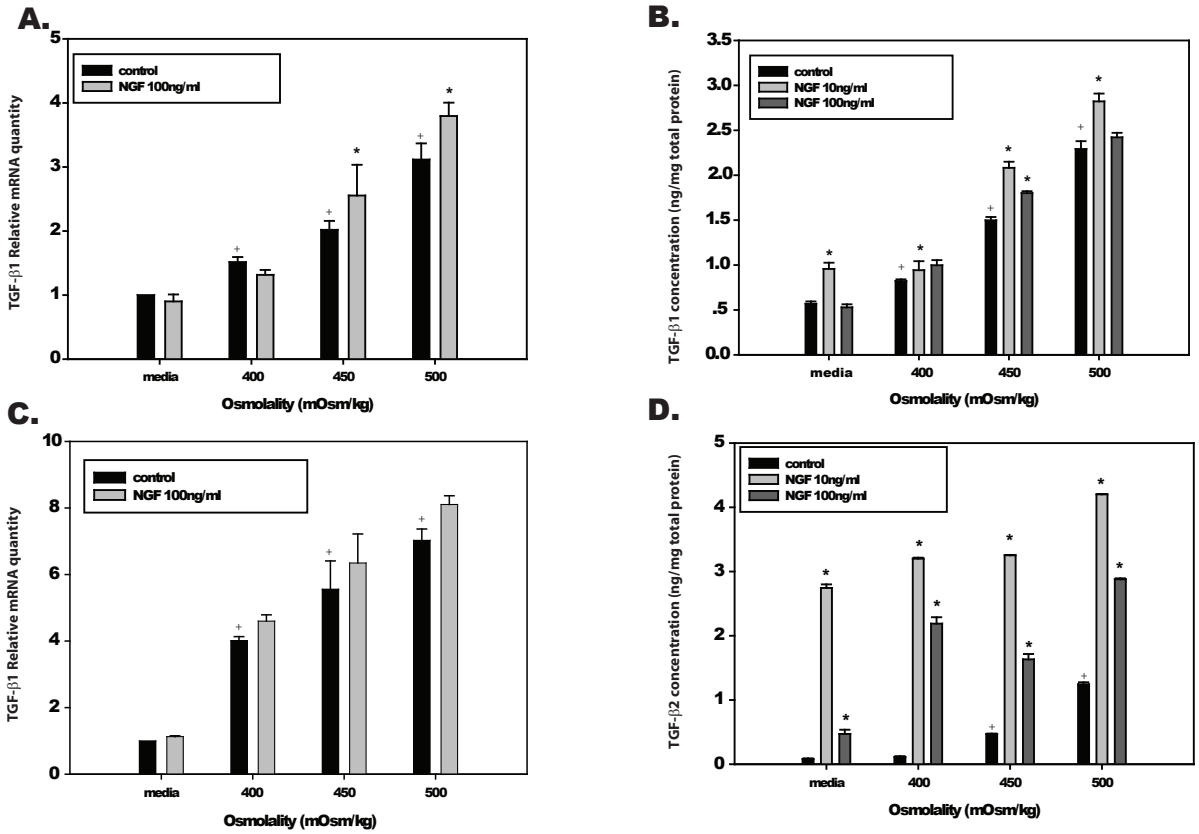
A.
control
NGF 100ng/ml
TGF-β1 Relative mRNA quantity
media
400
450
500
Osmolality (mOsm/kg)
B.
control
NGF 10ng/ml
NGF 100ng/ml
TGF-β1 concentration (ng/mg total protein)
media
400
450
500
Osmolality (mOsm/kg)
C.
control
NGF 100ng/ml
TGF-β1 Relative mRNA quantity
media
400
450
500
Osmolality (mOsm/kg)
D.
control
NGF 10ng/ml
NGF 100ng/ml
TGF-β2 concentration (ng/mg total protein)
media
400
450
500
Osmolality (mOsm/kg)

Figure 4.6 Effect of NGF on expression of TGF-β by SV40-HCEC.

TGF-β1 mRNA expression (A) and protein secretion (B) and TGF-β2 mRNA expression (C) and protein secretion (D) by SV40 -HCECs in response to hyperosmolar stress with and without 10 or 100ng/ml NGF (n = 3). * Indicates statistical significance compared with the control at the same osmolality. + Indicates statistical significance compared with the normal osmolality control ($p < 0.05$, Oneway ANOVA and post hoc t-test with Bonferonni correction).

A.

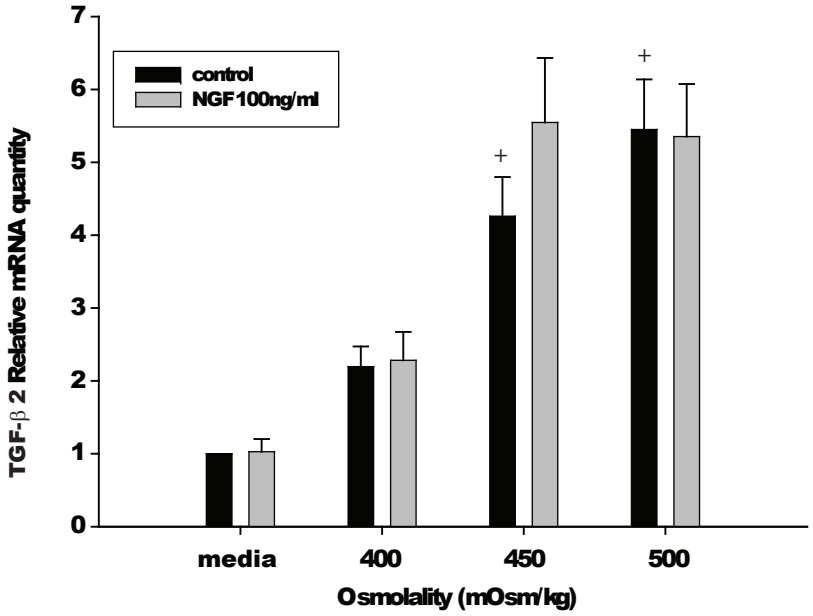
control
NGF100ng/ml
TGF-β 2 Relative mRNA quantity
0
1
2
3
4
5
6
7
+
+
media
400
450
500
Osmolality (mOsm/kg)

B.

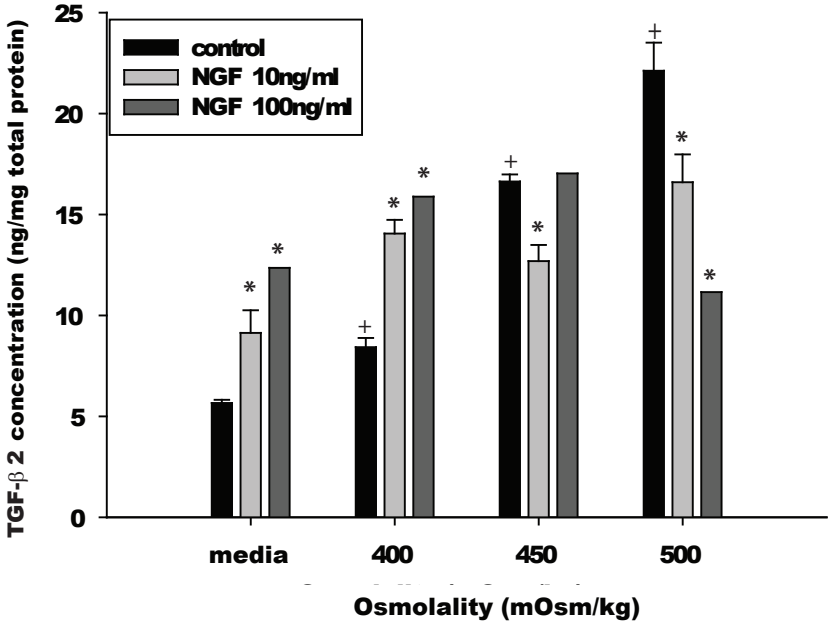
control
NGF 10ng/ml
NGF 100ng/ml
TGF-β 2 concentration (ng/mg total protein)
0
5
10
15
20
25
+
+
+
*
*
*
*
*
*
media
400
450
500
Osmolality (mOsm/kg)

Figure 4.7 Effect of NGF on expression of TGF-β2 by IOBA-NHC.

The cells were treated with NGF and/or hyperosmolar media for 24hrs. A. TGF-β2 mRNA expression (n = 3); B. TGF-β2 protein concentration in IOBA-NHC cell lysate (n = 3). * indicates statistical significance tested with paired t-test compared with the control at the same osmolality ($p < 0.05$, t-test). + indicates statistical significance compared with the normal osmolality control (post hoc t-test, $p < 0.05$).

IV. Discussion

To investigate a possible role for NGF on the structural cells at the ocular surface, particularly corneal and conjunctival epithelial cells, the effect of NGF on corneal and conjunctival epithelial cells in a hyperosmolar culture model which, in part, mimics a dry eye environment was studied. NGF was found to promote epithelial cell survival, decrease expression of some pro-inflammatory molecules such as IL-16, IL-13, TLR4 and increase TGF-β1 and 2 secretion. These results suggest that NGF can modulate the inflammatory response and facilitate epithelial proliferation and survival in response to hyperosmolar stress. Therefore NGF may play an important role in limiting ocular surface damage in inflammatory disorders such as dry eye.

The present study indicated that NGF is effective in promoting ocular surface epithelial cell survival in a hyperosmotic environment, likely through activation of TrkA, which was up-regulated with both hyperosmolar stress and NGF. This is consistent with a previous report by Lambiase et al., who showed that NGF increased corneal epithelial cell proliferation through activation of the TrkA receptor.[131] Similarly Chang et al. also reported that increased NGF production under hyperosmolar stress was related to decreased expression of Bax and caspase activities and might decrease apoptosis of corneal epithelial cells.[195] This may partially explain why NGF was reported to be beneficial for decreasing corneal surface staining in dry eye animals, corneal ulcer and enhancing wound healing after corneal surgeries.[123, 140, 196]

Previous studies have shown that inflammatory cytokines and growth factors such as IL-1β, can up-regulate the secretion of NGF.[184] However, the effect of NGF on

inflammatory responses remains unclear. It has been shown that NGF induced secretion of IL-10 from lymphocytes, and TGF-β from airway epithelial cells.[211-213] The present study showed that hyperosmolar stress increased expression of pro-inflammatory molecules such as TLR4, IL-13, IL-1 and this effect on TLR4 and IL-13 was partially blocked by NGF. Hyperosmolar stress also increased TGF- β (anti-inflammatory) expression by corneal and conjunctival epithelial cells and the effect was generally enhanced by NGF. Since most of the tested molecules are altered in inflammation at the ocular surface, it is possible that NGF may be anti-inflammatory at the ocular surface in dry eye.[214-217] However, MCP-1 and IL-1α mRNA and protein produced by SV40-HCECs under hyperosmolar stress were up-regulated by NGF, showing that NGF can also increase expression of some pro-inflammatory cytokines. Overall, NGF may regulate the inflammatory cytokines in dry eye, but its effect appears to be complex depending on the affected cytokines. The regulatory role of NGF on inflammatory cytokines may also contribute to its observed effect on enhancing wound healing and restroring normal corneal structure in previous patients and animal models.[123, 140, 196]

Both corneal and conjunctival epithelial cells were studied in the current experiment. The two cell types were treated with the same hyperosmolar stress. However, the largest alterations in TGF- β and TLR4 with NGF occurred at 450 mOsm/kg for IOBA-NHC, while the largest effect occurred at 500 mOsm/kg for SV40-HCECs. This could be explained by the difference in baseline osmolality of the two types of culture media, as the baseline osmolality of IOBA-NHC media is 60 mOsm/kg lower than the baseline osmolality of SHEM media for culture of SV40-HCECs. Thus, 500 mOsm/kg

was a relatively stronger stress on the NHC cells. Similarly, a significant amount of IOBA-NHC cell death was observed at 500mOsm/kg, but this was not the case for SV40-HCECs.

TGF-β2 mRNA expression and protein content were increased in the NHC cell lysates with NGF and/or hyperosmolar stress, but the concentration of secreted protein in the culture supernatant was not increased. Although the precise reason is unknown, one possible explanation would be that some key enzymes of the TGF-β2 secretion pathway were not increased with NGF,[218] therefore TGF-β2 could not be released. The secreted TGF-β2 molecule is composed of two identical disulfide-linked polypeptide chains which undergo cleavage and post-translational processing steps before secretion.[219] These steps are regulated by factors such as stress proteins, and plasmin.[220-221] However, there is no direct evidence in the literature regarding NGF modulation of these processes. However, in this experiment only the IOBA-NHC cell line was tested. Although this is a good model of studying conjunctival epithelial cells, this cell line may have some previously unidentified secretory deficits.[222] It will be important to test whether primary cultured conjunctival epithelial cells respond similarly.

The present study tested two commonly used concentrations of NGF for *in vitro* experiments: 10 and 100 ng/ml.[195] The effect of different concentrations (0.5 ng/ml to 200 ng/ml, data not shown) of NGF on TLR4, HLA-DR expression and cell survival was also tested. In this assay, 10 ng/ml was most effective in decreasing TLR4 expression in all tested cell lines, while 100 ng/ml was most effective in promoting cell survival.

Consistent with the current experiment, Sornelli et al. reported that 10 ng/ml of NGF was more effective in stimulating VEGF secretion than 100 ng/ml, when tested with corneal endothelial cells.[223] For cell viability, Lambiase et al. found that 100ng/ml of NGF increased corneal epithelial cell proliferation *in vitro*.[131] One possible explanation is that the regulatory effect of NGF on cytokines was saturated at 10ng/ml, similar to what Storm et al. found with PC12 cells.[224] With 100 ng/ml NGF, the altered cytokines may inhibit further activation of TrkA and the subsequent regulatory effect.[224] The effect of NGF on cell survival, however, may function through a different pathway and was not saturated at lower concentration.[225] Another possible explanation is that p75, a receptor with low affinity for NGF that was not specifically investigated in this experiment, was also altered and this subsequently affected the secretion of inflammatory cytokines and cell apoptosis.[226] High and low concentrations of NGF may activate similar downstream signaling pathways, therefore induce similar amount of cell apoptosis.[227] However, the effect of NGF on epithelial cell proliferation was dose-dependent so a higher concentration was more effective for cell viability.[131]

In conclusion, the study confirmed that NGF might play an anti-inflammatory role at the ocular surface and protect corneal and conjunctival epithelial barrier integrity in a dry eye environment. Therefore NGF may be useful in the treatment of dry eye.

Chapter 5. Nerve Growth Factor Induced Migration and Differentiation of Monocytic Lineage Cells *In Vivo* and *In Vitro*

I. Introduction

Circulating monocytic lineage cells migrate to peripheral tissues where they participate in the regulation of infection, inflammation, and wound healing.[18] For migration of these cells, expression of chemokines and local adhesion molecules are essential.[228-229] Knowledge of molecules involved in monocyte migration into peripheral tissues is rapidly increasing, however, the expression pattern of chemokines for recruitment of monocytic lineage cells in the cornea, and the effect of each chemokine remains unclear.

In mice, cells of the monocytic lineage originate from bone marrow hematopoetic stem cells (HSC).[5, [230] As shown by Randolph, et al. and Geissman et al., HSCs give rise to monocyte derived progenitor cells (MDP) which are primarily identified as CD115+ (macrophage colony stimulating factor 1 receptor), CD117 (C-kit receptor)^{low}, and CX3CR1+ (fractalkine receptor).[108-109, 231] MDPs enter the circulation and differentiate initially into CD11b+CD115+Gr (granulocyte receptor)1^{high} (classic) and then CD11b+CD115+Gr1^{low} (non-classic) subpopulations.[232] The non-classic subtype monocytes have also been considered as "resident" or "pro-inflammatory" as they produced lower amount of cytokines such as IL-10 in response to TLR4 agonists and do not respond to traditional chemokines such as MCP-1.[109, 232-233] In contrast, the classic subtype has been considered "inflammatory" as they respond to MCP-1, the most

important chemokine for monocytic lineage cells, and are rapidly recruited to sites of inflammation.[231] Depending upon the species, the percentage of $Gr1^{high}$ and $Gr1^{low}$ subpopulations in the blood is different. In humans, the classic population represents approximately 90%, whereas in mouse, only 50% is $Gr1^{high}$.[232, 234] MDPs may also remain undifferentiated in the circulation and may be trapped in terminal lymphoid organs and differentiate into plasmacytoid dendritic cells (pDC)s which were identified as conventional DCs which are CD11c+CD11b+CD4+ or CD11c+CD11b+CD8α+.[232, 235] The classic subtype, at a site of inflammation, may differentiate into CD115+CD11b+$Gr1^{high}$ inflammatory DCs or macrophages.[231, 236-237] The non-classic subtype, in peripheral tissues and spleen red pulp, may further differentiate into macrophages, Langerhans cells, and microglial cells.[236] A very small percentage of HSCs (less than 1%) may also directly enter the circulation and differentiate into resident DCs.[237] In this chapter, the term monocytic lineage cells refers to all cells that are derived from MDPs. The expression of markers used to define and characterize the cells is summarized in Appendix I. The cell types are summarized in Appendix II and Figure 5.1.

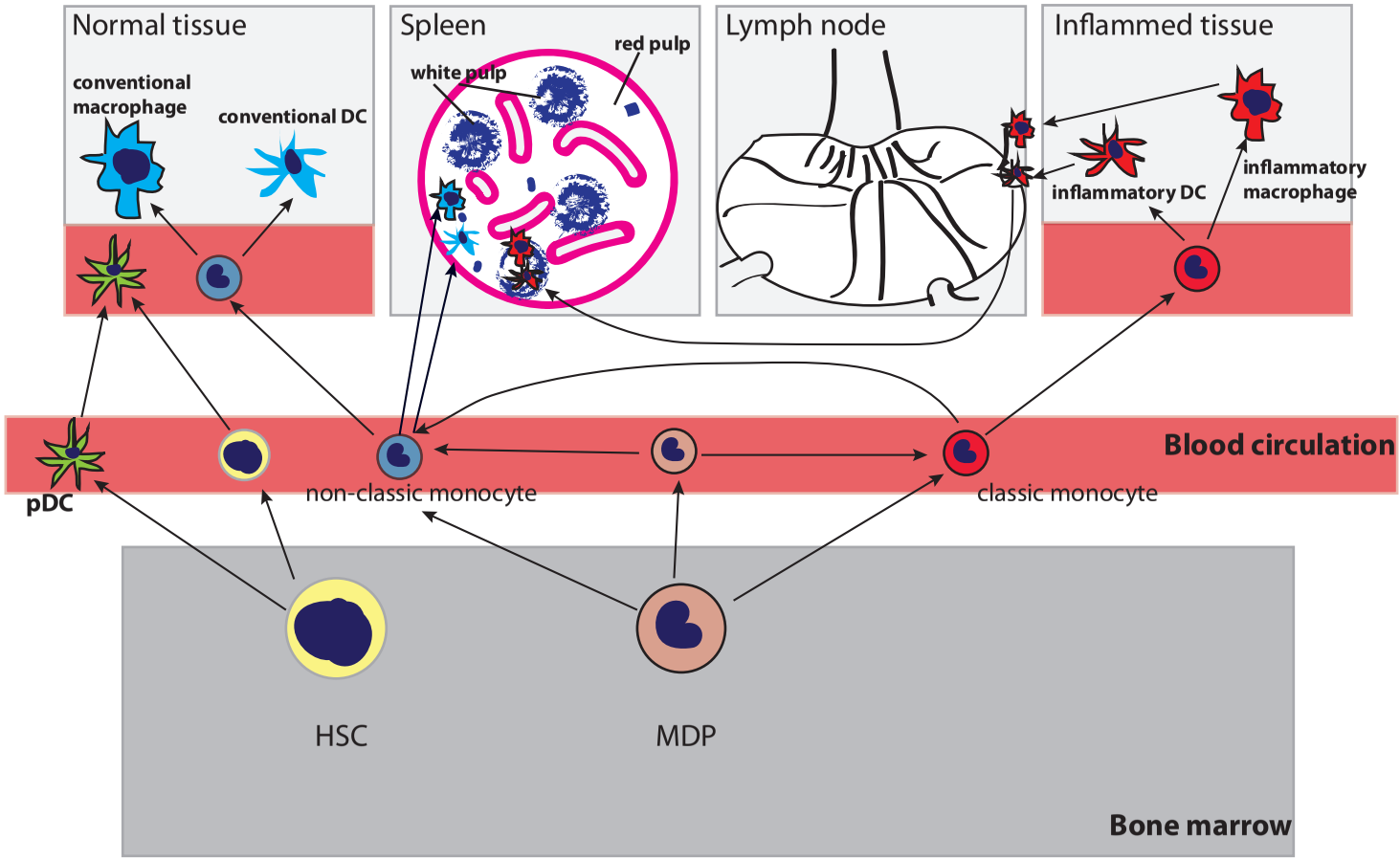
Normal tissue
conventional macrophage
conventional DC
Spleen
red pulp
white pulp
Lymph node
Inflammed tissue
inflammatory DC
inflammatory macrophage
Blood circulation
pDC
non-classic monocyte
classic monocyte
HSC
MDP
Bone marrow

Figure 5.1 Schematic for the differentiation process of monocytic lineage cells in the body.

HSC: hematopetic stem cells; MDP: monocyte derived progenitor cells; DC: dendritic cells; pDC: plasmacytoid dendritic cells.

Each subpopulation of monocytic lineage cells is equipped with specific chemokine receptors and adhesion molecules for the purpose of trafficking from blood to peripheral tissues.[238] Traditional chemokines, such as monocyte chemotactic protein-1 (MCP-1), mainly interact with the classic subtype only and do not have any effect on the non-classic subtype.[233] The non-classic subtype responds to other factors such as prostaglandin E2 and migrates to terminal tissues.[239] Although nerve growth factor has been shown to induce migration of monocytic lineage cells, it is not clear if NGF is specific for one subpopulation or not.[98]

Besides its effect on nervous system and structural cells, NGF has been identified as a pleiotropic factor which induces migration, proliferation, differentiation and apoptosis of immune cells.[76, 94] NGF may function as a key mediator between different tissues and regulate the crosstalk between nervous system and inflammatory and immune responses.[19] Expression of TrkA and p75 has been identified both on human and mouse blood monocytes.[99, 114, 240] However, the function of NGF on monocytic lineage cells is poorly understood. Kobayashi et al. showed that NGF induced migration of murine peritoneal macrophages *in vitro*;[98] but it is unclear if NGF has the same effect on other type of monocytic lineage cells.

Recently significant numbers of monocytic lineage cells were observed in the normal cornea and the number of cells increased profoundly with inflammation and immune responses.[However, the chemokines regulating the trafficking of monocytic lineage cells in the cornea are not known. Since migration of monocytic lineage cells is

very important for their physiologic and pathophysiologic function in the cornea, the effect of exogenous NGF on recruiting monocytic lineage cells was investigated. This study gives insight into the potential mechanism of NGF in regulating corneal immune responses and therefore in clinical therapy to enhance wound healing and resolve inflammation.

II. Methods

II A. Animals:

For this study, 8 to 14-week-old C57BL/6 mice (The Jackson laboratory, Bar Harbor, Maine, or from the UHCO breeding facility) were used. All protocols were approved by the University of Houston Animal Care and Use Committee, and all animal procedures followed the ARVO Statement for the use of animals in Ophthalmic and Vision Research. Mice were anesthetized using a mixture of ketamine and xylazine (120 and 20 mg/kg body weight, respectively) (Butler, Columbus, OH) via intraperitoneal injection before intrastromal injection was performed. For other procedures, mice were anesthetized using 3% isoflurane (Nicholas, San Diego, CA). Cells from 12 to 18-week-old transgenic mice expressing green fluorescent-protein linked to the actin promoter were obtained as a gift from Dr. Alan Burns (UHCO/Baylor College of Medicine, Houston, TX).

II B. Antibodies and chemicals:

The antibodies used were summarized in Table 5.1. Other chemicals used in the experiments included: NGF (mouse β NGF) and MCP-1 (both from R&D systems, San Diego, CA), GM-CSF and IL-4 (both gifts from Dr. Dequan Li, Baylor College of Medicine, Houston, TX) and fibronectin (BDPharmingen, San Diego, CA).

Table 5.1 Antibodies used for Chapter 5.

Antigen	Conjugate	Host	Manufacturer	Dilution	Catalog NO.
Mouse CD115	PE	rat	eBioscience	5μg/ml	12-1152
Rat IgG	PE	rat	eBioscience	5μg/ml	12-4321
Mouse CD11c	purified	mouse	R&D system	10μg/ml	MAB1777
Mouse IAd	purified	C57 mouse	BDPharmingen	10μg/ml	552857
Mouse IgG	purified	mouse	BDPharmingen	10μg/ml	559073
Mouse NGF	purified	rabbit	Noviscience	5μg/ml	431985
Mouse CD3	FITC	rat	BDPharmingen	5μg/ml	553239
Mouse F4/80	FITC	rat	eBioscience	10μg/ml	114801
Mouse IgG	FITC	rat	BDPharmingen	10μg/ml	556650
Mouse B220	biotin	rat	BDPharmingen	5μg/ml	553085
Mouse CD4	biotin	rat	BDPharmingen	5μg/ml	550280
Mouse CD8	biotin	rat	BDPharmingen	5μg/ml	555365
Mouse Thy1.1	FITC	goat	BDPharmingen	10μg/ml	555594
Mouse Thy1.2	PE	goat	BDPharmingen	10μg/ml	553014
Mouse β3-tubulin	purified	rabbit	Gift from Dr. Li Zhijie	4μg/ml	560340
Mouse CD11b	FITC	rat	BDPharmingen	10μg/ml	550282

II C. Cell isolation:

Mouse whole blood anticoagulated with 0.2% EDTA/PBS was obtained by cardiac puncture. Red blood cells were eliminated by adding 1 ml of RBC lysis buffer (Sigma-Aldrich, Carlsbad, CA) per 10^7 cells for 1 min. Monocyte lineage cells were enriched from peripheral blood with a continuous Percoll (GE Healthcare, Piscataway, NJ) density gradient (72, 67, 58, 50%), The upper-most monocyte band was collected using a syringe and cells washed with PBS for 1 min. For the density gradient enrichment, the cell suspension was firstly washed with 0.9% sodium chloride, and then centrifuged for 35 min at 2,200 rpm. The pellet of enriched cells was then suspended in cell staining buffer (PBS with 4% heat inactivated fetal calf serum, 0.1% sodium azide) on ice. The total cell number was determined using a hemocytometer and further purified using an immunomagnetic bead method. Briefly, the cells were diluted to a final concentration of $1\sim2\times10^7$ cells/ml with cell staining buffer and blocked with anti-CD16/32 Fc blocker for 15 mins on ice. Then the cells were incubated with biotinylated antibodies against CD4, CD8 and B220 for 20 mins on ice. The concentration of Fc blocker and antibodies used was 2.5 $\mu g/10^7$ cells. Then the cells were incubated with streptavidin particles at a concentration of 50 $\mu l/10^7$ cells for 30 mins at 4 °C. After each step the cells were washed with IMag buffer (PBS with 0.5% BSA, 2 mM EDTA, and 0.1% sodium azide) for 2 mins. The cells were suspended in RPMI-1640 media at a final concentration of $1\sim2\times10^7$ cells/ml and placed on the IMagnet for 8 mins at room temperature. After that the cells in suspension (purified monocytic lineage cells) were collected and maintained in RPMI-1640 media at room temperature for further experiments within 4 hrs.

Monocyte lineage cells were also obtained by peritoneal lavage after thioglycollate injection and from the spleen. To obtain cells from the peritoneal cavity, 1 ml sterile 3% thioglycollate (suspended in PBS and autoclaved) was injected intra-peritoneally. Five days after the injection, 5 ml PBS was injected into the peritoneal cavity. The peritoneal fluid containing extravasated macrophages was then drained with a 19-gauge needle. For isolation of monocytic lineage cells from the spleen, the mice were euthanized and the spleen removed. The adipose tissue and splenic vessels were carefully dissected out. Then the spleen was teased apart with forceps and washed twice with 0.2% EDTA/PBS. The wash fluid was collected and then filtered with a 40 μm filter. Cells collected by peritoneal lavage and from the spleen were then subjected to the isolation procedures described above for peripheral blood.

Wright staining was used to identify different types of leukocytes in whole blood smears. Briefly, a thick blood smear was made using fresh murine peripheral blood and fixed with methanol for 1 min. The slide was placed in hematoxylin for 20 secs followed by methylene blue for 6 secs. Each step was followed by washing in deionized water for 1min. The stained slide was then observed using a light microscope (Olympus BX51, Mountain View, CA).

II D. Non-specific esterase staining:

Non-specific esterase staining was performed following the manufacturer's instruction (Sigma-Aldrich, San Francisco, CA). For isolated cells, a smear slide of the sample was first made and fixed with methanol for 1 min, washed with deionized water,

then incubated with a pre-made mixture of 1 ml sodium nitrite solution, 1 ml fast blue base solution, 40 ml deionized water and 5 ml Trizmal buffer concentrate and 1 ml α-Naphthyl Acetate Solution at 37^{o}C for 30 mins. At the end of this incubation, the slides were then washed with running deionized water for 2 mins, and imaged using a light microscope (Olympus BX51, Mountain View, CA).

II E. *In vitro* migration assay:

The effect of NGF on migration of monocytic lineage cells was assessed using blind-well chambers. After resuspension in 1% BSA/DMEM media (25,000 cells/200 μl) monocytic lineage cells were placed in the top of each chamber, two replicates/condition. Migration through a nitrocellulose membrane with 5μm pores (Neuroprobe Inc., Gaithersburg, MD) was evaluated with different concentrations of NGF (1~200 ng/ml) in the bottom of the chambers for 3hrs at 37 °C. Positive controls were 2 % fibronectin or 5 ng/ml MCP-1. Media alone was used as the control. At the end of the incubation, the cells that remained in the top chamber were discarded and the top of the migration membranes was carefully cleaned to remove non-migrated cells. Then the membranes were fixed with methanol for 1min, followed with hematoxylin for 20 secs, and methylene blue for 6 secs. Three high power fields under a 40X objective (Olympus BX51, Mountain View, CA) in the center of each membrane were randomly picked and the total number of cells in each field was recorded.

To assess if the effect of NGF is specific to one subtype of monocytic lineage cells, the freshly isolated peritoneal macrophages or blood monocytes were cultured with

5% FBS for 4 hrs before the migration assay, then the cells were washed twice with PBS. Under these conditions, the surface antigen lost during the isolation process may be partially recovered to baseline level.[241] Immediately after the migration assay, the migration membranes were fixed with 1% paraformaldehyde at 4^{o}C overnight. Then the migration membranes were blocked with 2% BSA/PBS for 30 mins at room temperature before incubating with conjugated antibodies against CD11c, CD11b, IAb and F4/80 at 4 ^{o}C overnight. Finally the membranes were washed and mounted using airvol (a gift from Dr. A. Burns).

II F. NGF treatment *in vitro* and *in vivo*

To investigate the effect of NGF on monocyte differentiation, isolated blood monocytes were first cultured with RPMI-1640 media supplemented with 5% FBS overnight. Then the cells were treated with 100ng/ml NGF in 5% FBS/DMEM media for 24 hrs. At the end of the treatment, the cells were washed once with cold PBS and then stained immediately with antibodies against Ly6C, F4/80, CD11c as described later in the immunohistochemistry section. The combination of GM-CSF (2 ng/ml) and IL-4 (10ng/ml) were used as the positive control and media with 5% FBS was used as negative control.

To determine the effect of NGF on the status of monocytic cells *in vivo*, NGF was intrastromally injected into the mouse cornea. Briefly, 2 µl of NGF (1mg/ml) or the same amount of PBS was intrastromally injected into the corneas of anasesthetised animals. The injections were performed in the superior temporal quadrants of the right eye of each

animal. Immediately after injection, the ocular surface was washed with 0.5 ml of PBS. The animals were euthanised four hours after the injection, and the corneas were dissected for staining with antibodies against CD11b, CD11c, CD115 and Ly6C, Ly6G by flow cytometry as described below to measure the total number of monocytic lineage cells.

II G. Flow cytometric analysis of monocytic lineage cells

At the end of the NGF treatment, the cultured blood monocytes were collected and washed with cold PBS. Then the cells were incubated with 2% BSA/PBS for 15 mins to block nonspecific binding before incubating for 20 mins on ice with antibodies against CD11b (5 μg/ml), CD11c (10 μg/ml), CD115 (5 μg/ml) and Ly6C (10 μg/ml) to label all monocytic lineage cells. Labeled cells were washed with cold PBS twice and fixed with 0.5% paraformaldehyde before being analysed on a FACSCanto II flow cytometer (BD Biosciences, San Diego, CA). Analysis of the flow cytometry data was performed with Flowjo software (Flowjo, Boston, MA).

To assess monocytic lineage cells in the cornea, corneas were collected and the limbus was trimmed off 4 hrs after NGF intrastromal injection. Then the whole corneas were incubated with 20 mM EDTA/PBS for 30 mins at 37 °C before removing the epithelium with forceps. The endothelium was removed and discarded. Then epithelium and stromal samples were digested separately with collagenase (20 U/cornea, Sigma, St. Louis, MO) at 37 °C until a single cell suspension was obtained. Then DMEM media containing 10% FBS was added and the samples were filtered with a 40 μm filter (BD

Biosciences, San Diego, CA). The percentage of CD11c, Ly6C, MHC-II and CD115 positive cells in the epithelium and in the stroma was determined by flow cytometry as described above.

II H. Confocal analysis of corneas after subconjunctival injection of GFP expressing monocytes

Blood monocytic lineage cells were isolated from mice expressing the green fluorescent protein (GFP)-actin fusion gene. NGF or PBS intrastromal injection was performed on wild-type C57BL/6 mice as described above. Immediately following NGF injection, freshly isolated blood monocytes from GFP mice or normal wild-type mice were subconjunctivally injected into the same eye (4000 cells/50 μl of PBS). The animals were imaged 4 hrs post injection using a laser scanning in vivo confocal microscope with a Heidelberg Retina Tomograph II Rostock Cornea Module (HRT II/RCM; Heidelberg Engineering®, Heidelberg, Germany). A diode laser with a wavelength of 670 nm was used as the laser source. The images resolution was 384×384 pixels, covering 400×400 μm with transverse and longitudinal optical resolution of 2 μm and 4 μm, respectively, and an acquisition time of 0.024 s. Mice were anesthetized, a drop of gel was placed at the tip of the objective lens, and images of each layer of the cornea from epithelium to endothelium were recorded by focusing the microscope from anterior to posterior in the center of the cornea.

II I. Immunohistochemistry for corneal monocytic lineage cells

At 4 and 24 hrs after NGF intrastromal injection, animals were euthanized and the corneas collected. Full-thickness corneas were fixed in 1% paraformaldehyde for 1 hr on ice and then permeabilized with 0.02% Triton in PBS. To block non-specific staining, the tissues were incubated with 2% BSA/0.02% Triton-X/PBS for 1 hr at room temperature and anti- CD16/CD32 Fc blocker for 30 mins. Thereafter, the corneas were incubated with primary antibodies or isotype control antibodies overnight at 4^{o}C. If necessary, the tissues were then incubated with secondary antibodies for 1 hr at room temperature. Each step was followed by three thorough washings in PBS for 5 mins each. Finally, the corneas were mounted using Airvol with DAPI and examined using a Delta-Vision microscope (Delta-vision Spectrus, Applied Precision, Issaquah, WA). For each cornea, the expression of CD11c (10 μg/ml), Ly6C (10 μg/ml), Ly6G (4 μg/ml), MHC-II (10 μg/ml), CD115 (5 μg/ml), Thy1.1 (5 μg/ml), Thy1.2 (10 μg/ml) and β3-tubulin(4 μg/ml) was assessed separately in the periphery, paralimbal, para-central and central cornea. For CD11c, a FITC-conjugated goat-anti-mouse IgG was used as a secondary antibody. The remaining antibodies were conjugated directly to flurochromes.

II J. MCP-1 ELISA

For analysis of MCP-1 following *in vivo* injection of NGF, the mouse corneas were dissected and epithelium and stroma separated by incubating with 20 mM EDTA/PBS for 30 min at 37^{o}C. Then the samples were placed in Triton X-100 buffer: 50 mmol/L HEPES, 150 mmol/L NaCl, 1% Triton-X-100, 10% glycerol, 1 mmol phenylmethyl sulfonyl fluoride, 10 μg/ml aprotinin 10 μg/ml leupeptin, 1 mmol/L sodium orthovanadate. The samples were then homogenized and stored at -80 °C until

the ELISA for MCP-1 was performed following the manufacturer's instructions (R&D systems, San Francisco, CA).

II K. Keratocyte isolation and treatment

Murine keratocytes were isolated and cultured as previously described.[242] Briefly, corneas were dissected from the euthanized mice and the iris was removed. Then the corneas were cut into pieces and digested with collagenase (20 U/cornea, Sigma, St. Louis, MO) until a single cell suspension was obtained. Then the cell suspension was washed with serum free DMEM media twice, incubated with antibodies against PECAM and E-Cadherin for 15 mins at room temperature and then feritin particles for 15 mins at room temperature. Cells were then passed through a magnetic column (BD Biosciences, San Diego, CA) to negatively select out the epithelial cells and endothelial cells. The cells that flowed through the column were washed with PBS twice and cultured at 37^{o}C.

II L. Data analysis

For each antibody staining study, tissues samples from three to five mice were examined. For flow cytometric studies, at least three repeats were performed for each condition. Analysis of the difference between the number of marker positive cells in the PBS and NGF treated corneas was performed with Student's *t*-test or multiple comparison test. $P < 0.05$ was considered significant.

III. Results

III A. Purity of isolated monocytic lineage cells

To determine the purity of the cells isolated using the method described, the percentage of monocytic lineage cells in peripheral blood (Figure 5.2) and peritoneal lavage fluid (Figure 5.2) was first determined using flow cytometry. At each stages of the isolation process, staining for CD115+, F4/80+, and CD11c was used to distinguish monocytic lineage cells from other cell types. Also, in peripheral blood, neutrophils, monocytes and lymphocytes can be distinguished in flow cytometry by their distinct properties on forward scatter (FSC) and side scatter (SSC).[232] Consistent with previous reports, staining for CD115, CD11c and F4/80 was then analyzed by flow cytometry to confirm the cell types (Figure 5.2 B, second and third panel). 4% of the peripheral blood leukocytes were monocytes, and about 45% (1.7% of the whole blood leukocytes divided by the percentage for monocytes, 4%) of the monocytes were positive for CD11c (Figure 5.2 second and third panel). FSC and SSC showed that only 4% of the mouse peripheral blood leukocytes, after lysis of red blood cells, were monocytes (Figure 5.2 B, first panel), whereas 33% of the peritoneal lavage cells were macrophages (Figure 5.3, first panel). Only minimal F4/80 staining was found. In the peritoneal lavage fluid, 33% of the cells were macrophages based on their FSC and SSC properties and 26% of all the cells were F4/80 positive.

To determine the purity of isolated cells, the percentage of lymphocytes that remained after the isolation process was determined based on staining for CD3. Monocytes were identified using CD115. Density gradients have been widely used in the

isolation of blood leukocytes. However, here using a density gradient only 38%~40% of the cell fraction isolated from peripheral blood was found to be CD115+CD3- monocytes. 60% were CD115-CD3+ lymphocytes, and less than 1% were neutrophils based on the flow cytometry FSC and SSC (Figure 5.4 density gradient panel on left, panel A, B). Therefore, to use the monocytic lineage cells for experiments, further purification was needed to eliminate the large population of lymphocytes. Thus immunomagnetic beads were used to select out CD4+ or CD8+ or B220 lymphocytes, increasing the percentage of CD115+CD3- monocytes to 90~92%, and decreasing CD115-CD3+ lymphocytes to 7~9% (Figure 5.4, negative selection panel on left and panel C).

To further confirm the purity of monocytic lineage cells, the cells isolated from peripheral blood were stained by non-specific esterase staining. This stain is diffuse in the cytoplasm of cells from the monocyte and megakaryocyte series.[243] In comparison, neutrophils and lymphocytes also stain very weakly, but the staining pattern is discretely granular. Therefore the stain can be used to identify monocytic lineage cells.[244] The stain in isolated monocytes from peripheral blood showed a brown diffuse pattern in most of the isolated cells, indicating that they were monocytes (Figure 5.5).

The same isolation method was used to obtain purified macrophages from peritoneal lavage fluid and spleen and the purity investigated once for each. As for peripheral blood, the purity of the isolated monocytic lineage cells was greater than 90% (data not shown).

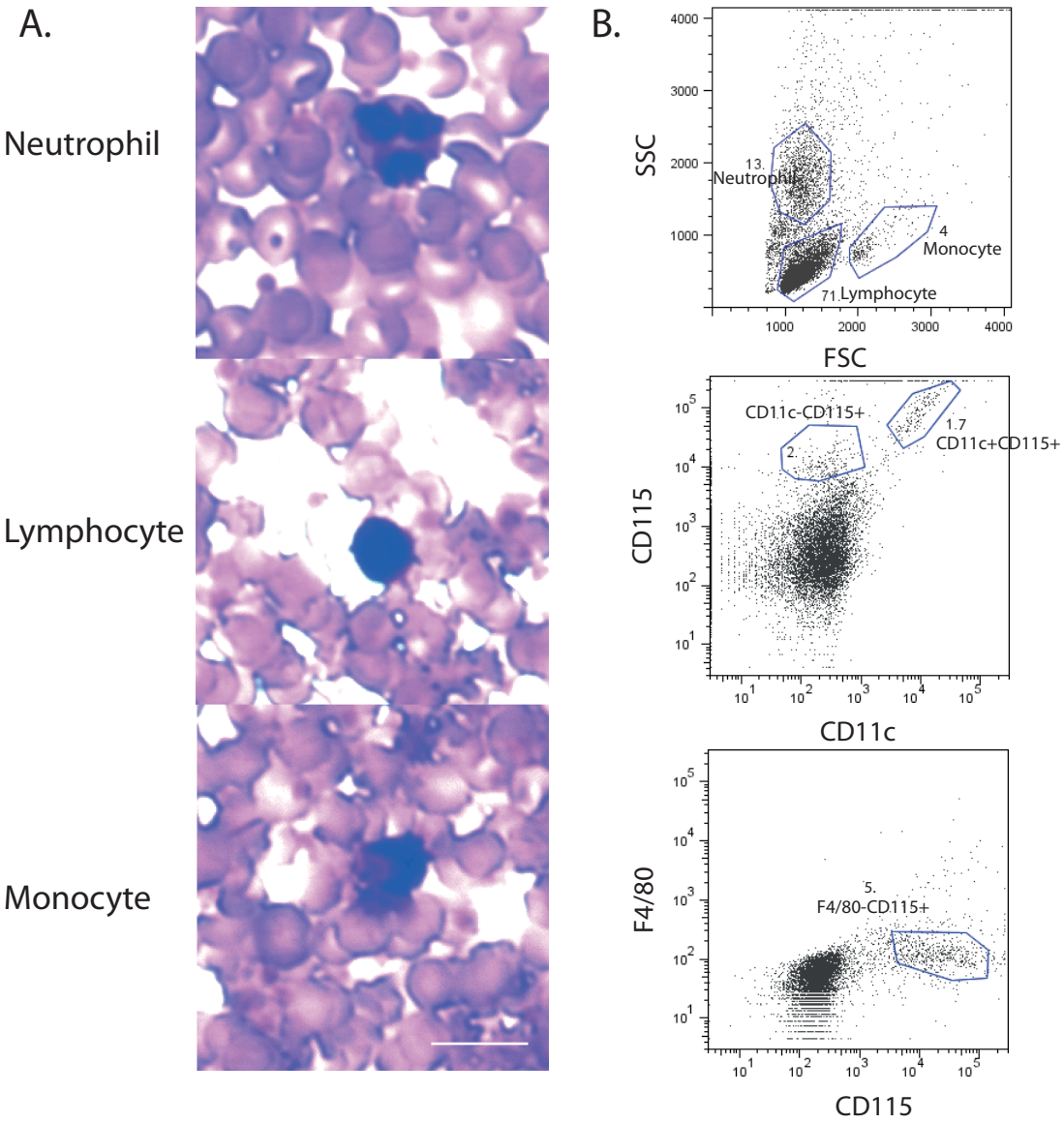
A.
Neutrophil
Lymphocyte
Monocyte
B.
SSC
FSC
13.
Neutrophil
4
Monocyte
71.Lymphocyte
CD115
CD11c
CD11c-CD115+
2.
1.7
CD11c+CD115+
F4/80
CD115
5.
F4/80-CD115+

Figure 5.2 Morphology and flow cytometric analysis of mouse whole blood leukocytes.

A. Wright staining of a thick blood smear of mouse peripheral blood. The majority of the cells (pink) were red blood cell and the cells with the deeply stained blue nucleus in the center are a neutrophil, lymphocyte and monocyte respectively. Scale bar: 20μm. B. Flow cytometric analysis of leukocytes. Neutrophils, lymphocytes and monocytes were gated based on FSC and SSC (top panel). Staining for CD115, CD11c and F4/80 was also analyzed to detect monocytes. Numbers in the charts show the percentages of the gated cells positive or negative for the specific markers. The experiment was repeated three times and the data shown here are one representative set.

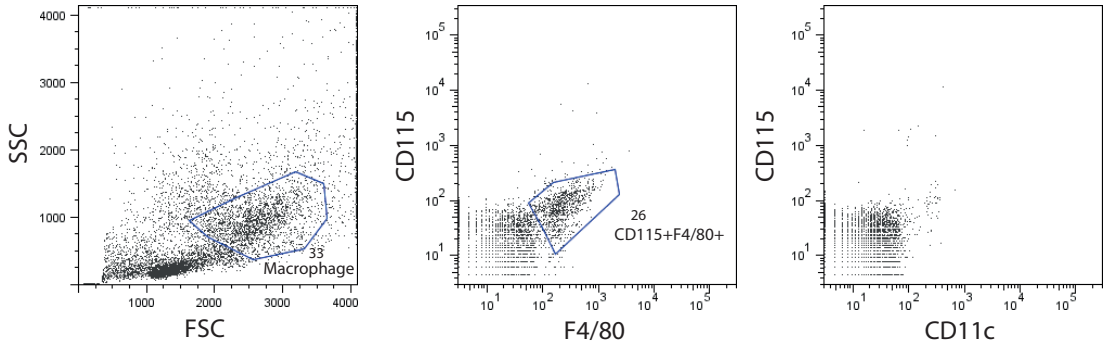

Figure 5.3 Flow cytometric analysis of peritoneal lavage fluid. Extravasated macrophages were gated based on FSC and SSC. Staining for CD115, CD11c and F4/80 was also analyzed to detect monocytes. Numbers in the charts show the percentage of the gated cells in the whole peritoneal lavage cells after lysis of red blood cells. The experiment was repeated three times and the data shown here are one representative set.

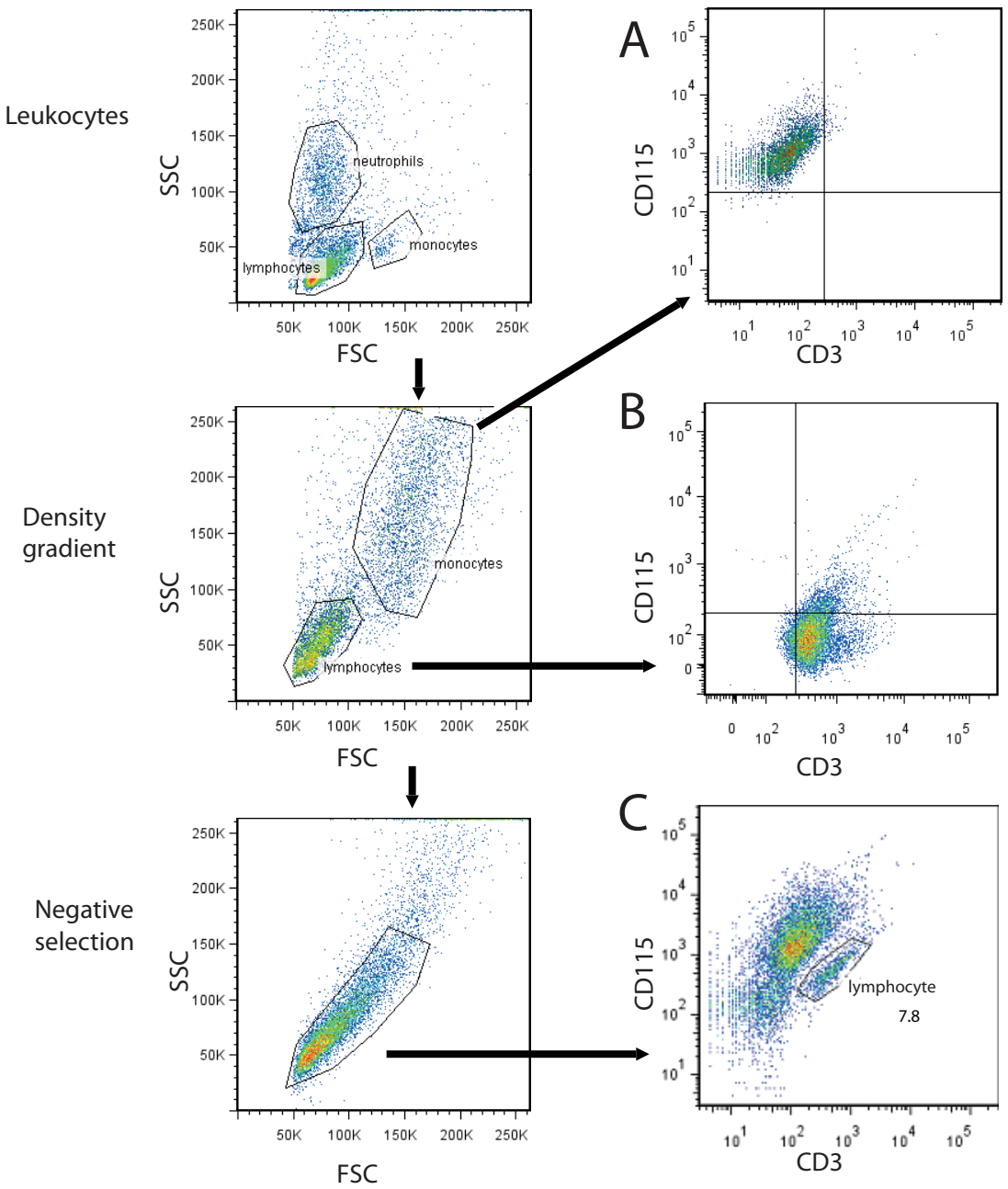
Leukocytes
Density gradient
Negative selection
SSC
FSC
neutrophils
monocytes
lymphocytes
A
B
C
CD115
CD3
lymphocyte
7.8

Figure 5.4 Flow cytometric analysis of the cells isolated from whole blood leukocytes at different stages of the isolation process.

The neutrophils and part of the lymphocytes in the peripheral blood leukocytes were eliminated with density gradient first then the remaining lymphocytes were further eliminated with immunomagnetic bead negative selection. Neutrophils, lymphocytes and monocytes were gated on FSC and SSC. The gated lymphocytes were identified as CD115-CD3+. The gated monocytes were identified as CD115+CD3-. Numbers in the charts show the percentage of the gated cells in the total cell population. The experiment has been repeated three times and the data shown here are one representative set.

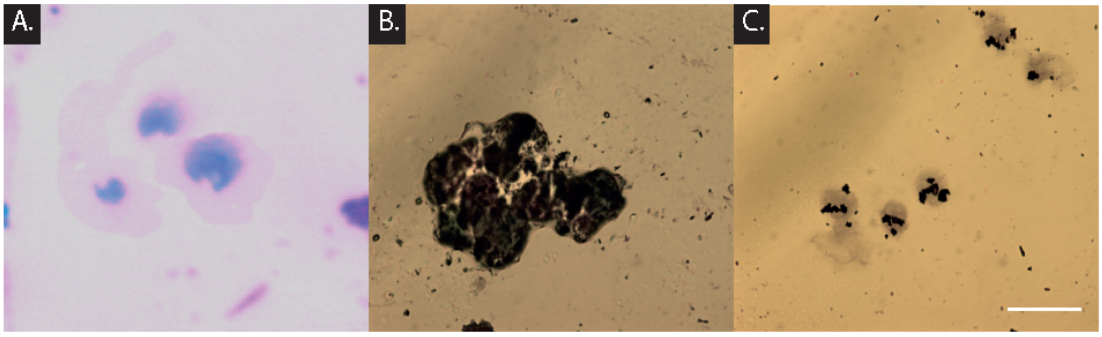

Figure 5.5 Staining characteristics of isolated peripheral blood leukocytes.

A. Wright staining of a smear of freshly isolated monocytes. B. Non-specific esterase staining of freshly isolated monocytes using a density gradient and then immunomagnetic selection. Diffuse brown staining was found in most of the cells. C. Non-specific esterase staining of freshly isolated neutrophils using a density gradient for comparison. Scale bar: 20μm.

III B. NGF induced migration of monocytic lineage cells *in vitro*

The optimal concentration of MCP-1, the key chemokine for recruitment of monocytic lineage cells, was determined by a concentration-response curve using increasing concentrations of MCP-1 and freshly isolated macrophages from peritoneal lavage fluid (Figure 5.6). The curve indicated that MCP-1 induced migration of monocytic lineage cells at a concentration lower than 1ng/ml. At 10 ng/ml, the effect of MCP-1 was almost saturated; therefore 5 ng/ml and 1 ng/ml were used as positive controls in subsequent experiments. The effect of NGF on monocytic lineage cell migration was compared to that of MCP-1 and fibronectin. NGF stimulated migration of monocytes isolated from peripheral blood in a concentration-dependent manner, with concentrations of 50ng/ml and above being as effective as MCP-1 (Figure 5.7A). Interestingly it was observed that upon migrating, cells exposed to 10 ng/ml NGF, but not MCP-1, became more “dendritic” like in morphology (Figure 5.8).

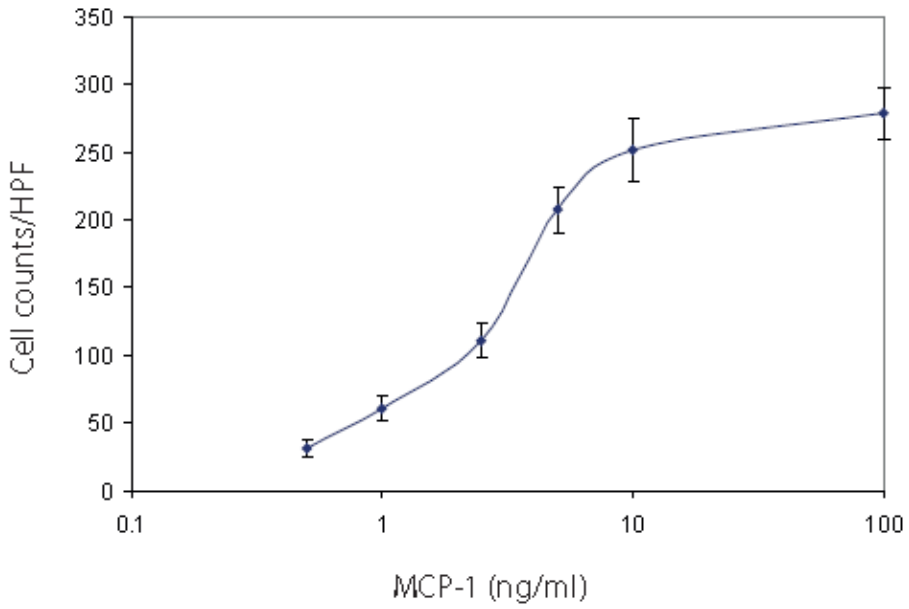

Figure 5.6 Effect of MCP-1 on migration of extravasated macrophages.

Freshly isolated macrophages from peritoneal lavage fluid were exposed to MCP-1 (0.5 ~100ng/ml) in blind-well chambers for 3hrs and the total number of cells that migrated was counted using a x40 objective. The experiment was repeated twice with two replicates in each experiment and the data shown are the average of two repeats. Error bar: standard deviation of two repeats. HPF: high power field.

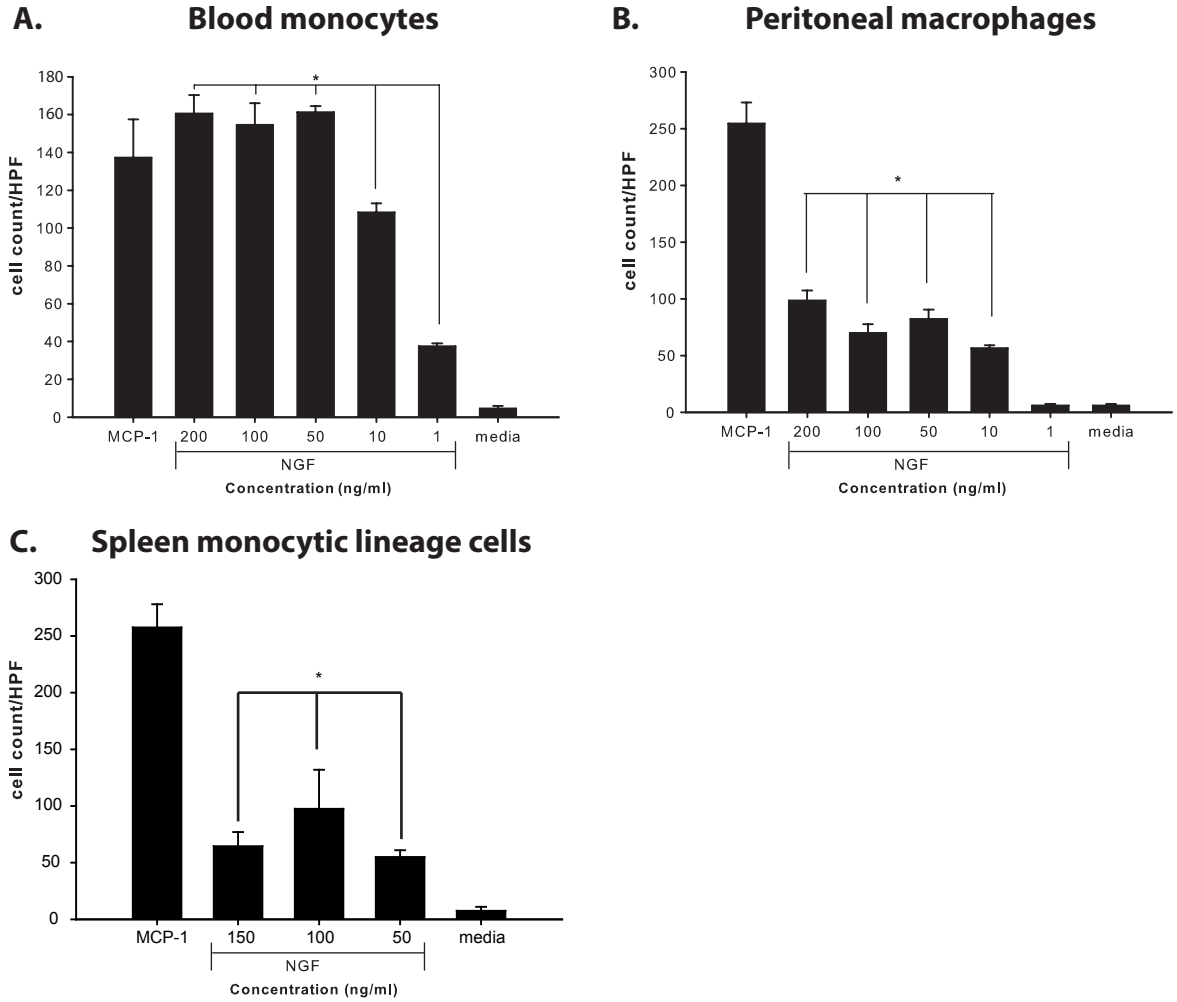
A.
Blood monocytes
cell count/HPF
180
160
140
120
100
80
60
40
20
0
*
MCP-1
200
100
50
10
1
media
NGF
Concentration (ng/ml)
B.
Peritoneal macrophages
cell count/HPF
300
250
200
150
100
50
0
*
MCP-1
200
100
50
10
1
media
NGF
Concentration (ng/ml)
C.
Spleen monocytic lineage cells
cell count/HPF
300
250
200
150
100
50
0
*
MCP-1
150
100
50
media
NGF
Concentration (ng/ml)

Figure 5.7 Effect of NGF on monocytic lineage cell migration.

Freshly isolated blood monocytes (A), macrophages from peritoneal lavage fluid (B) or spleen monocytic lineage cells (C) were treated with various concentrations of NGF (1~200ng/ml) for 3hrs and the total number of cells migrated counted using a x40 objective. MCP-1 (1ng/ml) was used as a positive control and serum free media was used as the control (media). The experiment was repeated three times with two replicates in each repeat and the data shown are the average of three repeats. * Indicates statistical significance compared with the control (one way ANOVA with post Dunett's test, $p<0.05$). Error bar: standard deviation. HPF: high power field.

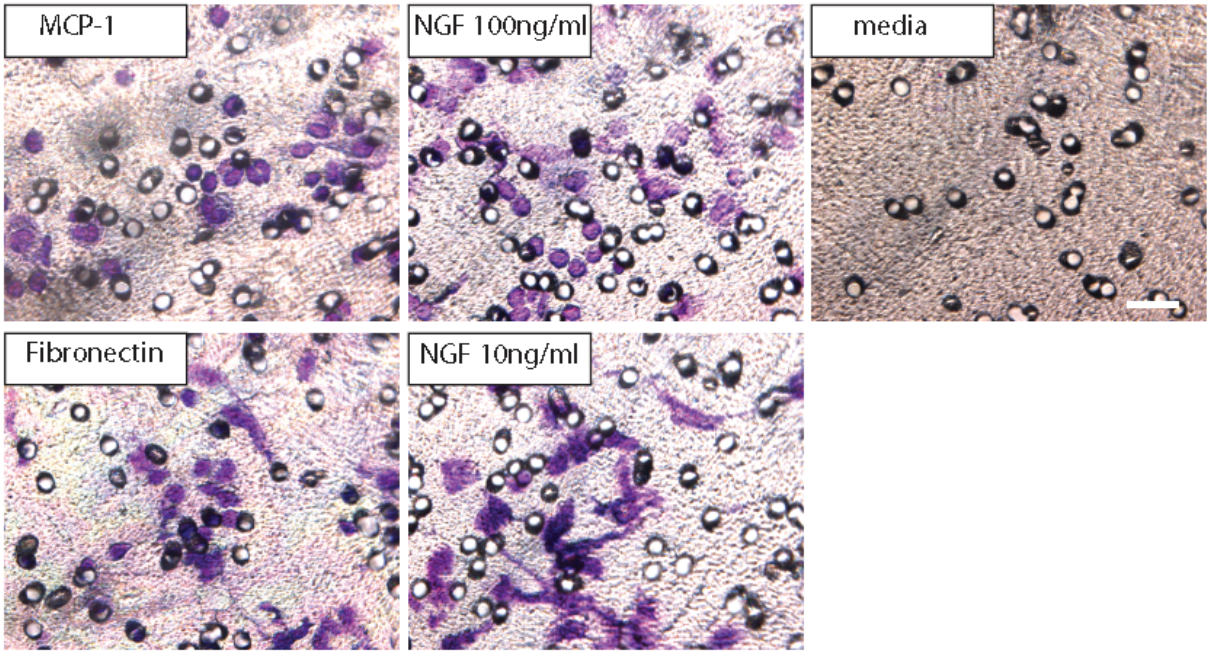
MCP-1
NGF 100ng/ml
media
Fibronectin
NGF 10ng/ml

Figure 5.8 Morphology of blood monocytes after the migration assay.

Freshly isolated blood monocytes were exposed to NGF in blind-well chambers for 3hrs then the migration membrane was stained by Wright staining. MCP-1 (1 ng/ml) and fibronectin (2%) were used as positive controls. Processes (arrows) were observed in cells migrating in response to fibronectin and particularly NGF (10 ng/ml) but not MCP-1. Scale bar: 20μm.

NGF also induced the migration of macrophages isolated from peritoneal fluid and monocytic lineage cells isolated from spleen (Figure 5.7 B, C). As shown in the figure, the number of cells migrating in response to NGF was lower than was seen with blood monocytes. Also the total number of monocytic lineage cells migrating in response to NGF was only half of the number of cells induced to migrate by MCP-1, indicating that in contrast to blood monocytes, NGF is not as effective as MCP-1 in macrophages and spleen cells.

In the *in vivo* situation, both NGF and MCP-1would be expected to increase in response to inflammation, therefore the combined effect of NGF and MCP-1 was also studied (Figure 5.9). For peripheral blood monocytes, the combination of a low concentration of NGF (1 ng/ml) and MCP-1 (5 ng/ml) increased the number of migrated cells, compared with NGF or MCP-1 alone, suggesting that NGF may have a small additive effect with MCP-1 *in vivo*. However, the combination of a high concentration of NGF (100 ng/ml) and MCP-1 resulted in fewer cells migrating that with either MCP-1 or NGF alone. Similar results were found with peritoneal macrophages. With spleen monocytic lineage cells, only the low concentration of NGF had an additive effect on with MCP-1 on migration.

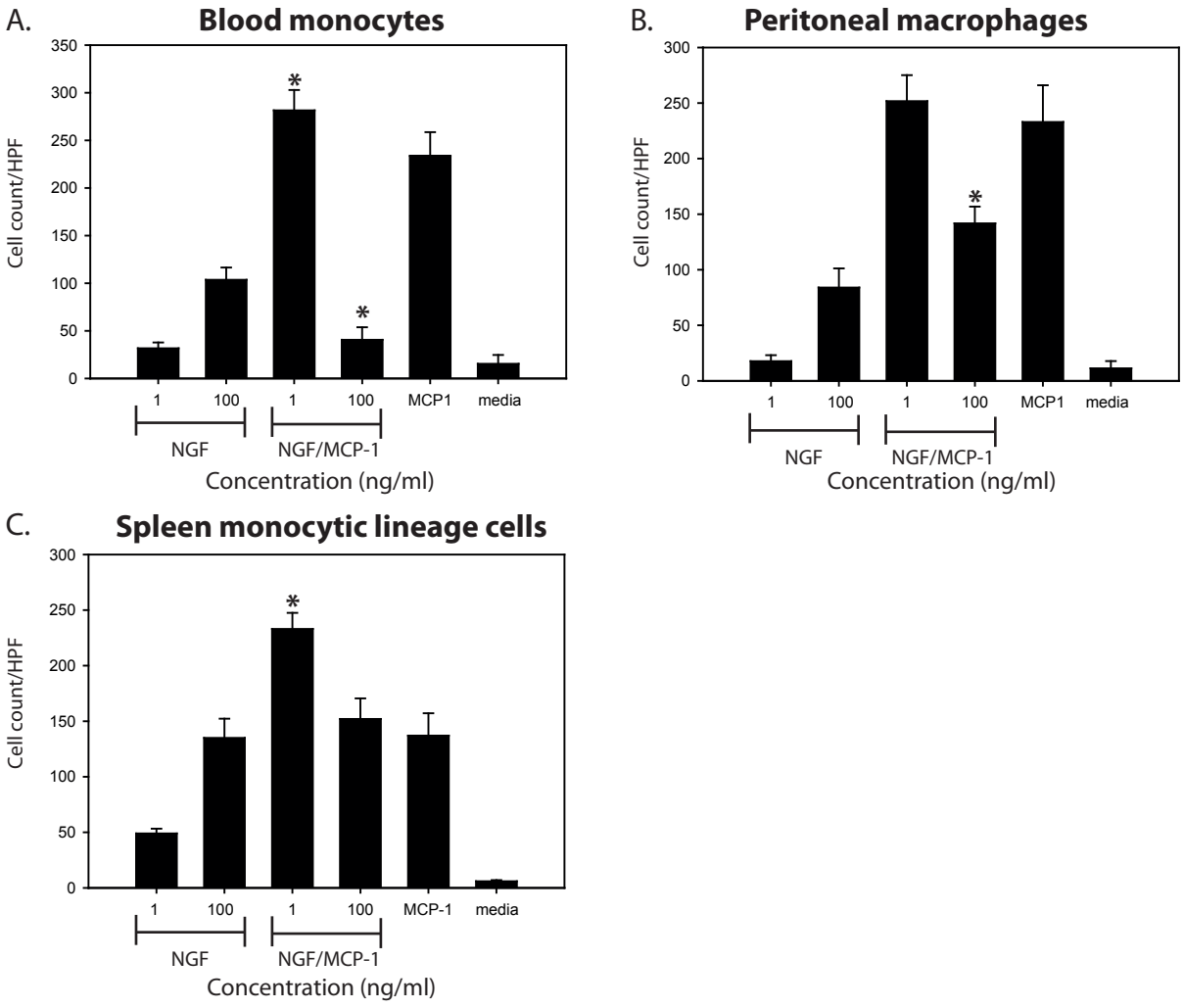
A.
Blood monocytes
Cell count/HPF
350
300
250
200
150
100
50
0
1
100
1
100
MCP1
media
NGF
NGF/MCP-1
Concentration (ng/ml)
B.
Peritoneal macrophages
Cell count/HPF
300
250
200
150
100
50
0
1
100
1
100
MCP1
media
NGF
NGF/MCP-1
Concentration (ng/ml)
C.
Spleen monocytic lineage cells
Cell count/HPF
300
250
200
150
100
50
0
1
100
1
100
MCP-1
media
NGF
NGF/MCP-1
Concentration (ng/ml)

Figure 5.9 Effect of NGF/MCP-1 combination on monocytic lineage cell migration.

Freshly isolated blood monocytes (A), macrophages from peritoneal lavage fluid (B) or spleen monocytic lineage cells (C) were exposed to various concentrations of NGF (1, 100ng/ml) and/or MCP-1(5ng/ml) in blind-well chambers for 3hrs and the total number of cells migrated counted using a x40 objective. Serum free media was used as the control (media). The experiment was repeated three times with two replicates in each repeats and the data shown are the average of three repeats. * Indicates statistical significance compared with the MCP-1 control (one way ANOVA with post Tukey's test, $p<0.05$). Error bar: standard deviation. HPF: high power field.

III C. NGF recruits primarily the classic subtype of monocytic lineage cells

The subtypes of monocytic lineage cells were assessed separately with samples from peripheral blood and peritoneal lavage for a better understanding about the cell specific effects of NGF. Ly6C staining was used to discriminate among the classic and non-classic subtypes. Approximately 50% of the blood monocytes were $Ly6C^{high}$, indicating they are classic subtype of monocytes (Figure 5.10 A). The remainder were $Ly6C^{low}$ and therefore belonged to the non-classic subtype (Figure 5.10 A). For peritoneal macrophages, flow cytometric analysis showed that 10% of the cells were $Ly6C^{high}$ (Figure 5.10 B, D). Spleenic monocytes were not tested.

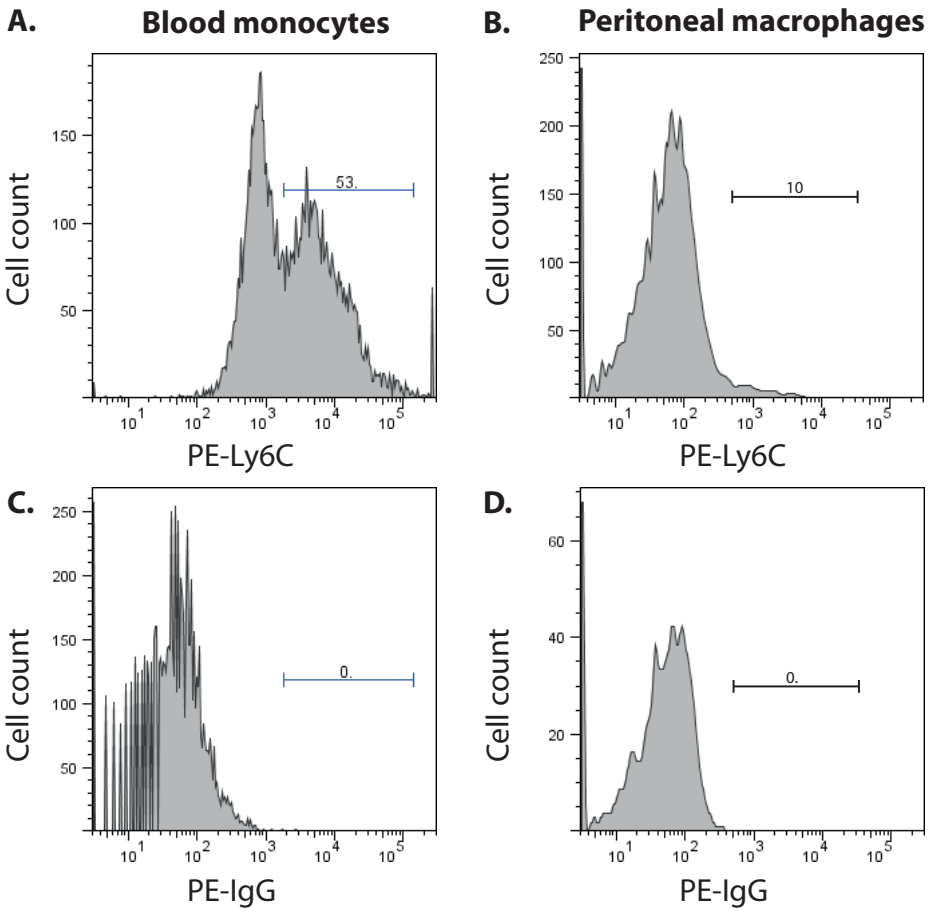

Figure 5.10 Flow cytometric analysis of Ly6C expression on blood monocytes and peritoneal macrophages.
Blood monocytes (A and C) or peritoneal macrophages (B and D) were first gated according to FSC and SSC and the histograms shown are from the gated populations. Panels A and B show results for staining with a specific antibody against Ly6C and panels C and D are for the isotype control. The two peaks in panel A indicated that blood monocytes include a Ly6Chigh group and a Ly6Clow group. Numbers on the plots show the percentage of the positive cells. The experiment was repeated three times and the data shown here are one representative set.

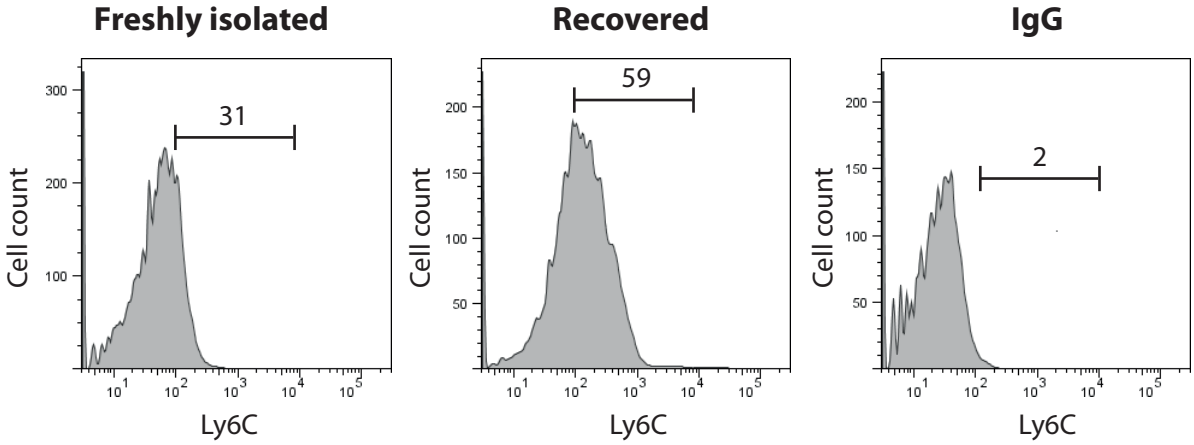

Figure 5.11 Flow cytometric analysis of Ly6C expression on blood monocytes and peritoneal macrophages.
Blood monocytes (A and C) or peritoneal macrophages (B and D) were first gated according to FSC and SSC and the histograms shown are from the gated populations. Panels A and B show results for staining with a specific antibody against Ly6C and panels C and D are for the isotype control. The two peaks in panel A indicated that blood monocytes include a Ly6Chigh group and a Ly6Clow group. Numbers on the plots show the percentage of the positive cells. The experiment was repeated three times and the data shown here are one representative set.

To test if NGF is selective for the classic subtype of monocytes, the expression of Ly6C on migrated moncytic lineage cells was tested. However, the Ly6C signals were decreased by the isolation process compared with the signals obtained from its staining level before any isolation step (data not shown), probably due to the multiple wash steps. However, for staining of the migration membrane (see below) which is not as sensitive as flow cytometric analysis, the signals due to Ly6C fluorescence needed to be improved. In previous experiments culturing with serum has been used to promote recovery of the surface markers,[241] therefore freshly isolated monocytic lineage cells were incubated with 5% FBS/PBS for 4 hrs before the migration assay was performed. As shown in the figure (Figure 5.11), Ly6C expression was significantly improved; meanwhile the percentage of Ly6C ^{high} cells remained at 50%, indicating that the recovery step did not alter the subtype of monocytic lineage cells. The recovery test was only performed on peritoneal macrophages; however it was presumed that other cell types of the monocytic lineage cells have the same response.

The migrated monocytes after the recovery step described above were stained with Ly6C. Nearly all cells that migrated through in response to NGF were positive for Ly6C, indicating they are the classic subtype (Figure 5.12, 5.13). MCP-1 was also selective for the classic subtype (Figure 5.12, 5.13), which is consistent with previous reports.[245] Similar observations were found with recovered peritoneal macrophages, which confirmed the selective effect of NGF and MCP-1 on classic subtype of monocytic lineage cells. Notably, nuclear fragmentation was observed more frequently in the NGF treated membrane (Figure 5.14), suggesting that NGF may also induce apoptosis. The

nuclear fragmentation was not observed with media or MCP-1, indicating that can be a specific effect of NGF.

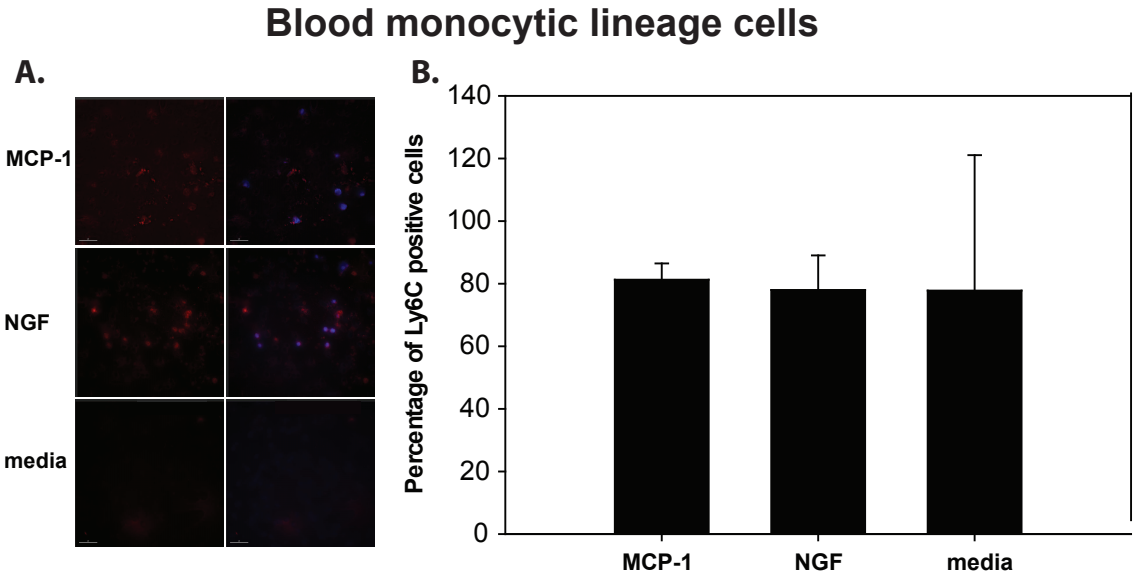
Blood monocytic lineage cells
A.
MCP-1
NGF
media
B.
Percentage of Ly6C positive cells
140
120
100
80
60
40
20
0
MCP-1
NGF
media

Figure 5.12 Ly6C staining of migrated monocytes isolated from peripheral blood. Freshly isolated monocytes were exposed to MCP-1 (5 ng/ml), NGF (100 ng/ml) or serum free media in blind-well chanbers for 3hrs then the membranes were stained for Ly6C. A. Ly6C staining on the migration membranes. Most of the migrated cells stained positively for Ly6C (red). The nuclei were counterstained with DAPI (blue). Scale bar: 20 μm. B.The percentage of Ly6C positive cells versus the total number of migrated cells found on the membrane. The data shown are the average of three experiments. Error bar: standard deviation.

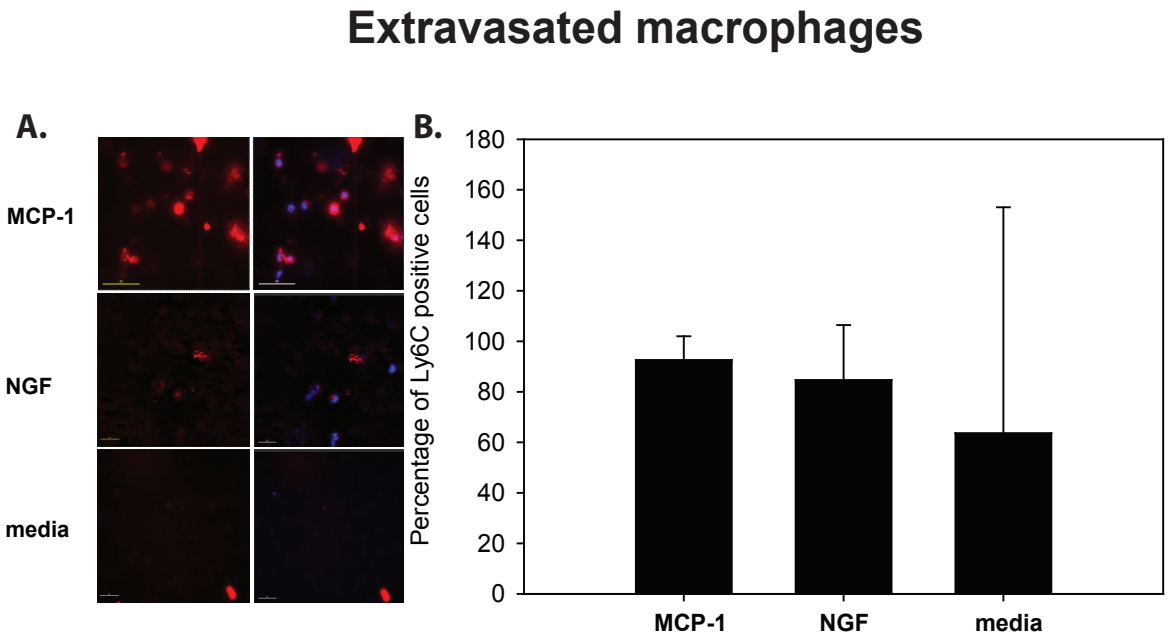
Extravasated macrophages
A.
MCP-1
NGF
media
B.
Percentage of Ly6C positive cells
180
160
140
120
100
80
60
40
20
0
MCP-1
NGF
media

Figure 5.13 Ly6C staining in migrated macrophages isolated from peritoneal lavage fluid.

Freshly isolated macrophages were treated with MCP-1, NGF or serum free media for 3 hrs and then staining for Ly6C on the migrated cells was assessed at the end of the treatment. A. Ly6C staining on the migration membranes. Most of the migrated cells stained positively for Ly6C (red). The nuclei were counterstained with DAPI (blue). B. The percentage of Ly6C positive cells versus the total number of migrated cells found on the membrane. NGF: 100 ng/ml, MCP-1: 5 ng/ml.Scale bar: 20 μm. The data shown are the average of three experiments. Error bar: standard deviation.

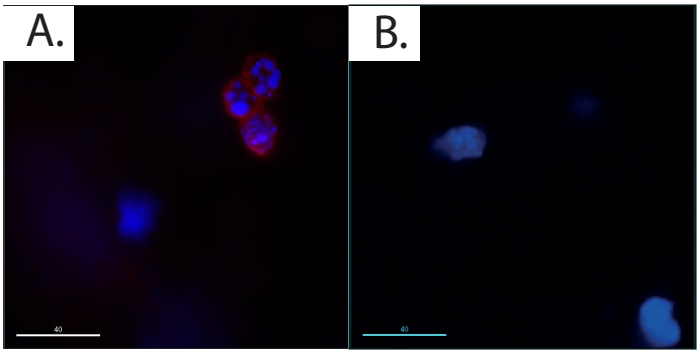

Figure 5.14 Nuclear fragmentation found in cells migrating in response to NGF. Freshly isolated macrophages from peritoneal lavage fluid were exposed to NGF (100 ng/ml) in blind-well chambers for 3 hrs before the staining was performed. A. Ly6C staining was found on the outer surface of the cells (red). B. Isotype control. The nuclei were counter-stained with DAPI (blue). Scale bar: 40 μm.

III D. NGF induced differentiation of monocytic lineage cells

The effect of NGF on monocytic lineage cell differentiation was then studied by flow cytometry (Figure 5.15). After 24hrs incubation with NGF monocytes isolated from peripheral blood were stained for IAb, CD11c, CD11b, F4/80. GM-CSF/IL-4, which has been reported to induce differentiation of monocytes into dendritic cells *in vitro*,[97] was used as positive control. As shown in the figure, GM-CSF/IL-4 significantly increased the percentage of CD11c positive cells, indicating that the cells differentiated into dendritic cells. NGF also induced about 10% of the cells to differentiate into CD11c positive cells but was not as effectively as GM-CSF/IL-4 (n = 3). In contrast, F4/80, the widely used macrophage marker, was not different from the control with 5% FBS. IAb expression was increased with both GM-CSF/IL-4 and NGF, suggesting that a small portion of the monocytes obtained antigen presenting capabiliities.

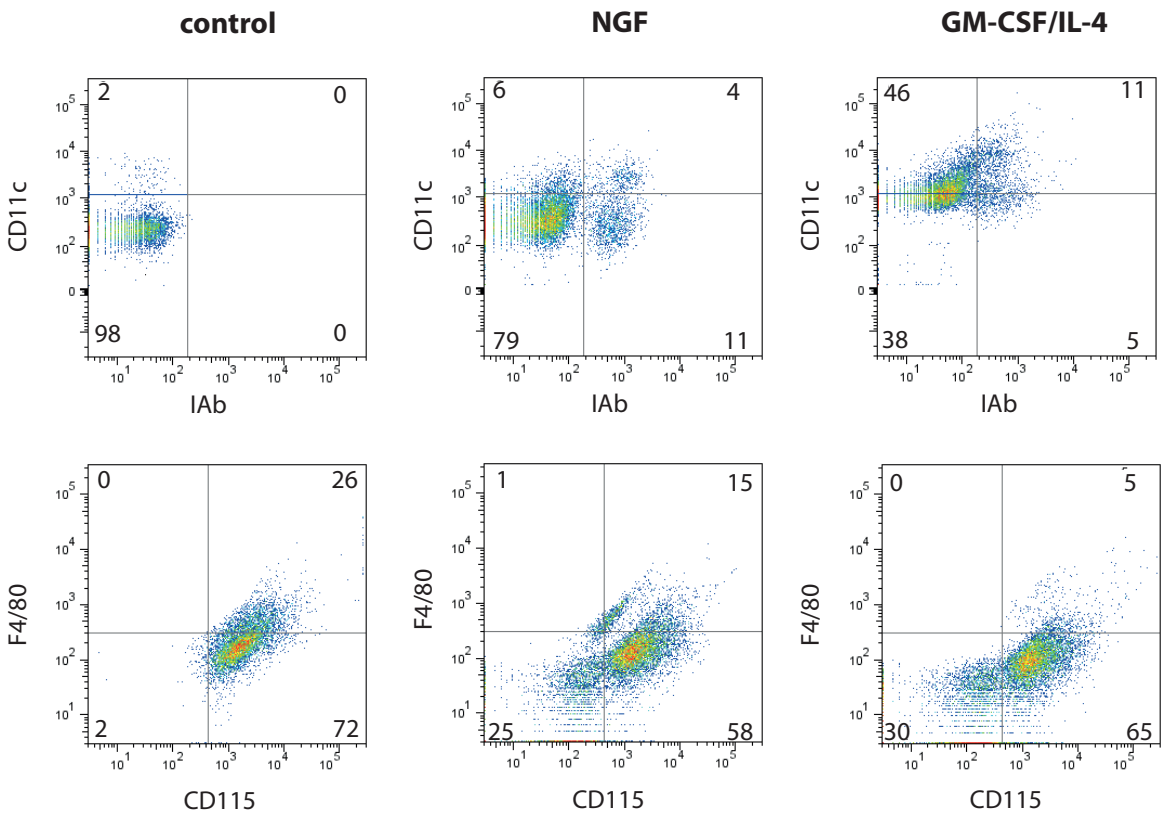
control
NGF
GM-CSF/IL-4
CD11c
IAb
F4/80
CD115
2
0
98
0
6
4
79
11
46
11
38
5
0
26
2
72
1
15
25
58
0
5
30
65

Figure 5.15 Flow cytometric analysis of blood monocyte differentiation status after 24 hrs exposure to NGF.

Freshly isolated monocytes were isolated from mouse peripheral blood and then treated with 100 ng/ml NGF in 5% FBS for 24 hrs. Numbers in the charts show the percentage of the cells in each quandrant. GM-CSF/IL-4 was used as a positive control and 5% FBS was used as the control.The experiment was repeated three times and the data shown here are one representative set.

III E. NGF induced migration of monocytic lineage cells from limbus

The effect of NGF on corneal monocytic lineage cell migration was then tested *in vivo* using intrastromal injection. To test the efficiency of our delivery method within the stroma *in vivo,* OCT imaging was performed after PBS intrastromal injection. It was observed that the injected PBS spread evenly through the entire stroma within minutes (Figure 5.16). Then to ensure that NGF was also evenly distributed with the injection, immunostaining for NGF was performed at 0, 4, 16, 24 hrs after the injection (Figure 5.17). Consistent with what was reported previously, [119, 122] NGF expression was only found in normal corneal epithelium and endothelium. At 4 hrs post intrastromal injection, NGF was evenly distributed through the entire corneal stroma. By 16 hrs, NGF staining in the central and paracental corneal stroma was significantly decreased, and it had almost completely disappeared by 24 hrs. Therefore subsequent *in vivo* experiments were performed at 4 hrs post injection.

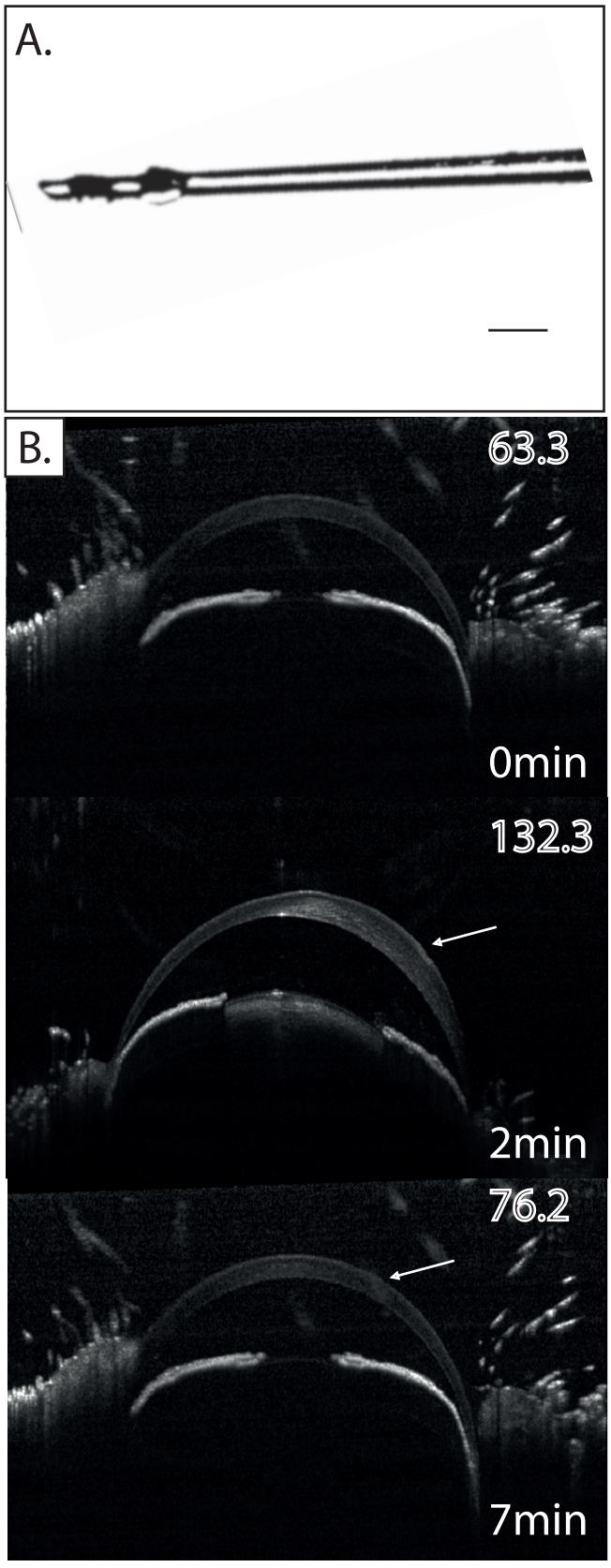
A.
B.
63.3
0min
132.3
2min
76.2
7min

Figure 5.16 The alterations in corneal stroma after PBS intrastromal injection. A. A glass capillary needle was used for the injection. The outer diameter of the needle was 35~40μm. Scale bar: 100μm. B. *In vivo* OCT imaging of a cornea before and after the intrastromal injection. The corneal thickness firstly increased near the injection site (arrow) and then PBS rapidly spread out to the whole stroma. Numbers in the right corner of each picture show the thickness of the corneas at the injection site or comparable position in the normal cornea (μm).

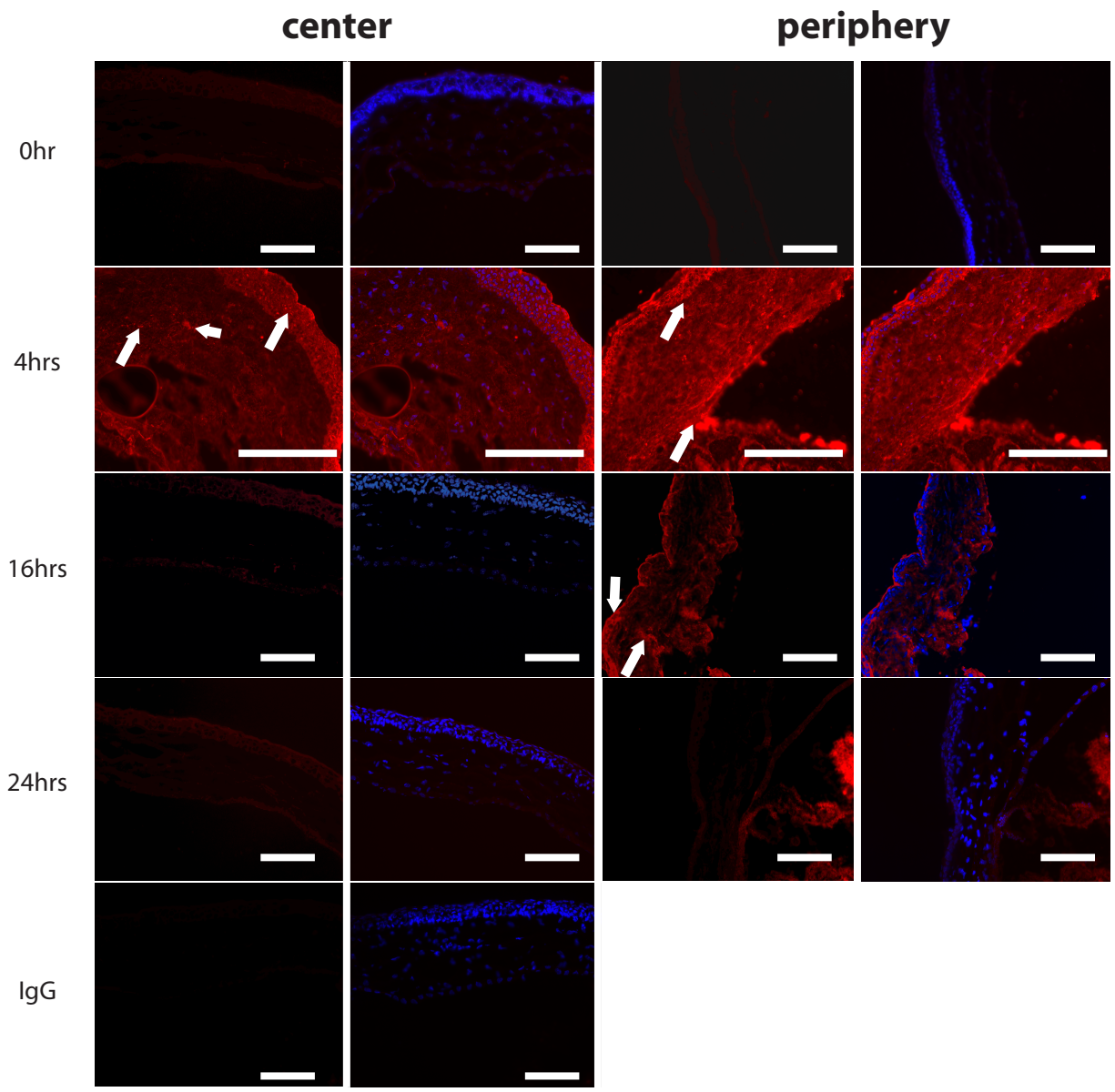
center
periphery
0hr
4hrs
16hrs
24hrs
IgG

Figure 5.17 NGF staining at 0, 4, 16, 24 hrs after the intrastromal injection. NGF staining (red, illustrated by white arrows) was found in central corneal stroma at 4 hrs, and in peripheral corneal stroma at 4 and 16 hrs after the intrastromal injection. The nuclei were counterstained with DAPI. Scale bars: 30 μm.

To test if intrastromal injection of NGF recruits monocytic lineage cells into the cornea, whole-mounted tissues were stained with antibodies against CD11b, CD11c, and CD115 (Figure 5.18). At 4 hrs post injection, the injury caused by the injection was not healed and immunostaining of whole-mount corneas demonstrated that CD11b+ cells were observed in the corneal stroma beneath the injection site (Figure 5.18, first row). In contrast, cells positive for CD11c, the dendritic cell marker, were mainly found inside the injection site. Only a small number of CD11b or CD11c positive cells were found near the PBS injection site. At 4 hrs and 16 hrs after the intrastromal injection of NGF, few if any CD115+ monocytic lineage cells were found near the injection site. However, by 24 hrs, a significant amount of CD115+ cells were observed surrounding the injection site. This population of cells may be the classic subtype of monocytic lineage cells which are recruited to sites of inflammation.[246]

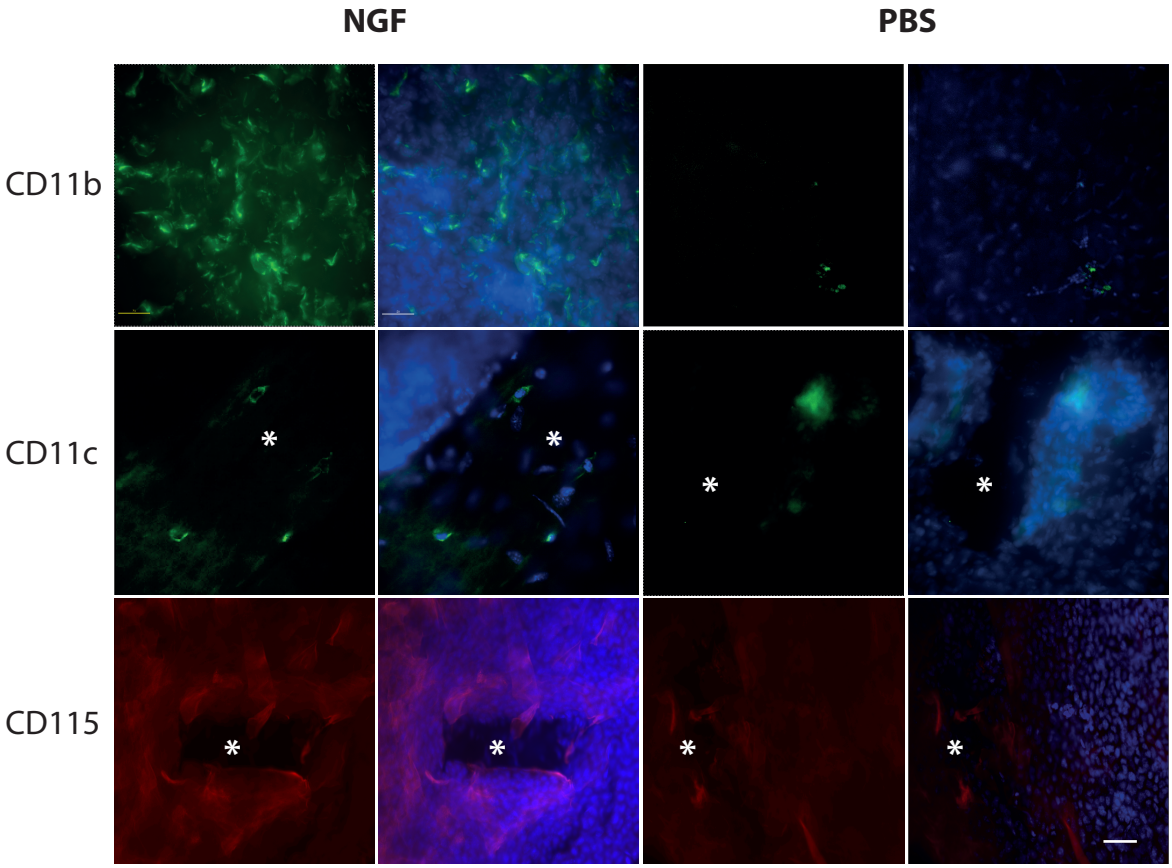
NGF
PBS
CD11b
CD11c
CD115

Figure 5.18 Immunostaining of mouse whole-mount corneas after NGF intrastromal injection.

The whole-mount corneas were imaged at the injection site (*) and expression of CD11b (green) or CD11c (green) was detected with antibodies at 4hrs after the injection. Expression of CD115 (red) was examined 24 hrs after the injection. The nuclei were counterstained with DAPI (blue). For CD11b, the images shown are a projected image. For CD11c and CD115, the images shown were taken in the anterior stroma. Scale bars: 20μm. The images shown are from one representive experiment and the experiment was repeated 4~6 times for each antibody.

The immunostaining results for CD11c and CD11b were not consistent among different repeats, which can probably be explained by antibody penetration problems. Therefore to quantify the infiltrating cells, flow cytometry was performed on corneal stroma cell suspensions (Figure 5.19). By this method, variation caused by antibody penetration problems was eliminated. The corneal single cell suspension was stained with antibodies against Ly6C, MHC-II, CD11c, and CD115 and quantitated by flow cytometry (Figure 5.18). 4.8% of cells were CD11c+, $Ly6C^{low}$ in NGF treated corneas, higher than the 1.1% found with PBS. Meanwhile, 7.2% were CD115+, MHC-II+ in NGF treated corneas, higher than the 2.1% found with PBS.

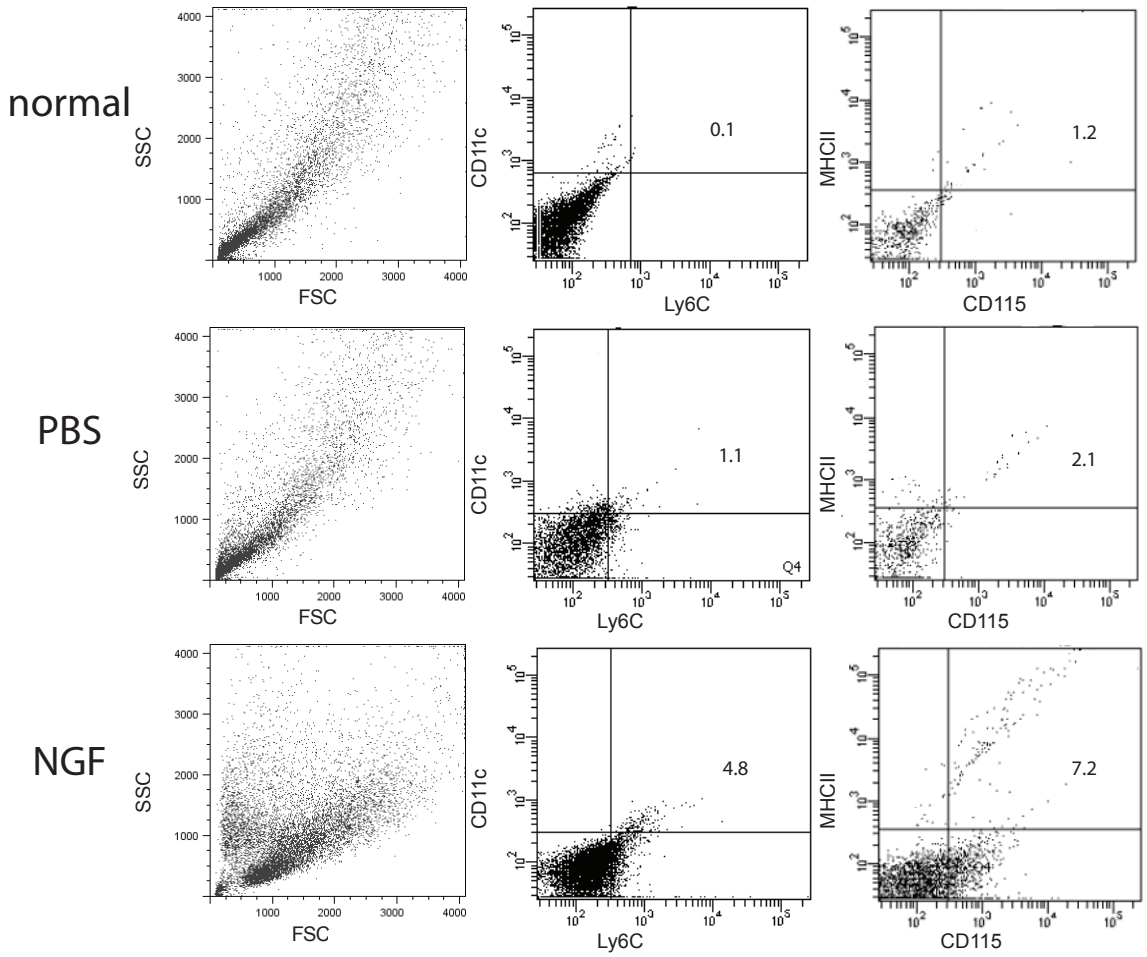
normal
PBS
NGF
SSC
FSC
CD11c
Ly6C
MHCII
CD115
0.1
1.2
1.1
2.1
4.8
7.2
Q4

Figure 5.19 Flow cytometric analysis of corneal stromal cells after NGF intrastromal injection.

At 4hrs after NGF (1μg/ml) or PBS injection, the corneal stroma was harvested; a single cell suspension was obtained and stained with antibodies against CD115, CD11c, MHCII, Ly6C. Numbers shown in the plots are the percentage of the cells in the quadrant. The experiment was repeated three times and the data shown is one representative set of data.

To assess if NGF was capable of inducing a local migration of monocytic lineage cells from the limbus or the sub-conjunctival space, GFP labeled monocytes were injected into the subconjunctival space following intrastromal injection of NGF. Both *in vivo* and *ex vivo* studies showed that more GFP cells were found in the NGF injected corneas (Figure 5.20). At 4 hrs post injection, more hyper-reflective cells were observed in the corneas with NGF injection (Figure 5.20 C, D, E, F), than the corneas injected with PBS control or normal monocytes only control. At 16 hrs post injection, a large number of neutrophils were seen in the corneal stroma. A few clusters of hyperreflective dots (Figure 5.20 I, white arrows) were observed in the NGF injected cornea, possibly due to apoptosis of GFP monocytes. In whole mount corneas, GFP cells were found in the corneal stroma in the injection site and the limbal stroma near the injection site (Figure 5.21 column A, B).

To assess the trafficking of the injected cells, the cervical lymph node and spleen were assessed at 4 hrs and 16 hrs after the injections. GFP cells were identified in the cervical node lymph at both 4 hrs and 16 hrs post injections indicating that the monocytic lineage cells injected into the subconjunctival space may travel to lymphatic tissues very quickly (Figure 5.21 column C, D, upper part). However, both in the spleen red and white pulp GFP cells were only found at 16 hrs post injection (Figure 5.21 column C, D, lower part).

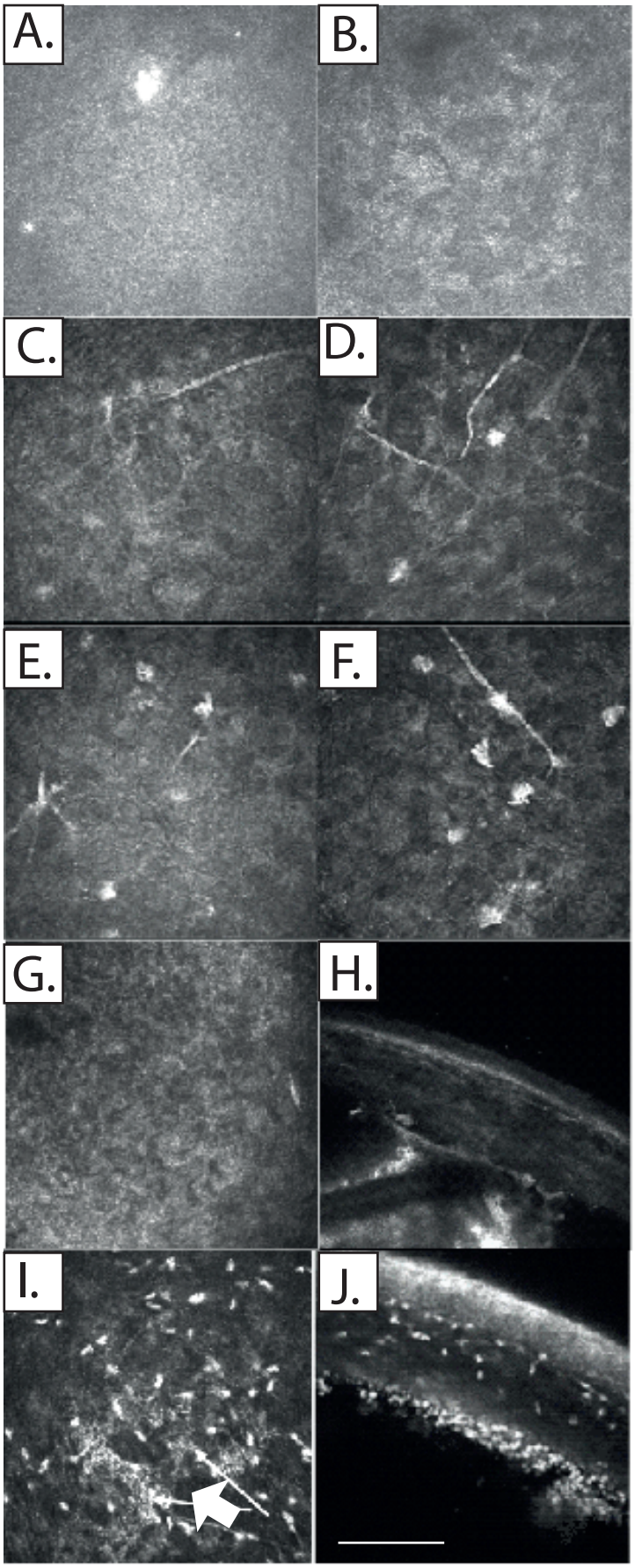
A.
B.
C.
D.
E.
F.
G.
H.
I.
J.

Figure 5.20 Migration of GFP monocytic lineage cells into the corneal stroma in response to NGF.

GFP monocytes were injected into the subconjunctival space immediately after intrastromal injection of NGF (1 μg/ml, 2 μl) or PBS as control. The corneas were imaged 4 and 16 hrs later by HRT *in vivo* confocal microscopy. A. Corneal epithelium 4 hrs after PBS intrastromal injection. B. Corneal epithelium 4 hrs after NGF intrastromal injection. C. Anterior corneal stroma 4 hrs after PBS intrastromal injection. D. Anterior corneal stroma 4 hrs after NGF intrastromal injection. E. Posterior corneal stroma 4 hrs after PBS intrastromal injection. F. Posterior corneal stroma 4 hrs after NGF intrastromal injection. G. Anterior corneal stroma 16 hrs after PBS intrastromal injection. H. Cross section of corneas at 16 hrs after PBS intrastromal injection. I. Anterior corneal stroma 16 hrs after NGF intrastromal injection. Degraded hyper-refletive cells were found (arrow). J. Cross section of corneas at 16 hrs after NGF intrastromal injection. Scale bars: 100 μm. The experiment was repeated three times and the images shown were taken from one representative experiment.

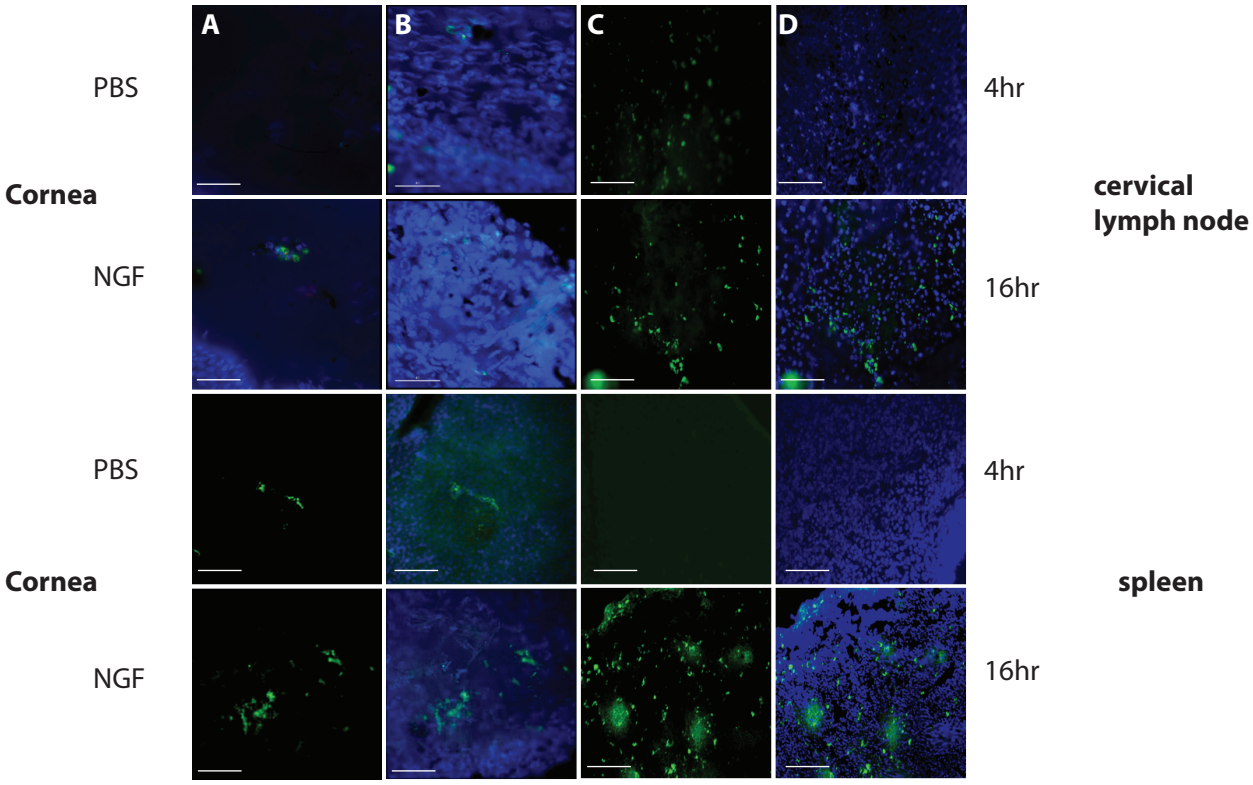
A
B
C
D
PBS
4hr
Cornea
cervical
lymph node
NGF
16hr
PBS
4hr
Cornea
spleen
NGF
16hr

Figure 5.21 GFP monocytic lineage cells in the cornea, cervical lymph node and spleen.

The tissue samples were harvested at 4 or 16 hrs after subconjunctival injection of GFP (green) monocytic cells and intrastromal injection of NGF (1 μg/ml). Images in columns A and B were taken at the injection site (upper) or one field away from the injection site (lower) of the corneas and those in columns C and D were from cervical lymph node (upper) or spleen (lower). GFP monocytic lineage cells are shown in green and the nuclei were counterstained with DAPI (blue, column B and D). Scale bar: 40μm. The experiment was repeated four times for the cornea and two times with cervical lymph node and spleen and the images shown were taken from one representative experiment.

III F. NGF up-regulated MCP-1 levels in the stroma

As MCP-1 is considered one of the most potent chemotactic factors for monocytic lineage cells *in vivo*,[146] its concentration was measured in the cornea 4 hrs after NGF injection to test if the recruitment of monocytic lineage cells corresponded with elevated MCP-1. The concentration of MCP-1 in normal untreated corneas was very low (45 +/-23 pg/mg tp) (Figure 5.22). With NGF, the concentration in the stroma was significantly increased up to 1458 +/- 139 pg /mg tp, which is significantly higher than the PBS vehicle control (289 +/- 37 pg/mg tp). Similarly in the epithelium, the concentration increased approximately 3-fold compared with the normal control. This suggested that NGF may induce secretion of MCP-1, which subsequently induced recruitment of monocytic lineage cells.

Next, the possible stromal sources of MCP-1 were studied. Based on previous findings,[229, 247] it was reasoned that MCP-1 may be secreted by infiltrating neutrophils. The total number of neutrophils was counted in wholemount corneas stained with antibodies against Ly6G (Figure 5.23). At 4 hrs after PBS or NGF intrastromal injections, small numbers of Ly6G+ cells were mainly found near the injection site as shown in Figure 5.22 B. Consistently, CD11b positive cells, mostly macrophages and neutrophils,[248] also accumulated near the injection site only with NGF (Figure 5.18). Thus it is not very likely that MCP-1 was only due to neutrophils; some other cellular components in the cornea, such as keratocytes, may also contribute to the significant increased level of MCP-1.

To test if the increased stromal MCP-1 was secreted by keratocytes in response to NGF, keratocytes were isolated from normal mouse corneas, cultured to give the corneal

fibroblast phenotype and incubated with 100 ng/ml of NGF. The isolated keratocytes showed the morphology of fibroblasts with the current culture conditions. After 24 hrs, secreted MCP-1 was detected in the NGF treated sample at a concentration of 143 +/- 31 pg/ml, much higher than with the media control (12 +/- 26 pg/ml) (Figure 5.24).

A.

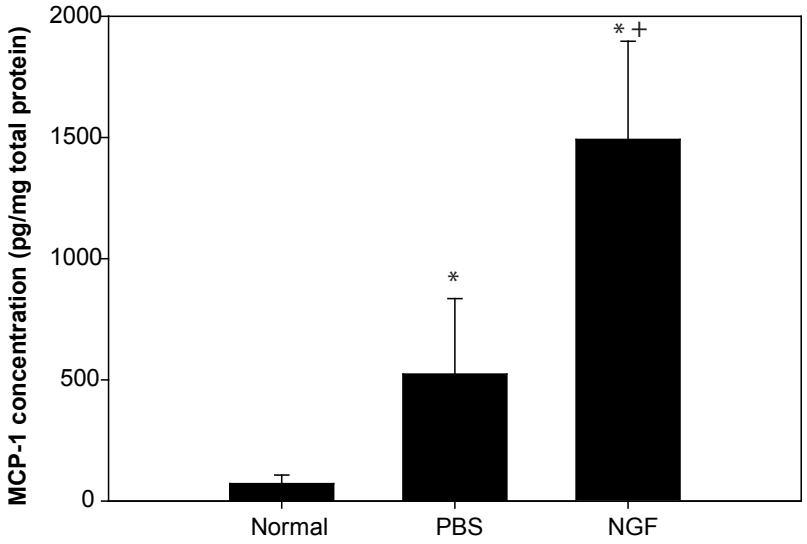
MCP-1 concentration (pg/mg total protein)
2000
1500
1000
500
0
*
*+
Normal
PBS
NGF

B.

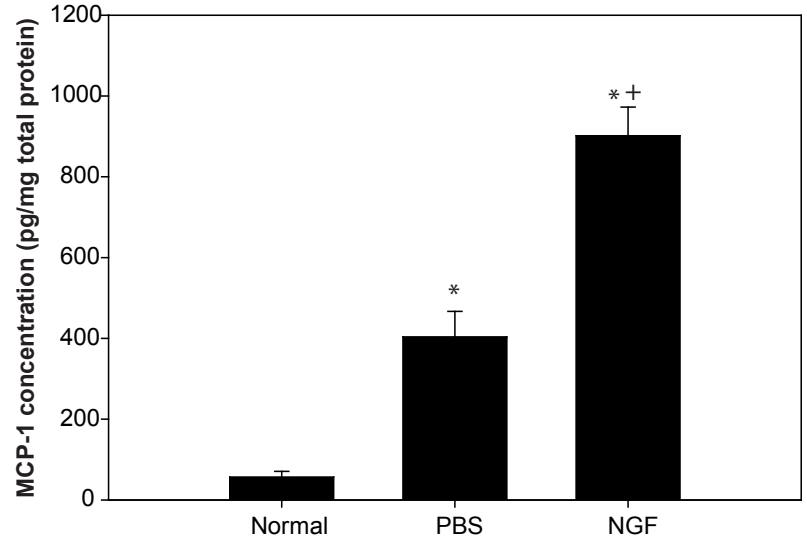
MCP-1 concentration (pg/mg total protein)
1200
1000
800
600
400
200
0
*
*+
Normal
PBS
NGF

Figure 5.22 Corneal MCP-1 levels in response to NGF.

At 4 hrs after NGF (1μg/ml) intrastromal injection, corneal epithelium and stroma were harvested separately and the concentration of MCP-1 was measured by ELISA. A. MCP-1 concentration in the stroma of NGF or PBS intrastromally injected corneas or normal untreated control. B. MCP-1 concentration in the epithelium. The experiment was repeated three times and the data shown are the average of three repeats. * Indicates statistical significance compared with the normal control. + Indicates statistical significance compared with the PBS control (two sample t-test, $p<0.05$). Error bar: standard deviation.

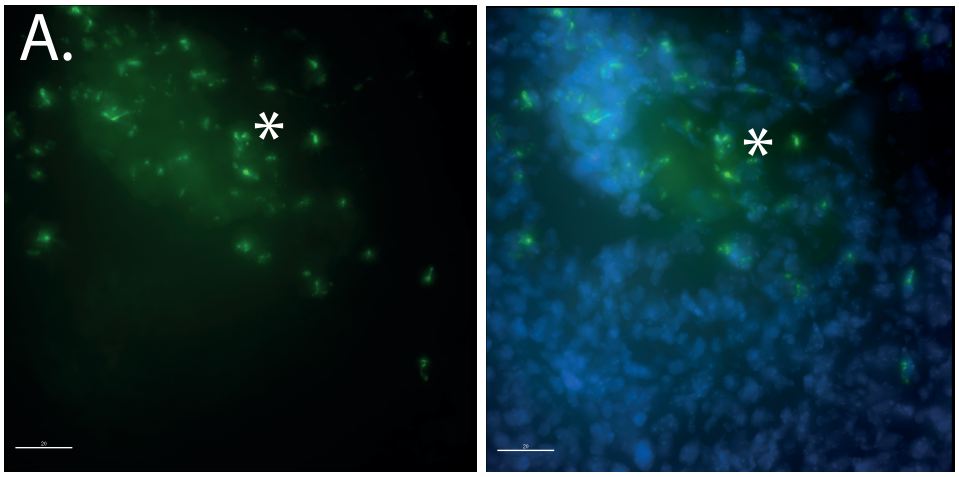
A.
*
*

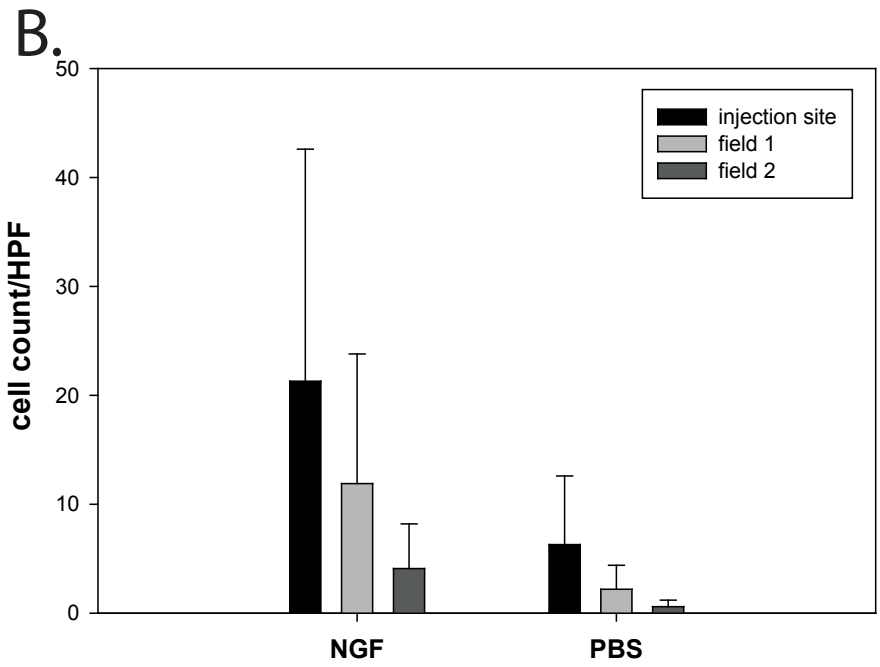
B.
50
40
30
20
10
0
cell count/HPF
injection site
field 1
field 2
NGF
PBS

Figure 5.23 Neutrophils at the intrastromal injection site.

Neutrophils were stained with an antibody against Ly6G and the number of positive cells was counted. A. Ly6G positive cells in the injection site of a NGF injected cornea. Scale bar: 20μm. B. The total cell count of Ly6G positive cells in the injection site, one and two fields away from the injection site towards the central cornea. The experiment was repeated three times and the data shown are the average of three repeats. No statistically significant differences were found among the counted fields (two-sample t-test, $p<0.05$). Error bar: standard deviation. HPF: high power field.

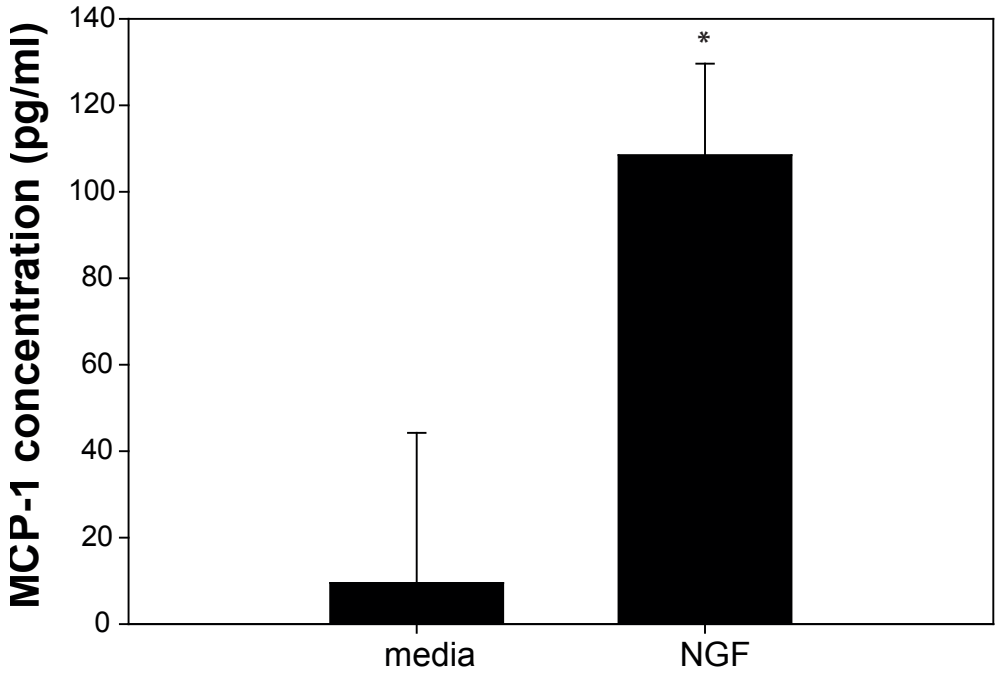

Figure 5.24 Fibroblasts derived from mouse keratocytes secreted MCP-1 when stimulated by NGF in vitro. Keratocytes isolated from mouse corneas were treated with NGF (100ng/ml, 24hrs) and the concentration of MCP-1 secreted into the culture media was measured by ELISA. The experiment was repeated three times and the data shown are the average of three repeats. * Indicates statistical significance (two-sample t-test, $p<0.05$). Error bar: standard deviation.

To further test if the keratocytes are activated into fibroblasts in vivo, similar to the condition we used *in vitro*, staining for thy1.1 in the cornea was performed.[249] As expected, the number of Thy1.1 positive cells increased with NGF injection (Figure 5.25). MCP-1 concentration in the aqueous was also significantly increased in both PBS and NGF treated corneas, which may also contribute to the increased corneal MCP-1 (data not shown).

A.

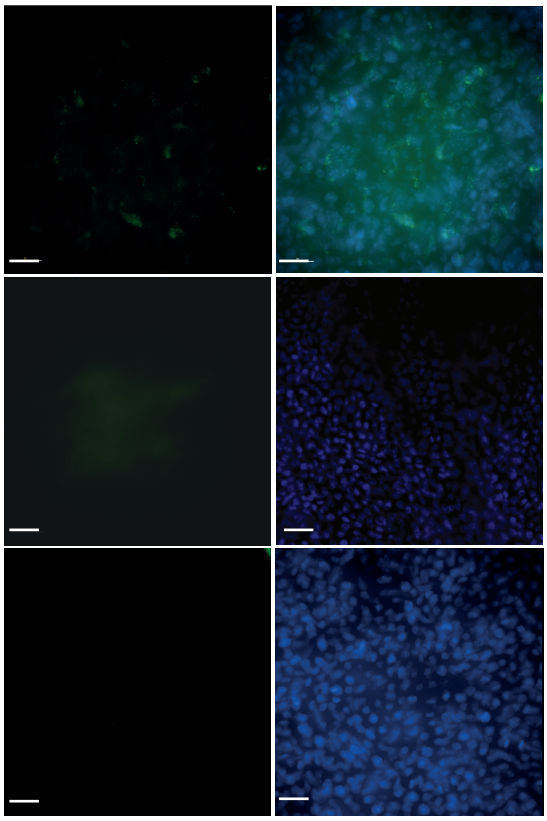

B.

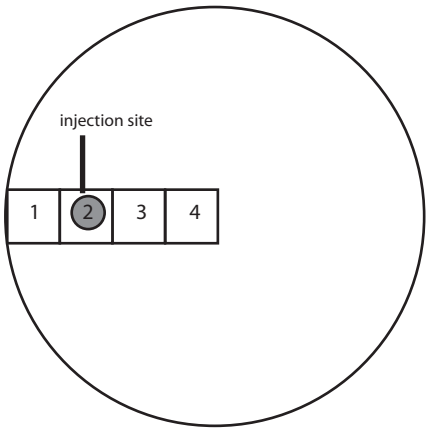
injection site
1
2
3
4

C.

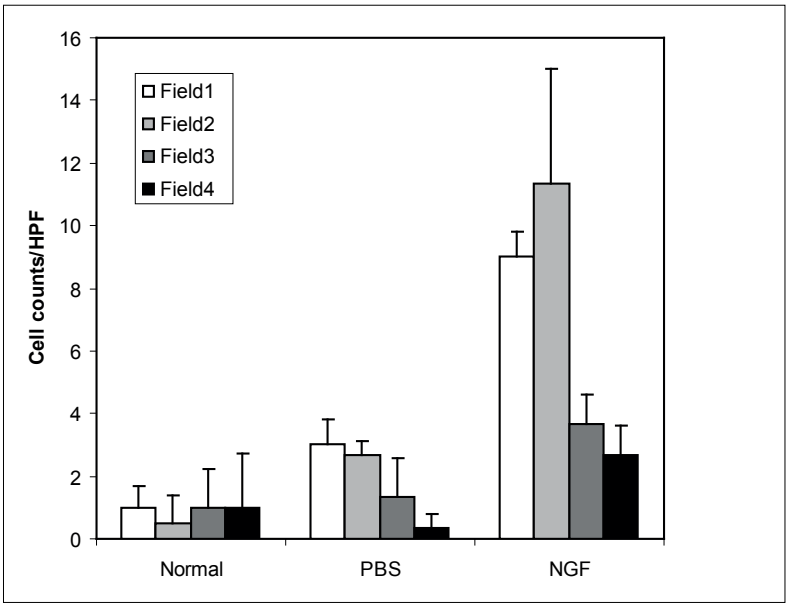
Field1
Field2
Field3
Field4
Cell counts/HPF
0
2
4
6
8
10
12
14
16
Normal
PBS
NGF

Figure 5.25 Thy1.1 staining in corneas after NGF intrastromal injection.

The corneas were harvested at 4hrs after NGF (1μg/ml) intrastromal injection then stained for thy1.1 (green). A. Staining for Thy1.1 in the injection region. Scale bar = ??? B. The thy1.1 positive cells were counted in four different fields as demonstrated. C. Number of positive cells per field. The experiment was repeated three times and the data shown are the average of three repeats. * Indicates statistical significance between PBS and NGF treatment (two-sample t-test, $p = 0.009$). Error bar: standard deviation.

IIIG. Effect of NGF on corneal innervation

Apart from its action on immune cells, NGF has also been shown to stimulate axonal growth. To assess the effect of NGF on innervation, corneal nerves were stained with antibodies against β3-tubulin (Figure 5.26). As expected, the corneal nerves were disrupted at the injection site. At the basal epithelium level, we observed that the corneas which had been injected with NGF had more staining for β3-tubulin (Figure 5.26 D~F), possibly suggesting axon growth.

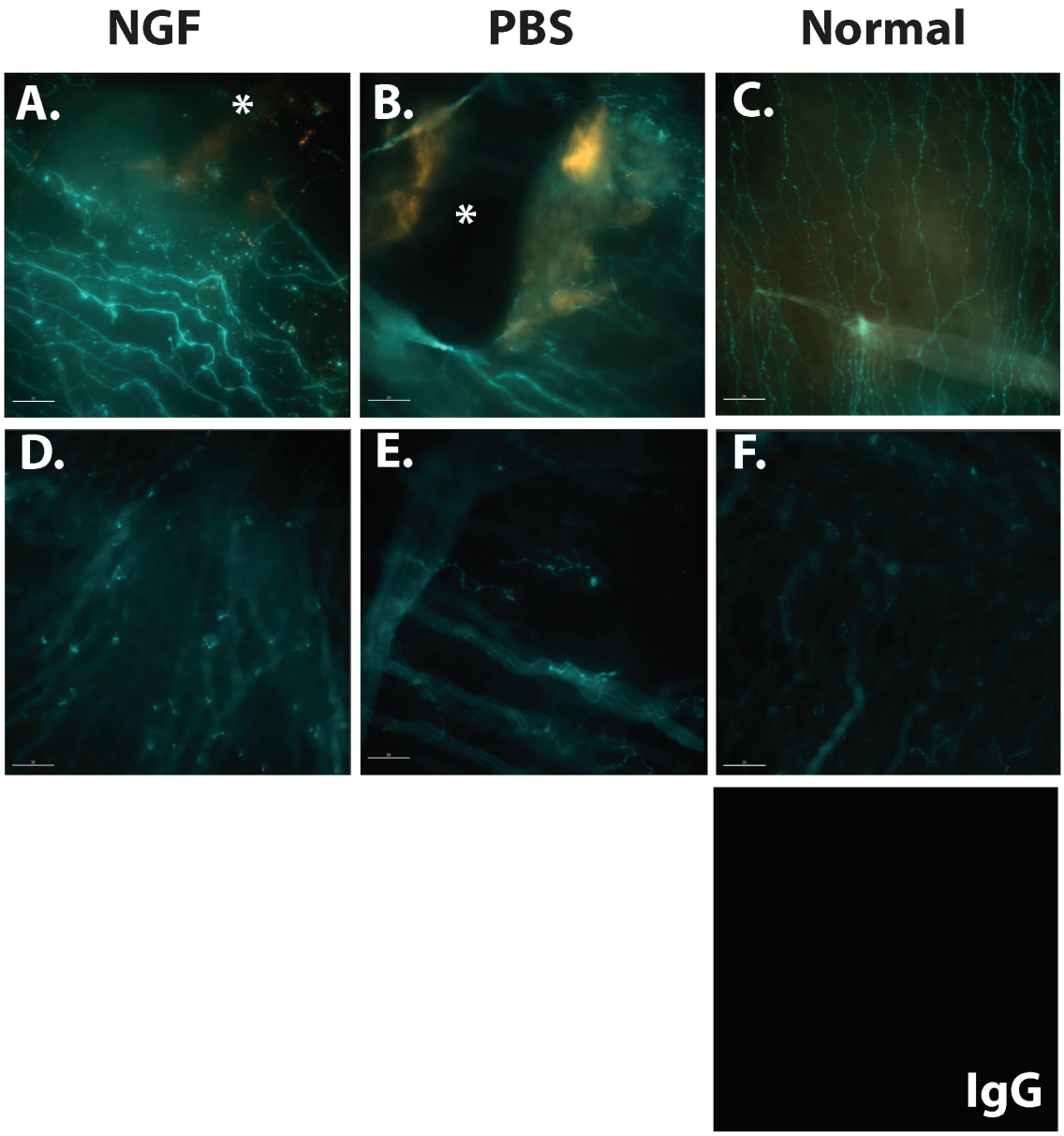
NGF
PBS
Normal
A.
B.
C.
D.
E.
F.
IgG

Figure 5.26 The effect of NGF intrastromal injection on corneal nerves.

At 4 hrs after NGF (1μg/ml) injection, the corneas were stained with antibodies against β3-tubulin (light blue). A~B. Projected images at the injection site. C. Projected image at the paralimbal region, where the intrastromal injection was usually performed. D~F. Nerve endings at the basal epithelium at the central region of the cornea. IgG: isotype control. * Indicates the site of injection. Scale bar: 20μm. The experiment has been repeated three times and the images were taken from one representative experiment.

IV. Discussion

Recent studies indicate that the cornea is endowed with monocytes and macrophages, and those cells contribute significantly to local immune responses.[142] However, the identity of the cytokines and chemokines that induce this effect and how they are regulated by the local environment in normal and disease states remains unclear. Here NGF, a factor which was effective in treating dry eye, corneal ulcer and promoting wound healing,[123, 130, 133, 140] was studied to determine if it may play a role in regulating the recruitment and differentiation of monocytic lineage cells at the ocular surface. The data indicate that NGF induced migration of monocytic lineage cells, including blood monocytes, peritoneal macrophages and spleen monocytic lineage cells and promoted differentiation of blood monocytes into dendritic like cells *in vitro*. A role for NGF modulation of monocytic lineage cells in the cornea *in vivo* was confirmed, and results showed that increased MCP-1 in response to NGF application may contribute to the effect.

NGF induced migration of monocytic lineage cells *in vitro* and the effect was mostly selective for classic monocytes. According to Randolph et al. [6,11] the non-classic subtype of blood monocytes are constantly replaced by the classic subtype of monocytes.[28] The classic subtype is considered the precursor for the other, as it is the first subtype that reappears after depletion of all monocytic lineage cells in the body.[29] The classic subpopulation may also travel back to the bone marrow and induce proliferation of specific MDPs.[30] By comparing the effect of NGF on migration of

monocytic lineage cells isolated from three different sources, it was shown here that NGF is more effective on migration of peripheral blood monocytes and the classic subtype of monocytes, suggesting that the main effect of NGF may be to induce monocytes to exit the circulation and migrate to tissues. This effect may be crucial during inflammation, in which substantial monocytic lineage cells are needed to initiate innate and adaptive immune response. However, the current experiments were performed *in vitro* where the cells were living in a simple environment. *In vivo*, the monocytes in the circulation first attach to the endothelium and then extravasate to the peripheral tissues. It remains unclear if NGF will be active in inducing the extravasation or the migration of extravasated cells only.[235] Further studies about the effect of NGF on monocyte-vascular endothelial cell interactions are needed to clarify the mechanism of how NGF acts to promote monocytic lineage cell migration.

Recently Hamrah et al. reported that normal corneas are endowed with a significant amount of resident dendritic cells and macrophages.[142] Previous researchers also showed that the corneal limbus and conjunctiva have substantial monocytic lineage cells.[250-251] The migration of these cells may be regulated by chemokines such as MCP-1 as indicated by Ebihara et al. by their *in vitro* studies.[146] The experiments here further indicated that NGF may also contribute to this. As illustrated in Figure 5.27, intrastromal injection led to discontinuation of epithelial cells and death of keratocytes at the injection site. NGF was evenly delivered into the stroma, and likely stimulated stromal cells to secret MCP-1 and induced influx of resident monocytic lineage cells to the site of injection. Meanwhile, NGF may also directly

induce migration. Possibly by diffusing into limbal vessels, similar to observed effect with MCP-1, NGF may further recruit the classic subpopulation of monocytes. The monocytic lineage cells recruited to the site of inflammation or injury, secrete cytokines and growth factors that affect corneal epithelial cells and keratocytes to facilitate wound healing.[142, 252] Moreover, differentiated macrophages and dendritic cells may function as antigen presenting cells or phagocytoze pathogens directly to regulate innate and adaptive immune responses at the ocular surface.[108, 252]

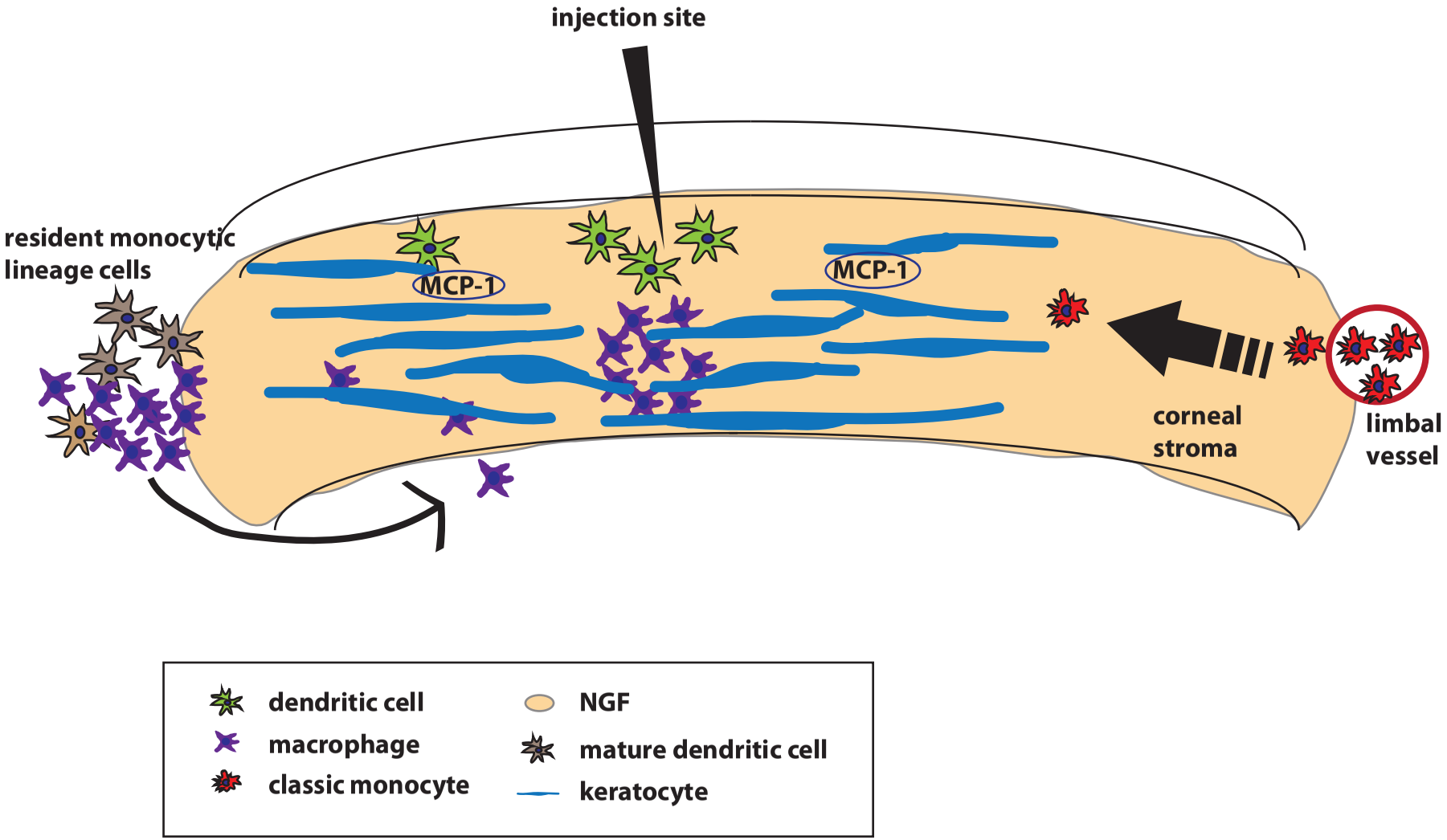
injection site
resident monocytic lineage cells
MCP-1
MCP-1
corneal stroma
limbal vessel
dendritic cell
macrophage
classic monocyte
NGF
mature dendritic cell
keratocyte

Figure 5.27 Schematic for the effect of exogenous NGF on migration of the monocytic lineage cells in the cornea.

NGF may act directly or through MCP-1 secreted from stromal cells to recruit monocytes.

Moreover, most of the *in vivo* experiments were performed at 4 hrs post injection. Compared to related studies in other tissues, this is a fairly short time period.[17,24] This was justified by the fact that the peak staining with NGF post injection in corneal stroma was at 4 hrs, and decreased gradually and almost disappeared at 24hrs. Besides, unlike other tissues such as central cornea or skin, the limbus has a great amount of monocytic lineage cells.[32] Those cells may act as a reservoir and may respond quickly to immune challenge in the cornea. However, in contrast to other studies with more severe inflammation, when we extended the observation period to 72 hrs there was not a significant recruitment of monocytic lineage cells (data not shown).[33,34] By 72 hrs, the epithelial injury caused by the injection was completely healed. Possibly the injury caused by the injection needle was comparatively weak and did not induce a significant amount of migration of MDPs.

The study has some limitations. First, the immunostaining with CD11c and CD11b in the cornea was not consistent between experiments, possibly due to an antibody penetration problem.[253] In order to quantify the migrated monocytic lineage cells, flow cytometric analysis was used to calculate the percentage of monocytic lineage cells in a single cell suspension of corneal cells. As the percentage of corneal bone marrow derived cells is very small, a pool of 10~12 corneas was required for each sample. Thus the absolute changes within each individual cornea were not determined. Flow cytometric analysis also does not provide information on which region of the cornea the cells were located. Further, very recent studies have identified additional new markers which indicate that each population of the monocytic lineage cells are related and

probably can be divided into several subpopulations. In my experiment the monocytic lineage cells were classified into classic vs. non-classic. However more markers may need to be tested for better estimation of their functions. In addition, although it was observed that NGF was capable of inducing migration of monocytic lineage cells directly *in vitro*, it is unclear if *in vivo,* NGF induces a transendothelial migration, or simply affects expression of other cytokines that promote monocytic cell migration.

In summary, these experiments showed that NGFis effective in inducing the migration of monocytic lineage cells both *in vitro* and in the cornea *in vivo* and therefore may enhance the immune responses initiated by monocytic lineage cells. This study provided some evidence that NGF may be useful in clinical therapy for corneal injuries via its effect on monocytic lineage cells.

Chapter 6. General conclusion and discussion

Previous studies in animal models of dry eye, corneal ulcer, and refractive surgeries support the concept that NGF is beneficial in increasing recovery of corneal innervation and wound healing responses. These studies have indicated that NGF and mimetics may be promising in clinical therapy. However, compared with studies conducted in other organs of the body, such as brain, skin and bronchus, the effects of NGF at the ocular surface, especially its effect on structural and immune cells, are not well understood. In the current study, a significant correlation between endogeneous NGF and TGF-β was found in established contact lens wearers, indicating that NGF may play a role in regulating cytokines involved in ocular surface inflammation. This was further confirmed by *in vitro* studies that exogenous NGF application to corneal and conjunctival epithelial cells under hyperosmolar stress decreased pro-inflammatory molecules and increased anti-inflammatory molecules. These findings support an anti-inflammatory role for NGF in the cornea. The effect of NGF on monocytic lineage cells at the ocular surface was also studied using a murine model. Consistent with previous reports, NGF enhanced migration and differentiation of the monocytic lineage cells *in vitro* and *in vivo,* suggesting that NGF may also regulate immune responses at the ocular surface.

Generally, the effect of NGF can be classified into three categories based on its target cells: on immune cells and structural cells and on cells in the nervous system. In the following section the possible role of NGF at the ocular surface will be discussed in these three categories.

I. Effect of NGF on immune cells at the ocular surface

The significant new finding presented in this work is that NGF induced migration of monocytic lineage cells, both *in vivo* and *in vitro* in the current study. This effect was probably via MCP-1, the key chemokine for recruiting monocytic lineage cells in the body.[229] NGF is likely to have promoted secretion of MCP-1 from activated keratocytes, after which, it diffused into the limbus and conjunctiva and induced influx of monocytic lineage cells. MCP-1 may also diffuse into the anterior chamber and attract monocytes and macrophages into the anterior chamber. In this work MCP-1 was detected using ELISA, although this did not allow identification of the cellular source of the MCP-1 that was produced. Although NGF increased MCP-1 secretion from keratocytes, it remains unclear if keratocytes are the only or even the major source of MCP-1. Other potential sources such as corneal epithelial cells, endothelial cells, Schwann cells, influxed neurotrophils and lacrimal gland (which may secrete NGF into the tear film) may also contribute to the increased level of MCP-1. Expression of CCR2, the MCP-1 receptor should also be determined in future studies using immunostaining.

The current study only tested the effect of NGF on monocytic lineage cells. However, according to the literature, NGF also affects migration, differentiation and function of other immune cells such as neutrophils, mast cells, and lymphocytes in inflammation.[18] The migration pattern of these cells needs also to be tested to fully understand the effect of NGF on corneal immune responses.

II.Effect of NGF on structural cells at the ocular surface

The current study tested the effect of NGF on a corneal epithelial cell line, a conjunctival epithelial cell line and human primary corneal epithelial cells *in vitro* and found that NGF increased cell viability in response to hyperosmolar stress. The observed effect of NGF can be explained by a combination of increased cell proliferation and decreased cell death which is supported by previous studies by Lambiase et al. and Chang et al.[194, 254] Moreover, NGF was also found to regulate production of cytokines and growth factors at the ocular surface and therefore likely plays an anti-inflammatory role.

Although not tested in the current study, NGF has also been shown to regulate the proliferation, survival, and functions of other structural cells *in vitro*. Lambiase et al. reported that NGF increases proliferation of goblet cells and MUC5AC mRNA and protein expression. The differentiation of keratocytes into myofibroblasts was also enhanced by NGF *in vitro*, indicating that NGF may be important for wound closure. [118] This evidence suggests that NGF plays an important role in maintaining normal structure and functions of the ocular surface. Under stress, NGF may increase the proliferation and differentiation of corneal and conjunctival epithelial cells, and keratocytes and therefore facilitate wound healing.

The current study, however, only used *in vitro* cell lines. In the literature, there have been several phase 1 and phase 2 studies that also reported that NGF facilitates recovery of corneal epithelial cells from stress *in vivo* such as the study by Lambiase et al.

on corneal ulcer subjects, and Gong et al. on rats with corneal transplant.[129, 255] Although very promising, NGF has not yet been approved for clinical therapy.

III. Effect of NGF on corneal innervation

Although not the major focus of the present study, some information reagarding the effects of NGF on corneal nerves can be draw from the results. The results in the mouse model supported that NGF enhanced the nerve growth. At the site of the intrastromal injection, the nerves were clearly disrupted. Meanwhile, the injected NGF can induce growth of nerves nearby and finally may lead to recovery of normal corneal innervation. This supports the findings by Lambiase et al. that NGF was beneficial for recovery from neurodegenerative corneal ulcer and from Lee et al. that NGF may be useful in increasing nerve recovery after refractive surgeries.[130, 193] In subjects with established contact lens wear and dry eye, in conflict with previous reports, the data indicated that increased NGF did not correlate with increased corneal innervation. This can be explained by the fact that these patients only have minimal nerve damage that did not stimulate NGF production. In order to delineate the specific effects of NGF on human corneal innervation, it is critical to include control groups with severe nerve injuries, such as patients with neurodegenerative corneal ulcer, or patients after refractive surgeries.

The current study with intrastromal injection of NGF indicated that staining of β3-tubulin, a microtubule protein, was increased with NGF intrastromal application, suggesting that NGF may stimulate the sprouting of axonal terminals through rearrangement of microtubules. Heerssen et al. showed that NGF regulated the

rearrangement of microtubules and actin and then stimulated axonal growth.[256] Subsequently the transportation of other neurotransmitters, such as substance P, CGRP and opion (a central neurotranmitter for pain sensation) may be affected. For better understanding of the functions of NGF on corneal nerve axons, additional studies to define changes in the ultrastructure, and the effect of NGF on expression of neuropeptides secreted in the cornea will be required.

Although previous studies have reported that TrkA and p75 are expressed on nerve axons in other tissues,[257] the present study did not measure the expression of these receptors *in vivo*. However it was observed, from the *in vitro* study, that TrkA receptor was up-regulated with exogenous NGF. Therefore the injection of NGF in the present mouse model was hypothesized to increase TrkA on affected axons, resulting in increased formation of the TrkA-NGF complex, which would be internalized to modulate transcription of target genes necessary for nerve growth.[258] To justify this speculation, further studies need to be performed to investigate the presence of TrkA receptors on corneal nerves in normal and injured corneas.

Mature myelinating Schwann cells in adults downregulate NGF expression to undetectable levels, but after nerve injury, reactive and dedifferentiated Schwann cells markedly upregulate NGF production *in vivo*. *In vitro*, NGF expression by Schwann cells is upregulated by cytokines and other inflammatory mediators.[259-260] In the cornea, Schwann cell expression of NGF has never been tested; however it is presumed that Schwann cells also secrete NGF and express TrkA and p75 receptor under stress.

In general, NGF may act as a mediator between the structural, nervous and immune systems at the ocular surface. In normal status, NGF helps maintain homeostasis, and structure. With inflammatory or immune stimuli, NGF may be up-regulated and facilitate wound healing and decrease inflammatory responses.

Appendix I. Summary of major cell surface antigens used in this thesis and their expression in mouse.

Major characterizing antigen	Description	Expression
B220	CD45R	**B lymphocytes**; plasmacytoid dendritic cells
CD3	Associated with T cell receptor	**T-lymphocytes**
CD4	Co-receptor that assists the T cell receptor	Thymocytes, subpopulation of mature **T cells** and dendritic cells
CD8	Co-receptor that assists the T cell receptor	Subpopulation of mature **T cells** and dendritic cells
CD115	A receptor for macrophage colony stimulating factor or colony stimulating factor-1	**Monocytes, macrophages**, osteoclasts, and some epithelial cells
CD11b	Integrin α_M. Associates with CD18 to form $\alpha_M\beta_2$ integrin (Mac-1)	**Macrophages**, NK cells, **granulocytes**, **activated lymphocytes and mouse B-1 cells**
CD11c	Integrin α_X. Associates with β_2 integrin to form the CD11c/CD18 heterodimer	**Dendritic cells, a subset of monocytes** and some activated T cells
CX3CR1	A chemokine receptor	Spleen cells; some epithelial cells, fibroblasts, **a subset of monocytes, a subset of macrophages**
E-cadherin	Epithelial cadherin, involved in intercellular adhesion	**Epithelial cells**
F4/80	Member of the EGF TM7 family	**Mature macrophages, Langerhans cells, all bone marrow cells stimulated *in vitro* with M-CSF**
IA^b	MHC class II molecule	**Antigen presenting cells**
Ly6C	A GPI-linked protein of the Ly6 family	**Monocytes/macrophages**, endothelial cells and granulocytes as well as a subset of lymphocytes

Major characterizing antigen	Description	Expression
Ly6G	Myeloid differentiation antigen Gr-1	Bone marrow granulocytes, peripheral **neutrophils**
Thy1.1	CD90.1	Hematopoietic stem cells, mature T cells, thymocytes, neurons, inflammed endothelia and **fibroblasts**
Thy1.2	CD90.2	Thymocytes and mature T cells as well as **neurons, fibroblasts and myofibroblasts**
β3-tubulin	Microtubule subunit	Embryonic stem cells, **neurons and axons**

- Bold text indicates the major cell types which the specific surface marker was used to identify in the literature.
- The description and expression data were cited from the information provided by the manufacturer of the antibodies.

Appendix II. Summary of the widely used surface antigens in murine monocytic lineage cells and related cells

Cell type	Major characterizing antigens
Monocytes Classic subtype	CD115+, CD204+, CCR2+, CX3CR1^{low} , GR1+, CD62L+, CD11c-, CD43-
Monocytes Non-Classic subtype	CD115+, CD204+, CCR2-, CX3CR1^{high} and GR1-, CD11c+, CD43+, CD62L-
Conventional Macrophages	F4/80+, CD204+, Dectin1+, CCR2+, CX3CR1^{low} , GR1+
Inflammatory macrophages	F4/80+, CD204+, Dectin1+, CCR2-, CX3CR1^{high} and GR1-
Conventional dendritic cells	CD11c+, CD11b+/-, CD8α–
Inflammatory dendritic cells	CD115+, CD11b+, GR1+
Plasmacytoid DC	CD11c– CD123^{high}, CD40-, CCR7+
MDP	CD115+, CD117^{low}, CX3CR1+ CD40+

- References for the information in the table: [109-110, 245, 261-263]

Appendix III. Matlab programme for measurement of corneal nerve density

```
function varargout = Axon_Length(varargin)
% AXON_LENGTH M-file for Axon_Length.fig
%      AXON_LENGTH, by itself, creates a new AXON_LENGTH or
raises the existing
%      singleton*.
%
%      H = AXON_LENGTH returns the handle to a new AXON_LENGTH or
the handle to
%      the existing singleton*.
%
%      AXON_LENGTH('CALLBACK',hObject,eventData,handles,...)
calls the local
%      function named CALLBACK in AXON_LENGTH.M with the given
input arguments.
%
%      AXON_LENGTH('Property','Value',...) creates a new
AXON_LENGTH or raises the
%      existing singleton*.  Starting from the left, property
value pairs are
%      applied to the GUI before Axon_Length_OpeningFunction gets
called.  An
%      unrecognized property name or invalid value makes property
application
%      stop.  All inputs are passed to Axon_Length_OpeningFcn via
varargin.
%
%      *See GUI Options on GUIDE's Tools menu.  Choose "GUI
allows only one
%      instance to run (singleton)".
%
% See also: GUIDE, GUIDATA, GUIHANDLES

% Copyright 2002-2003 The MathWorks, Inc.

% Edit the above text to modify the response to help Axon_Length

% Last Modified by GUIDE v2.5 09-Nov-2006 11:54:19

% Begin initialization code - DO NOT EDIT
gui_Singleton = 1;
gui_State = struct('gui_Name',       mfilename, ...
                   'gui_Singleton',  gui_Singleton, ...
                   'gui_OpeningFcn', @Axon_Length_OpeningFcn, ...
                   'gui_OutputFcn',  @Axon_Length_OutputFcn, ...
                   'gui_LayoutFcn',  [] , ...
                   'gui_Callback',   []);
if nargin && ischar(varargin{1})
    gui_State.gui_Callback = str2func(varargin{1});
end
```

```
    if nargout
        [varargout{1:nargout}] = gui_mainfcn(gui_State, varargin{:});
    else
        gui_mainfcn(gui_State, varargin{:});
    end
    % End initialization code - DO NOT EDIT


    % --- Executes just before Axon_Length is made visible.
    function Axon_Length_OpeningFcn(hObject, eventdata, handles,
varargin)
    % This function has no output args, see OutputFcn.
    % hObject    handle to figure
    % eventdata  reserved - to be defined in a future version of
MATLAB
    % handles    structure with handles and user data (see GUIDATA)
    % varargin   command line arguments to Axon_Length (see VARARGIN)

    set(handles.text1, 'HitTest', 'off');
    set(handles.text2, 'HitTest', 'off');
    set(handles.fileinfo, 'String', [], 'HitTest', 'off');
    set(handles.text2, 'HitTest', 'off');
    set(handles.openfile, 'Enable', 'on', 'HitTest', 'off');
    set(handles.start, 'Enable', 'off', 'HitTest', 'off');
    set(handles.finish, 'Enable', 'off', 'HitTest', 'off');
    set(handles.reset, 'Enable', 'off', 'HitTest', 'off');
    set(handles.length, 'String', [], 'HitTest', 'off');
    set(handles.axes1, 'HitTest', 'on');

    axes(handles.axes1);
    axis off;

    handles.point1 = [];
    handles.point2 = [];
    handles.distance = 0;

    % Choose default command line output for Axon_Length
    handles.output = hObject;

    % Update handles structure
    guidata(hObject, handles);

    % UIWAIT makes Axon_Length wait for user response (see UIRESUME)
    % uiwait(handles.figure1);


    % --- Outputs from this function are returned to the command line.
    function varargout = Axon_Length_OutputFcn(hObject, eventdata,
handles)
    % varargout  cell array for returning output args (see VARARGOUT);
    % hObject    handle to figure
    % eventdata  reserved - to be defined in a future version of
MATLAB
    % handles    structure with handles and user data (see GUIDATA)
```

```
      % Get default command line output from handles structure
      varargout{1} = handles.output;



      function fileinfo_Callback(hObject, eventdata, handles)
      % hObject    handle to fileinfo (see GCBO)
      % eventdata  reserved - to be defined in a future version of
MATLAB
      % handles    structure with handles and user data (see GUIDATA)

      % Hints: get(hObject,'String') returns contents of fileinfo as
text
      %        str2double(get(hObject,'String')) returns contents of
fileinfo as a double


      % --- Executes during object creation, after setting all
properties.
      function fileinfo_CreateFcn(hObject, eventdata, handles)
      % hObject    handle to fileinfo (see GCBO)
      % eventdata  reserved - to be defined in a future version of
MATLAB
      % handles    empty - handles not created until after all
CreateFcns called

      % Hint: edit controls usually have a white background on Windows.
      %       See ISPC and COMPUTER.
      if ispc && isequal(get(hObject,'BackgroundColor'),
get(0,'defaultUicontrolBackgroundColor'))
          set(hObject,'BackgroundColor','white');
      end



      % --- Executes on button press in openfile.
      function openfile_Callback(hObject, eventdata, handles)
      % hObject    handle to openfile (see GCBO)
      % eventdata  reserved - to be defined in a future version of
MATLAB
      % handles    structure with handles and user data (see GUIDATA)

      [filename, pathway] = uigetfile('*.jpg', 'Please select the JPEG
file you want to process:');

      if filename ~= 0

          colormap(gray(256));

          handles.image2process = imread([pathway, filename]);
          axes(handles.axes1);
          image(handles.image2process);
          axis off;

          set(handles.text1, 'HitTest', 'off');
```

```
            set(handles.text2, 'HitTest', 'off');
            set(handles.fileinfo, 'String', [pathway, filename],
'HitTest', 'off');
            set(handles.openfile, 'Enable', 'on', 'HitTest', 'off');
            set(handles.start, 'Enable', 'on', 'HitTest', 'off');
            set(handles.finish, 'Enable', 'off', 'HitTest', 'off');
            set(handles.reset, 'Enable', 'off', 'HitTest', 'off');
            set(handles.length, 'String', [], 'HitTest', 'off');
            set(handles.axes1, 'HitTest', 'on');

            handles.point1 = [];
            handles.point2 = [];
            handles.distance = 0;

        else

        end

        guidata(hObject, handles);




        % --- Executes on button press in start.
        function start_Callback(hObject, eventdata, handles)
        % hObject    handle to start (see GCBO)
        % eventdata  reserved - to be defined in a future version of
MATLAB
        % handles    structure with handles and user data (see GUIDATA)

        handles.point1 = [];
        handles.point2 = [];
        handles.distance = 0;

        axes(handles.axes1);
        hold on;

        while 1

            [m,n] = ginput(1);

            if m > 768 | m < 0 | n > 576 | n < 0

                break

            else

                handles.point1 = handles.point2;
                handles.point2 = [m,n];

                if ~isempty(handles.point1)
```

```
                    handles.distance = handles.distance +
(sum((handles.point2 - handles.point1) .^ 2)) ^ 0.5 / 1.78;
                    axes(handles.axes1);
                    plot(handles.point1(1), handles.point1(2), 'yo',...
                        'MarkerFaceColor', 'y', 'MarkerSize', 1.5);
                    plot(handles.point2(1), handles.point2(2), 'yo',...
                        'MarkerFaceColor', 'y', 'MarkerSize', 1.5);
                    axis off;
                    grid off;

                else

                    axes(handles.axes1);
                    plot(handles.point2(1), handles.point2(2), 'yo',...
                        'MarkerFaceColor', 'y', 'MarkerSize', 1.5);
                    axis off;
                    grid off;

                end

                set(handles.finish, 'Enable', 'on');
                set(handles.reset, 'Enable', 'on');

            end

        end

        axes(handles.axes1);
        hold off;

        guidata(hObject, handles);




        % --- Executes on button press in finish.
        function finish_Callback(hObject, eventdata, handles)
        % hObject    handle to finish (see GCBO)
        % eventdata  reserved - to be defined in a future version of
MATLAB
        % handles    structure with handles and user data (see GUIDATA)

        set(handles.length, 'String', [num2str(handles.distance), '
micron']);




        % --- Executes on button press in reset.
        function reset_Callback(hObject, eventdata, handles)
        % hObject    handle to reset (see GCBO)
        % eventdata  reserved - to be defined in a future version of
MATLAB
```

```
      % handles    structure with handles and user data (see GUIDATA)

      axes(handles.axes1);
      image(handles.image2process);
      axis off;
      hold off;

      set(handles.openfile, 'Enable', 'on', 'HitTest', 'off');
      set(handles.start, 'Enable', 'on', 'HitTest', 'off');
      set(handles.finish, 'Enable', 'off', 'HitTest', 'off');
      set(handles.reset, 'Enable', 'off', 'HitTest', 'off');
      set(handles.length, 'String', [], 'HitTest', 'off');




      function length_Callback(hObject, eventdata, handles)
      % hObject    handle to length (see GCBO)
      % eventdata  reserved - to be defined in a future version of
MATLAB
      % handles    structure with handles and user data (see GUIDATA)

      % Hints: get(hObject,'String') returns contents of length as text
      %        str2double(get(hObject,'String')) returns contents of
length as a double


      % --- Executes during object creation, after setting all
properties.
      function length_CreateFcn(hObject, eventdata, handles)
      % hObject    handle to length (see GCBO)
      % eventdata  reserved - to be defined in a future version of
MATLAB
      % handles    empty - handles not created until after all
CreateFcns called

      % Hint: edit controls usually have a white background on Windows.
      %       See ISPC and COMPUTER.
      if ispc && isequal(get(hObject,'BackgroundColor'),
get(0,'defaultUicontrolBackgroundColor'))
          set(hObject,'BackgroundColor','white');
      end
```

Appendix IV. Ocular surface dry eye index (OSDI) questionnaire

Ocular Surface Disease Index© (OSDI©)[2]

Ask your patients the following 12 questions, and circle the number in the box that best represents each answer. Then, fill in boxes A, B, C, D, and E according to the instructions beside each.

Have you experienced any of the following *during the last week*?	All of the time	Most of the time	Half of the time	Some of the time	None of the time
1. Eyes that are sensitive to light? . .	4	3	2	1	0
2. Eyes that feel gritty?	4	3	2	1	0
3. Painful or sore eyes?	4	3	2	1	0
4. Blurred vision?	4	3	2	1	0
5. Poor vision?	4	3	2	1	0

Subtotal score for answers 1 to 5 (A)

Have problems with your eyes limited you in performing any of the following *during the last week*?	All of the time	Most of the time	Half of the time	Some of the time	None of the time	N/A
6. Reading?.	4	3	2	1	0	N/A
7. Driving at night?	4	3	2	1	0	N/A
8. Working with a computer or bank machine (ATM)?.	4	3	2	1	0	N/A
9. Watching TV?	4	3	2	1	0	N/A

Subtotal score for answers 6 to 9 (B)

Have your eyes felt uncomfortable in any of the following situations *during the last week*?	All of the time	Most of the time	Half of the time	Some of the time	None of the time	N/A
10. Windy conditions?.	4	3	2	1	0	N/A
11. Places or areas with low humidity (very dry)?	4	3	2	1	0	N/A
12. Areas that are air conditioned?. . .	4	3	2	1	0	N/A

Subtotal score for answers 10 to 12 (C)

Add subtotals A, B, and C to obtain D
(D = sum of scores for all questions answered) (D)

Total number of questions answered
(do not include questions answered N/A) (E)

Please turn over the questionnaire to calculate the patient's final OSDI© score.

Evaluating the OSDI© Score[1]

The OSDI© is assessed on a scale of 0 to 100, with higher scores representing greater disability. The index demonstrates sensitivity and specificity in distinguishing between normal subjects and patients with dry eye disease. The OSDI© is a valid and reliable instrument for measuring dry eye disease (normal, mild to moderate, and severe) and effect on vision-related function.

Assessing Your Patient's Dry Eye Disease[1, 2]

Use your answers D and E from side 1 to compare the sum of scores for all questions answered (D) and the number of questions answered (E) with the chart below.* Find where your patient's score would fall. Match the corresponding shade of red to the key below to determine whether your patient's score indicates normal, mild, moderate, or severe dry eye disease.

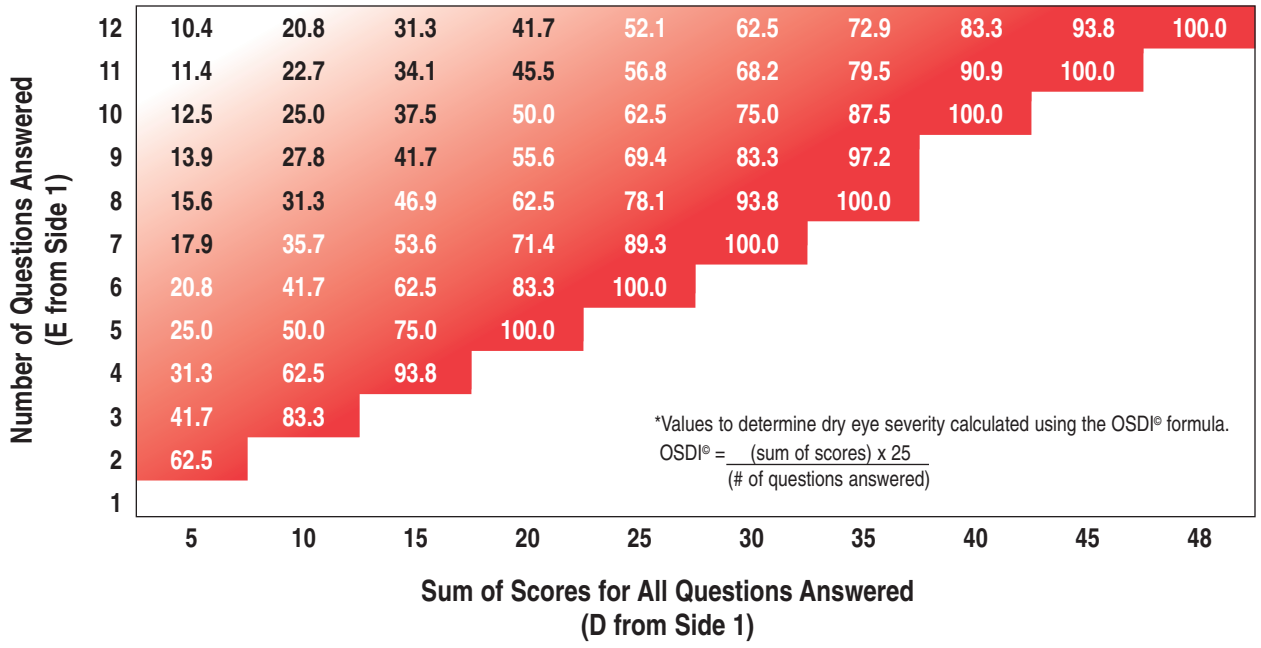

Normal **Mild** **Moderate** **Severe**

Patient's Name: _____ **Date:** _____

How long has the patient experienced dry eye disease? _____

Eye Care Professional's Comments: _____

_____

_____

_____

_____

1. Data on file, Allergan, Inc.
2. Schiffman RM, Christianson MD, Jacobsen G, Hirsch JD, Reis BL. Reliability and validity of the Ocular Surface Disease Index. *Arch Ophthalmol.* 2000;118:615-621

Appendix V. Original picture of inflammatory cytokine array film.

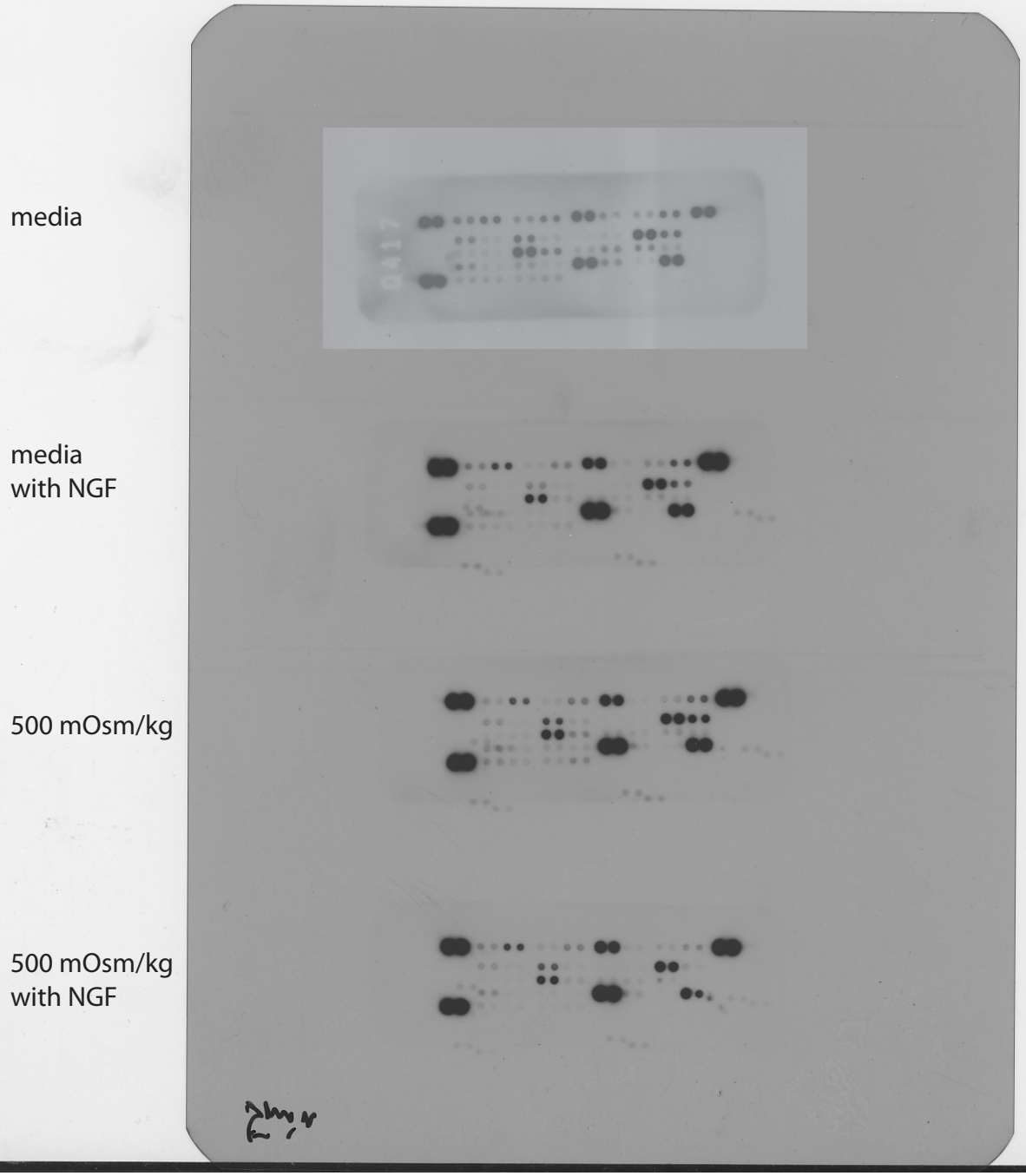

Appendix VI. PCR primer validation

	Sequence
GAPDH	forward 5'-GCCAAGGTCATCCATGACAAC-3', reverse 5'-GTCCACCACCCTGTTGCTGTA-3
Expected product size: 495 bp Melting temperature: 59℃ Dissociation curve: two peaks Efficiency: 90%	
TLR4	forward 5′ - AGCCACGCATTCACAGGG -3′ , reverse 5′ - CATGGCTGGGATCAGAGTCC -3′
Expected product size: 131 bp Melting temperature: 58℃ Dissociation curve: one peak Efficiency: 95%	
TLR9	forward 5′ -ACTGTTCAGCCGGAGATGTTT -3′ , reverse 5′ -TCAGGGCCTTCAGCTGGTTTC -3
Expected product size: 622 bp Melting temperature: 60℃ Dissociation curve: one peak Efficiency: 98%	
HLA-DR	forward: 5’-GGGCATTCCATAGCAGAGACA-3’ reverse: 5’-TGGGACCATCTTCATCATCAA-3’
Expected product size: 1118 bp Melting temperature: 58℃ Dissociation curve: one peak Efficiency: 96%	
TGF-β1	forward 5'- TTCAAGCAGAGTACACACAGCATA -3', reverse 5'- ACTCCGGTGACATCAAAAGATAAC -3'
Expected product size: 1328 bp Melting temperature: 58℃ Dissociation curve: one peak Efficiency: 102%	
TGF-β2	forward 5'- AGACTTGAGTCACAACAGACCAAC -3', reverse 5'- TATATAAGCTCAGGACCCTGCTGT -3'
Expected product size: 553 bp Melting temperature: 58℃ Dissociation curve: one peak Efficiency: 98%	
NGFB	forward 5'- TACTGTGGACCCCAGGCTGT -3', reverse 5'- TCTTATCCCCAACCCACACG -3'
Expected product size: 230 bp Melting temperature: 59℃ Dissociation curve: one peak	

Efficiency: 92%	
NTRK1	forward 5'- CTGTGCTGGCTCCAGAGGAT -3', reverse 5'- AGGAGGTTGTGGCACTCAGC -3'
Expected product size: 729 bp Melting temperature: 58℃ Dissociation curve: one peak Efficiency: 97%	
IL-13[204]	forward 5'- GCCCTGGAATCCCTGATCA -3', reverse 5'- GCTCAGCATCCTCTGGGTCTT -3'
Expected product size: 66 bp Melting temperature: 58℃ Dissociation curve: one peak Efficiency: 95%	
IL-16[205]	forward 5'- AAGGGGCATCTCCAACATCATCAT -3', reverse 5'- CTCCTGCCAAGCTGAACCCAAGAC -3'
Expected product size: 357 bp Melting temperature: 61℃ Dissociation curve: one peak Efficiency: 91%	
IL-1α[206]	forward 5'- TGGCTCATTTTCCCTCAAAAGTTG -3', reverse 5'- AGAAATCGTGAAATCCGAAGTCAAG -3'
Expected product size: 171 bp Melting temperature: 60℃ Dissociation curve: one peak Efficiency: 92%	
MCP-1[207]	forward 5'- CGCCTCCAGCATGAAAGTCT -3', reverse 5'- ATGAAGGTGGCTGCTATG -3'
Expected product size: 63 bp Melting temperature: 57℃ Dissociation curve: one peak Efficiency: 91%	

Reference:

1. Levi-Montalcini, R. and V. Hamburger, *Selective growth stimulating effects of mouse sarcoma on the sensory and sympathetic nervous system of the chick embryo.* J Exp Zool, 1951. **116**(2): p. 321-61.
2. Bueker, E.D., *Implantation of tumors in the hind limb field of the embryonic chick and the developmental response of the lumbosacral nervous system.* Anat Rec, 1948. **102**(3): p. 369-89.
3. Levi-Montalcini, R., *The nerve growth factor: thirty-five years later.* EMBO J, 1987. **6**(5): p. 1145-54.
4. Cohen, S., *Purification of a Nerve-Growth Promoting Protein from the Mouse Salivary Gland and Its Neuro-Cytotoxic Antiserum.* Proc Natl Acad Sci U S A, 1960. **46**(3): p. 302-11.
5. Toschi, G., et al., *Characteristics of labelled RNA from spinal ganglia of chick embryo and the action of a specific growth factor (NGF).* J Neurochem, 1966. **13**(7): p. 539-44.
6. Max, S.R., et al., *Nerve growth factor-mediated induction of tyrosine hydroxylase in rat superior cervical ganglia in vitro.* J Biol Chem, 1978. **253**(22): p. 8013-5.
7. Simson, J.A., et al., *Secretagogue-mediated discharge of nerve growth factor from granular tubules of male mouse submandibular glands: an immunocytochemical study.* Anat Rec, 1978. **192**(3): p. 375-87.
8. Fanger, G.R., J.R. Jones, and R.A. Maue, *Differential regulation of neuronal sodium channel expression by endogenous and exogenous tyrosine kinase receptors expressed in rat pheochromocytoma cells.* J Neurosci, 1995. **15**(1 Pt 1): p. 202-13.
9. Mesner, P.W., et al., *A timetable of events during programmed cell death induced by trophic factor withdrawal from neuronal PC12 cells.* J Neurosci, 1995. **15**(11): p. 7357-66.
10. Yoo, Y.E., et al., *Iron enhances NGF-induced neurite outgrowth in PC12 cells.* Mol Cells, 2004. **17**(2): p. 340-6.
11. Nemoto, K., et al., *Gene expression of neurotrophins and their receptors in cultured rat vascular smooth muscle cells.* Biochem Biophys Res Commun, 1998. **245**(1): p. 284-8.
12. Olgart, C. and N. Frossard, *Human lung fibroblasts secrete nerve growth factor: effect of inflammatory cytokines and glucocorticoids.* Eur Respir J, 2001. **18**(1): p. 115-21.
13. Pons, F., et al., *Nerve growth factor secretion by human lung epithelial A549 cells in pro- and anti-inflammatory conditions.* Eur J Pharmacol, 2001. **428**(3): p. 365-9.
14. Bruni, A., et al., *Interaction between nerve growth factor and lysophosphatidylserine on rat peritoneal mast cells.* FEBS Lett, 1982. **138**(2): p. 190-2.
15. Lambiase, A., et al., *Increased plasma levels of nerve growth factor in vernal keratoconjunctivitis and relationship to conjunctival mast cells.* Invest Ophthalmol Vis Sci, 1995. **36**(10): p. 2127-32.

16. Aalto, K., et al., *Nerve growth factor in serum of children with systemic lupus erythematosus is correlated with disease activity.* Cytokine, 2002. **20**(3): p. 136-9.
17. Lambiase, A., et al., *Nerve growth factor and the immune system: old and new concepts in the cross-talk between immune and resident cells during pathophysiological conditions.* Curr Opin Allergy Clin Immunol, 2004. **4**(5): p. 425-30.
18. Freund, V. and N. Frossard, *[Nerve growth factor (NGF) in inflammation and asthma].* Rev Mal Respir, 2004. **21**(2 Pt 1): p. 328-42.
19. Bonini, S., et al., *Nerve growth factor and asthma.* Allergy, 2002. **57 Suppl 72**: p. 13-5.
20. Bax, B., et al., *Prediction of the three-dimensional structures of the nerve growth factor and epidermal growth factor binding proteins (kallikreins) and an hypothetical structure of the high molecular weight complex of epidermal growth factor with its binding protein.* Protein Sci, 1993. **2**(8): p. 1229-41.
21. Wiesmann, C. and A.M. de Vos, *Nerve growth factor: structure and function.* Cell Mol Life Sci, 2001. **58**(5-6): p. 748-59.
22. http://genome.ucsc.edu/, 2008.
23. ensemble, archive.ensembl.org, 2008. **5**.
24. Edwards, R.H. and W.J. Rutter, *Use of vaccinia virus vectors to study protein processing in human disease. Normal nerve growth factor processing and secretion in cultured fibroblasts from patients with familial dysautonomia.* J Clin Invest, 1988. **82**(1): p. 44-7.
25. Delsite, R. and D. Djakiew, *Characterization of nerve growth factor precursor protein expression by human prostate stromal cells: a role in selective neurotrophin stimulation of prostate epithelial cell growth.* Prostate, 1999. **41**(1): p. 39-48.
26. Fahnestock, M., *Structure and biosynthesis of nerve growth factor.* Curr Top Microbiol Immunol, 1991. **165**: p. 1-26.
27. Farhadi, H., et al., *Prohormone convertases in mouse submandibular gland: co-localization of furin and nerve growth factor.* J Histochem Cytochem, 1997. **45**(6): p. 795-804.
28. Fahnestock, M., et al., *The nerve growth factor precursor proNGF exhibits neurotrophic activity but is less active than mature nerve growth factor.* J Neurochem, 2004. **89**(3): p. 581-92.
29. Lee, F.S., et al., *The uniqueness of being a neurotrophin receptor.* Curr Opin Neurobiol, 2001. **11**(3): p. 281-6.
30. Bradshaw, R.A., *Nerve growth factor.* Annu Rev Biochem, 1978. **47**: p. 191-216.
31. Murphy, R.A., et al., *Molecular properties of the nerve growth factor secreted in mouse saliva.* Proc Natl Acad Sci U S A, 1977. **74**(7): p. 2672-6.
32. Bocchini, V. and P.U. Angeletti, *The nerve growth factor: purification as a 30,000-molecular-weight protein.* Proc Natl Acad Sci U S A, 1969. **64**(2): p. 787-94.
33. Buxser, S., P. Puma, and G.L. Johnson, *Properties of the nerve growth factor receptor. Relationship between receptor structure and affinity.* J Biol Chem, 1985. **260**(3): p. 1917-26.

34. Martin-Zanca, D., S.H. Hughes, and M. Barbacid, *A human oncogene formed by the fusion of truncated tropomyosin and protein tyrosine kinase sequences.* Nature, 1986. **319**(6056): p. 743-8.
35. Frade, J.M. and Y.A. Barde, *Nerve growth factor: two receptors, multiple functions.* Bioessays, 1998. **20**(2): p. 137-45.
36. Huang, C.M., et al., *Proteomic analysis of proteins in PC12 cells before and after treatment with nerve growth factor: increased levels of a 43-kDa chromogranin B-derived fragment during neuronal differentiation.* Brain Res Mol Brain Res, 2001. **92**(1-2): p. 181-92.
37. Friedman, W.J., *Neurotrophins induce death of hippocampal neurons via the p75 receptor.* J Neurosci, 2000. **20**(17): p. 6340-6.
38. Windisch, J.M., R. Marksteiner, and R. Schneider, *Nerve growth factor binding site on TrkA mapped to a single 24-amino acid leucine-rich motif.* J Biol Chem, 1995. **270**(47): p. 28133-8.
39. Chao, M.V. and B.L. Hempstead, *p75 and Trk: a two-receptor system.* Trends Neurosci, 1995. **18**(7): p. 321-6.
40. Squinto, S.P., et al., *trkB encodes a functional receptor for brain-derived neurotrophic factor and neurotrophin-3 but not nerve growth factor.* Cell, 1991. **65**(5): p. 885-93.
41. Koide, T., et al., *Localization of trkB and low-affinity nerve growth factor receptor mRNA in the developing rat retina.* Neurosci Lett, 1995. **185**(3): p. 183-6.
42. Rose, C.R., et al., *Truncated TrkB-T1 mediates neurotrophin-evoked calcium signalling in glia cells.* Nature, 2003. **426**(6962): p. 74-8.
43. Yamauchi, J., J.R. Chan, and E.M. Shooter, *Neurotrophin 3 activation of TrkC induces Schwann cell migration through the c-Jun N-terminal kinase pathway.* Proc Natl Acad Sci U S A, 2003. **100**(24): p. 14421-6.
44. Greene, L.A. and A.S. Tischler, *Establishment of a noradrenergic clonal line of rat adrenal pheochromocytoma cells which respond to nerve growth factor.* Proc Natl Acad Sci U S A, 1976. **73**(7): p. 2424-8.
45. Stephens, R.M., et al., *Trk receptors use redundant signal transduction pathways involving SHC and PLC-gamma 1 to mediate NGF responses.* Neuron, 1994. **12**(3): p. 691-705.
46. Vetter, M.L., et al., *Nerve growth factor rapidly stimulates tyrosine phosphorylation of phospholipase C-gamma 1 by a kinase activity associated with the product of the trk protooncogene.* Proc Natl Acad Sci U S A, 1991. **88**(13): p. 5650-4.
47. Neri, L.M., et al., *Increase in nuclear phosphatidylinositol 3-kinase activity and phosphatidylinositol (3,4,5) trisphosphate synthesis precede PKC-zeta translocation to the nucleus of NGF-treated PC12 cells.* FASEB J, 1999. **13**(15): p. 2299-310.
48. Berninger, B., et al., *BDNF and NT-3 induce intracellular Ca2+ elevation in hippocampal neurones.* Neuroreport, 1993. **4**(12): p. 1303-6.
49. Woo, C.W., E. Lucarelli, and C.J. Thiele, *NGF activation of TrkA decreases N-myc expression via MAPK path leading to a decrease in neuroblastoma cell number.* Oncogene, 2004. **23**(8): p. 1522-30.

50. Wang, L.H., A.J. Paden, and E.M. Johnson, Jr., *Mixed-lineage kinase inhibitors require the activation of Trk receptors to maintain long-term neuronal trophism and survival.* J Pharmacol Exp Ther, 2005. **312**(3): p. 1007-19.
51. Fiori, J.L., et al., *Dysregulation of the BMP-p38 MAPK signaling pathway in cells from patients with fibrodysplasia ossificans progressiva (FOP).* J Bone Miner Res, 2006. **21**(6): p. 902-9.
52. Brodie, C., et al., *Protein kinase C-epsilon plays a role in neurite outgrowth in response to epidermal growth factor and nerve growth factor in PC12 cells.* Cell Growth Differ, 1999. **10**(3): p. 183-91.
53. Pierchala, B.A., et al., *Nerve growth factor promotes the survival of sympathetic neurons through the cooperative function of the protein kinase C and phosphatidylinositol 3-kinase pathways.* J Biol Chem, 2004. **279**(27): p. 27986-93.
54. Davis, P.K., S.M. Dudek, and G.V. Johnson, *Select alterations in protein kinases and phosphatases during apoptosis of differentiated PC12 cells.* J Neurochem, 1997. **68**(6): p. 2338-47.
55. Ashcroft, M., et al., *The selective and inducible activation of endogenous PI 3-kinase in PC12 cells results in efficient NGF-mediated survival but defective neurite outgrowth.* Oncogene, 1999. **18**(32): p. 4586-97.
56. Yasui, H., et al., *Differential responses to nerve growth factor and epidermal growth factor in neurite outgrowth of PC12 cells are determined by Rac1 activation systems.* J Biol Chem, 2001. **276**(18): p. 15298-305.
57. Wooten, M.W., et al., *A role for zeta protein kinase C in nerve growth factor-induced differentiation of PC12 cells.* Cell Growth Differ, 1994. **5**(4): p. 395-403.
58. Ohmichi, M., S.J. Decker, and A.R. Saltiel, *Nerve growth factor stimulates the tyrosine phosphorylation of a 38-kDa protein that specifically associates with the src homology domain of phospholipase C-gamma 1.* J Biol Chem, 1992. **267**(30): p. 21601-6.
59. Segal, R.A., et al., *Differential utilization of Trk autophosphorylation sites.* J Biol Chem, 1996. **271**(33): p. 20175-81.
60. Fabian, R.H. and C.E. Hulsebosch, *Plasma nerve growth factor access to the postnatal central nervous system.* Brain Res, 1993. **611**(1): p. 46-52.
61. Obara, Y., et al., *PKA phosphorylation of Src mediates Rap1 activation in NGF and cAMP signaling in PC12 cells.* J Cell Sci, 2004. **117**(Pt 25): p. 6085-94.
62. Wood, K.W., et al., *The cytoplasmic raf oncogene induces a neuronal phenotype in PC12 cells: a potential role for cellular raf kinases in neuronal growth factor signal transduction.* Proc Natl Acad Sci U S A, 1993. **90**(11): p. 5016-20.
63. Lutz, M., et al., *Nerve growth factor mediates activation of the Smad pathway in PC12 cells.* Eur J Biochem, 2004. **271**(5): p. 920-31.
64. Kendall, S.E., et al., *Expression analysis of a novel p75(NTR) signaling protein, which regulates cell cycle progression and apoptosis.* Mech Dev, 2002. **117**(1-2): p. 187-200.
65. Mischel, P.S., et al., *The extracellular domain of p75NTR is necessary to inhibit neurotrophin-3 signaling through TrkA.* J Biol Chem, 2001. **276**(14): p. 11294-301.

66. Huebner, K., et al., *The nerve growth factor receptor gene is at human chromosome region 17q12-17q22, distal to the chromosome 17 breakpoint in acute leukemias.* Proc Natl Acad Sci U S A, 1986. **83**(5): p. 1403-7.
67. Medina, M.L., et al., *Transient vesicle leakage initiated by a synthetic apoptotic peptide derived from the death domain of neurotrophin receptor, p75NTR.* J Pept Res, 2002. **59**(4): p. 149-58.
68. Roux, P.P. and P.A. Barker, *Neurotrophin signaling through the p75 neurotrophin receptor.* Prog Neurobiol, 2002. **67**(3): p. 203-33.
69. Benzel, I., Y.A. Barde, and E. Casademunt, *Strain-specific complementation between NRIF1 and NRIF2, two zinc finger proteins sharing structural and biochemical properties.* Gene, 2001. **281**(1-2): p. 19-30.
70. Salehi, A.H., S. Xanthoudakis, and P.A. Barker, *NRAGE, a p75 neurotrophin receptor-interacting protein, induces caspase activation and cell death through a JNK-dependent mitochondrial pathway.* J Biol Chem, 2002. **277**(50): p. 48043-50.
71. Adams, I., et al., *Perineuronal nets in the rhesus monkey and human basal forebrain including basal ganglia.* Neuroscience, 2001. **108**(2): p. 285-98.
72. Hirata, H., et al., *Nerve growth factor signaling of p75 induces differentiation and ceramide-mediated apoptosis in Schwann cells cultured from degenerating nerves.* Glia, 2001. **36**(3): p. 245-58.
73. Deshmukh, M. and E.M. Johnson, Jr., *Evidence of a novel event during neuronal death: development of competence-to-die in response to cytoplasmic cytochrome c.* Neuron, 1998. **21**(4): p. 695-705.
74. Mamidipudi, V., X. Li, and M.W. Wooten, *Identification of interleukin 1 receptor-associated kinase as a conserved component in the p75-neurotrophin receptor activation of nuclear factor-kappa B.* J Biol Chem, 2002. **277**(31): p. 28010-8.
75. Ito, H., H. Nomoto, and S. Furukawa, *Growth arrest of PC12 cells by nerve growth factor is dependent on the phosphatidylinositol 3-kinase/Akt pathway via p75 neurotrophin receptor.* J Neurosci Res, 2003. **72**(2): p. 211-7.
76. Korsching, S., *The neurotrophic factor concept: a reexamination.* J Neurosci, 1993. **13**(7): p. 2739-48.
77. Djouhri, L., et al., *Time course and nerve growth factor dependence of inflammation-induced alterations in electrophysiological membrane properties in nociceptive primary afferent neurons.* J Neurosci, 2001. **21**(22): p. 8722-33.
78. Landis, S.C., J.R. Fredieu, and M. Yodlowski, *Neonatal treatment with nerve growth factor antiserum eliminates cholinergic sympathetic innervation of rat sweat glands.* Dev Biol, 1985. **112**(1): p. 222-9.
79. Gryz, E.A. and S.O. Meakin, *Acidic substitution of the activation loop tyrosines in TrkA supports nerve growth factor-independent cell survival and neuronal differentiation.* Oncogene, 2000. **19**(3): p. 417-30.
80. Ieda, M., et al., *Nerve growth factor is critical for cardiac sensory innervation and rescues neuropathy in diabetic hearts.* Circulation, 2006. **114**(22): p. 2351-63.
81. Bennett, D.L., et al., *trkA, CGRP and IB4 expression in retrogradely labelled cutaneous and visceral primary sensory neurones in the rat.* Neurosci Lett, 1996. **206**(1): p. 33-6.

82. Stucky, C.L., et al., *Overexpression of nerve growth factor in skin selectively affects the survival and functional properties of nociceptors.* J Neurosci, 1999. **19**(19): p. 8509-16.
83. Mousa, S.A., et al., *Nerve growth factor governs the enhanced ability of opioids to suppress inflammatory pain.* Brain, 2007. **130**(Pt 2): p. 502-13.
84. Chada, S.R. and P.J. Hollenbeck, *Nerve growth factor signaling regulates motility and docking of axonal mitochondria.* Curr Biol, 2004. **14**(14): p. 1272-6.
85. Salehi, A., J.D. Delcroix, and D.F. Swaab, *Alzheimer's disease and NGF signaling.* J Neural Transm, 2004. **111**(3): p. 323-45.
86. Chiarelli, F., F. Santilli, and A. Mohn, *Role of growth factors in the development of diabetic complications.* Horm Res, 2000. **53**(2): p. 53-67.
87. De Rosa, R., et al., *Intranasal administration of nerve growth factor (NGF) rescues recognition memory deficits in AD11 anti-NGF transgenic mice.* Proc Natl Acad Sci U S A, 2005. **102**(10): p. 3811-6.
88. Sofroniew, M.V., C.L. Howe, and W.C. Mobley, *Nerve growth factor signaling, neuroprotection, and neural repair.* Annu Rev Neurosci, 2001. **24**: p. 1217-81.
89. Varilek, G.W., et al., *Nerve growth factor synthesis by intestinal epithelial cells.* Am J Physiol, 1995. **269**(3 Pt 1): p. G445-52.
90. Ishida, K., et al., *Expression of neurotrophic factors in cultured human retinal pigment epithelial cells.* Curr Eye Res, 1997. **16**(2): p. 96-101.
91. Cantarella, G., et al., *Nerve growth factor-endothelial cell interaction leads to angiogenesis in vitro and in vivo.* FASEB J, 2002. **16**(10): p. 1307-9.
92. Mitsuma, N., et al., *Wide range of lineages of cells expressing nerve growth factor mRNA in the nerve lesions of patients with vasculitic neuropathy: an implication of endoneurial macrophage for nerve regeneration.* Neuroscience, 2004. **129**(1): p. 109-17.
93. Freund, V. and N. Frossard, *Expression of nerve growth factor in the airways and its possible role in asthma.* Prog Brain Res, 2004. **146**: p. 335-46.
94. Levi-Montalcini, R., *The nerve growth factor: thirty-five years later.* Biosci Rep, 1987. **7**(9): p. 681-99.
95. Frossard, N., V. Freund, and C. Advenier, *Nerve growth factor and its receptors in asthma and inflammation.* Eur J Pharmacol, 2004. **500**(1-3): p. 453-65.
96. Ehrhard, P.B., et al., *Expression of nerve growth factor and nerve growth factor receptor tyrosine kinase Trk in activated CD4-positive T-cell clones.* Proc Natl Acad Sci U S A, 1993. **90**(23): p. 10984-8.
97. Jiang, Y., et al., *Nerve growth factor promotes TLR4 signaling-induced maturation of human dendritic cells in vitro through inducible p75NTR 1.* J Immunol, 2007. **179**(9): p. 6297-304.
98. Kobayashi, H. and A.P. Mizisin, *Nerve growth factor and neurotrophin-3 promote chemotaxis of mouse macrophages in vitro.* Neurosci Lett, 2001. **305**(3): p. 157-60.
99. Susaki, Y., et al., *Functional properties of murine macrophages promoted by nerve growth factor.* Blood, 1996. **88**(12): p. 4630-7.
100. Podlesniy, P., et al., *Pro-NGF from Alzheimer's disease and normal human brain displays distinctive abilities to induce processing and nuclear translocation of*

intracellular domain of p75NTR and apoptosis. Am J Pathol, 2006. **169**(1): p. 119-31.
101. Fox, A.J., et al., *Release of nerve growth factor by human pulmonary epithelial cells: role in airway inflammatory diseases.* Eur J Pharmacol, 2001. **424**(2): p. 159-62.
102. Levi-Montalcini, R., et al., *Nerve growth factor: from neurotrophin to neurokine.* Trends Neurosci, 1996. **19**(11): p. 514-20.
103. Ajizian, S.J., B.K. English, and E.A. Meals, *Specific inhibitors of p38 and extracellular signal-regulated kinase mitogen-activated protein kinase pathways block inducible nitric oxide synthase and tumor necrosis factor accumulation in murine macrophages stimulated with lipopolysaccharide and interferon-gamma.* J Infect Dis, 1999. **179**(4): p. 939-44.
104. Bracci-Laudiero, L., et al., *Increased levels of NGF in sera of systemic lupus erythematosus patients.* Neuroreport, 1993. **4**(5): p. 563-5.
105. Tuveri, M.A., et al., *Nerve growth factor and mast cell distribution in the skin of patients with systemic sclerosis.* Clin Exp Rheumatol, 1993. **11**(3): p. 319-22.
106. Bonini, S., et al., *Circulating nerve growth factor levels are increased in humans with allergic diseases and asthma.* Proc Natl Acad Sci U S A, 1996. **93**(20): p. 10955-60.
107. Lambiase, A., et al., *Expression of nerve growth factor receptors on the ocular surface in healthy subjects and during manifestation of inflammatory diseases.* Invest Ophthalmol Vis Sci, 1998. **39**(7): p. 1272-5.
108. Randolph, G.J., C. Jakubzick, and C. Qu, *Antigen presentation by monocytes and monocyte-derived cells.* Curr Opin Immunol, 2008. **20**(1): p. 52-60.
109. Ziegler-Heitbrock, L., et al., *Nomenclature of monocytes and dendritic cells in blood.* Blood, 2010.
110. Ginhoux, F., et al., *Langerhans cells arise from monocytes in vivo.* Nat Immunol, 2006. **7**(3): p. 265-73.
111. Rost, B., et al., *Monocytes of allergics and non-allergics produce, store and release the neurotrophins NGF, BDNF and NT-3.* Regul Pept, 2005. **124**(1-3): p. 19-25.
112. Mizutani, H., et al., *Role of increased production of monocytes TNF-alpha, IL-1beta and IL-6 in psoriasis: relation to focal infection, disease activity and responses to treatments.* J Dermatol Sci, 1997. **14**(2): p. 145-53.
113. Weihrauch, D., et al., *Importance of monocytes/macrophages and fibroblasts for healing of micronecroses in porcine myocardium.* Mol Cell Biochem, 1995. **147**(1-2): p. 13-9.
114. la Sala, A., et al., *Ligand activation of nerve growth factor receptor TrkA protects monocytes from apoptosis.* J Leukoc Biol, 2000. **68**(1): p. 104-10.
115. Bracci-Laudiero, L., et al., *Endogenous NGF regulates CGRP expression in human monocytes, and affects HLA-DR and CD86 expression and IL-10 production.* Blood, 2005. **106**(10): p. 3507-14.
116. Barouch, R., et al., *Nerve growth factor regulates TNF-alpha production in mouse macrophages via MAP kinase activation.* J Leukoc Biol, 2001. **69**(6): p. 1019-26.

117. Muzi, S., et al., *Nerve Growth Factor in the Developing and Adult Lacrimal Glands of Rat With and Without Inherited Retinitis Pigmentosa.* Cornea, 2010.
118. Micera, A., et al., *Nerve growth factor effect on human primary fibroblastic-keratocytes: possible mechanism during corneal healing.* Exp Eye Res, 2006. **83**(4): p. 747-57.
119. Li, X., et al., *Nerve growth factor modulate proliferation of cultured rabbit corneal endothelial cells and epithelial cells.* J Huazhong Univ Sci Technolog Med Sci, 2005. **25**(5): p. 575-7.
120. Qi, H., et al., *Nerve growth factor and its receptor TrkA serve as potential markers for human corneal epithelial progenitor cells.* Exp Eye Res, 2008. **86**(1): p. 34-40.
121. Lambiase, A., et al., *Nerve Growth Factor promotes in vitro human conjunctival epithelial cells differentiation and mucin gene expression.* Invest Ophthalmol Vis Sci, 2009.
122. Qi, H., et al., *Patterned expression of neurotrophic factors and receptors in human limbal and corneal regions.* Mol Vis, 2007. **13**: p. 1934-41.
123. Lee, H.K., et al., *Topical 0.1% prednisolone lowers nerve growth factor expression in keratoconjunctivitis sicca patients.* Ophthalmology, 2006. **113**(2): p. 198-205.
124. Liu, Q., A.M. McDermott, and W.L. Miller, *Elevated Nerve Growth Factor in Dry Eye Associated With Established Contact Lens Wear.* Eye Contact Lens, 2009.
125. Bradley, J.C., et al., *Serum growth factor analysis in dry eye syndrome.* Clin Experiment Ophthalmol, 2008. **36**(8): p. 717-20.
126. Park, K.S., et al., *Serum and tear levels of nerve growth factor in diabetic retinopathy patients.* Am J Ophthalmol, 2008. **145**(3): p. 432-7.
127. Lambiase, A., et al., *Molecular basis for keratoconus: lack of TrkA expression and its transcriptional repression by Sp3.* Proc Natl Acad Sci U S A, 2005. **102**(46): p. 16795-800.
128. Lewin, G.R., A.M. Ritter, and L.M. Mendell, *Nerve growth factor-induced hyperalgesia in the neonatal and adult rat.* J Neurosci, 1993. **13**(5): p. 2136-48.
129. Lambiase, A., et al., *Topical treatment with nerve growth factor for corneal neurotrophic ulcers.* N Engl J Med, 1998. **338**(17): p. 1174-80.
130. Lee, H.K., et al., *Nerve growth factor concentration and implications in photorefractive keratectomy vs laser in situ keratomileusis.* Am J Ophthalmol, 2005. **139**(6): p. 965-71.
131. Lambiase, A., et al., *Nerve growth factor promotes corneal healing: structural, biochemical, and molecular analyses of rat and human corneas.* Invest Ophthalmol Vis Sci, 2000. **41**(5): p. 1063-9.
132. Aloe, L., P. Tirassa, and A. Lambiase, *The topical application of nerve growth factor as a pharmacological tool for human corneal and skin ulcers.* Pharmacol Res, 2008. **57**(4): p. 253-8.
133. Cellini, M., et al., *The use of nerve growth factor in surgical wound healing of the cornea.* Ophthalmic Res, 2006. **38**(4): p. 177-81.
134. Mauro, C., L. Pietro, and C.C. Emilio, *The use of nerve growth factor in herpetic keratitis: a case report.* J Med Case Reports, 2007. **1**: p. 124.

135. Micera, A., et al., *Nerve growth factor involvement in the visual system: implications in allergic and neurodegenerative diseases.* Cytokine Growth Factor Rev, 2004. **15**(6): p. 411-7.
136. Levi-Schaffer, F., et al., *Nerve growth factor and eosinophils in inflamed juvenile conjunctival nevus.* Invest Ophthalmol Vis Sci, 2002. **43**(6): p. 1850-6.
137. Huang, X., et al., *TLR4 is required for host resistance in Pseudomonas aeruginosa keratitis.* Invest Ophthalmol Vis Sci, 2006. **47**(11): p. 4910-6.
138. Marx, J., *NGF and Alzheimer's: hopes and fears.* Science, 1990. **247**(4941): p. 408-10.
139. Park, H.J., et al., *Up-regulation of VEGF expression by NGF that enhances reparative angiogenesis during thymic regeneration in adult rat.* Biochim Biophys Acta, 2007. **1773**(9): p. 1462-72.
140. Lambiase A, M.D., Mollinari C, Bonini P, Rinaldi AM, D' Amato M, Micera A, Coassin M, Rama P, Bonini S, Garaci E., *Molecular basis for keratoconus: lack of TrkA expression and its transcriptional repression by Sp3.* Proc Natl Acad Sci U S A., 2005. **102**(46): p. 16795-800.
141. Hamrah, P., et al., *Novel characterization of MHC class II-negative population of resident corneal Langerhans cell-type dendritic cells.* Invest Ophthalmol Vis Sci, 2002. **43**(3): p. 639-46.
142. Hamrah, P., et al., *The corneal stroma is endowed with a significant number of resident dendritic cells.* Invest Ophthalmol Vis Sci, 2003. **44**(2): p. 581-9.
143. Catry, L., et al., *Morphologic and immunophenotypic heterogeneity of corneal dendritic cells.* Graefes Arch Clin Exp Ophthalmol, 1991. **229**(2): p. 182-5.
144. Nakamura, T., et al., *Characterization and distribution of bone marrow-derived cells in mouse cornea.* Invest Ophthalmol Vis Sci, 2005. **46**(2): p. 497-503.
145. J. Huang, D.E.P., S.E. Wilson, *Monocyte influx into the mouse corneal stroma following epithelial scrape injury* Invest Ophthalmol Vis Sci, 2003. **ARVO**(44): p. E-Abstract 888.
146. Ebihara, N., et al., *Involvement of C-C chemokine ligand 2-CCR2 interaction in monocyte-lineage cell recruitment of normal human corneal stroma.* J Immunol, 2007. **178**(5): p. 3288-92.
147. Qi H, C.E., Yoon KC, de Paiva CS, Shine HD, Jones DB, Pflugfelder SC, Li DQ., *Patterned expression of neurotrophic factors and receptors in human limbal and corneal regions.* Mol Vis., 2007. **13**: p. 1934-41.
148. Ríos JD, G.E., Gu J, Hodges RR, Dartt DA., *Role of neurotrophins and neurotrophin receptors in rat conjunctival goblet cell secretion and proliferation.* Invest Ophthalmol Vis Sci., 2007. **48**(4): p. 1543-51.
149. Ghinelli E, J.J., Ríos JD, Chen LL, Zoukhri D, Hodges RR, Dartt DA., *Presence and localization of neurotrophins and neurotrophin receptors in rat lacrimal gland.* Invest Ophthalmol Vis Sci., 2003. **44**(8): p. 3352-7.
150. Micera A, L.A., Puxeddu I, Aloe L, Stampachiacchiere B, Levi-Schaffer F, Bonini S, Bonini S., *Nerve growth factor effect on human primary fibroblastic-keratocytes: possible mechanism during corneal healing.* Exp Eye Res. , 2007. **83**(4): p. 747-57.

151. Bonini S, A.L., Bonini S, Rama P, Lamagna A, Lambiase A., *Nerve growth factor (NGF): an important molecule for trophism and healing of the ocular surface.* Adv Exp Med Biol., 2002. **506**: p. 531-7.
152. Lee HK, L.K., Kim HC, Lee SH, Kim EK., *Nerve growth factor concentration and implications in photorefractive keratectomy vs laser in situ keratomileusis.* Am J Ophthalmol., 2007. **139**(6): p. 965-71.
153. Joo MJ, Y.K., Hyon JY, Lai H, Hose S, Sinha D, O'Brien TP., *The effect of nerve growth factor on corneal sensitivity after laser in situ keratomileusis.* Arch Ophthalmol., 2004. **122**(9): p. 1338-41.
154. Bonini S, L.A., Rama P, Caprioglio G, Aloe L., *Topical treatment with nerve growth factor for neurotrophic keratitis.* Ophthalmology., 2000. **107**(7): p. 1347-51.
155. Esquenazi S, B.H., Bui V, He J, Kim DB, Bazan NG, *Topical combination of NGF and DHA increases rabbit corneal nerve regeneration after photorefractive keratectomy* Invest Ophthalmol Vis Sci., 2005. **46**(9): p. 3121-7.
156. Lambiase A, B.S., Bonini S, Micera A, Magrini L, Bracci-Laudiero L, Aloe L., *Increased plasma levels of nerve growth factor in vernal keratoconjunctivitis and relationship to conjunctival mast cells.* Invest Ophthalmol Vis Sci., 1995. **36**(10): p. 2127-32.
157. Bonini S, L.A., Bonini S, Angelucci F, Magrini L, Manni L, Aloe L., *Circulating nerve growth factor levels are increased in humans with allergic diseases and asthma.* Proc Natl Acad Sci U S A. , 1996. **93**(20): p. 10955-60.
158. Lee HK, R.I., Seo KY, Hong S, Kim HC, Kim EK., *Topical 0.1% prednisolone lowers nerve growth factor expression in keratoconjunctivitis sicca patients.* Ophthalmology., 2006. **113**(2): p. 198-205.
159. Levi-Montalcini, R., *The nerve growth factor: thirty-five years later.* The EMBO Journal, 1987. **6**(5): p. 1145–1154.
160. Freund-Michel V, F.N., *The nerve growth factor and its receptors in airway inflammatory diseases.* Pharmacol Ther. , 2008. **117**(1): p. 52-76.
161. Yongchaitrakul T, P.P., *Transforming growth factor-beta1 up-regulates the expression of nerve growth factor through mitogen-activated protein kinase signaling pathways in dental pulp cells.* Eur J Oral Sci. , 2007. **115**(1): p. 57-63.
162. Jiang Y, C.G., Zhang Y, Lu L, Liu S, Cao X., *Nerve growth factor promotes TLR4 signaling-induced maturation of human dendritic cells in vitro through inducible p75NTR 1.* J Immunol., 2007. **179**(9): p. 6297-304.
163. Bracci-Laudiero L, A.L., Caroleo MC, Buanne P, Costa N, Starace G, Lundeberg T, *Endogenous NGF regulates CGRP expression in human monocytes, and affects HLA-DR and CD86 expression and IL-10 production.* Blood., 2005. **106**(10): p. 3507-14.
164. Micera A, P.I., Lambiase A, Antonelli A, Bonini S, Bonini S, Aloe L, Pe'er J, Levi-Schaffer F., *The pro-fibrogenic effect of nerve growth factor on conjunctival fibroblasts is mediated by transforming growth factor-beta.* Clin Exp Allergy., 2005. **35**(5): p. 650-6.
165. Patel SV, M.J., Hodge DO, Bourne WM., *In vivo confocal microscopy of the human cornea.* Invest Ophthalmol Vis Sci., 2002. **43**(4): p. 995-1003.

166. Chalmers RL, B.C., *Dryness symptoms among an unselected clinical population with and without contact lens wear.* Cont Lens Anterior Eye. , 2006. **29**(1): p. 25-30.
167. Begley CG, C.R., Mitchell GL, *Characterization of ocular surface symptoms from optometric practices in North America.* . Cornea, 2001. **20**: p. 610-8.
168. McMahon TT, Z.K., *Twenty-five years of contact lenses: the impact on the cornea and ophthalmic practice.* . Cornea, 2000. **19**: p. 730-40.
169. Ozcura F, A.S., Helvaci MR., *Ocular surface disease index for the diagnosis of dry eye syndrome.* Ocul Immunol Inflamm., 2007. **15**(5): p. 389-93.
170. Beuerman RW, M.J., *Comparative clinical assessment of corneal sensation with a new aesthesiometer.* Am J Ophthalmol., 1978. **86**(6): p. 812-5.
171. Meadows DL, P.J., Joshi A, Mordaunt J, *A novel method to evaluate residence time in humans using a nonpenetrating fluorescent tracer.* Invest Ophthalmol Vis Sci., 2002. **43**(4): p. 1032-9.
172. Linna TU, V.M., Pérez-Santonja JJ, Petroll WM, Alió JL, Tervo TM., *Effect of myopic LASIK on corneal sensitivity and morphology of subbasal nerves.* Invest Ophthalmol Vis Sci., 2000. **41**(2): p. 393-7.
173. Battat L, M.A., Dursun D, Pflugfelder SC, *Effects of laser in situ keratomileusis on tear production, clearance, and the ocular surface.* Ophthalmology., 2001. **108**(7): p. 1230-5.
174. Russo PA, B.C., Galasso JM, *Extended-wear silicone hydrogel soft contact lenses in the management of moderate to severe dry eye signs and symptoms secondary to graft-versus-host disease.* Eye Contact Lens., 2007. **33**(3): p. 144-7.
175. Park KS, K.S., Kim JC, Kim HC, Im YS, Ahn CW, Lee HK., *Serum and tear levels of nerve growth factor in diabetic retinopathy patients.* Am J Ophthalmol., 2008. **145**(3): p. 432-7.
176. Hermonat PL, L.D., Yang B, Mehta JL., *Mechanism of action and delivery possibilities for TGFbeta1 in the treatment of myocardial ischemia.* Cardiovasc Res., 2007. **74**(2): p. 235-43.
177. Benítez-Del-Castillo JM, A.M., Wassfi MA, Díaz-Valle D, Gegúndez JA, Fernandez C, García-Sánchez J., *Relation between corneal innervation with confocal microscopy and corneal sensitivity with noncontact esthesiometry in patients with dry eye.* Invest Ophthalmol Vis Sci., 2007. **48**(1): p. 173-81.
178. du Toit R, S.P., Simpson T, Fonn D., *The effects of six months of contact lens wear on the tear film, ocular surfaces, and symptoms of presbyopes.* Optom Vis Sci. , 2001. **78**(6): p. 455-62.
179. Woo HM, B.E., Campbell SF, Marfurt CF, Murphy CJ, *Nerve growth factor and corneal wound healing in dogs.* Exp Eye Res., 2005. **80**(5): p. 633-42.
180. Levi-Montalcini, R., *The nerve growth factor 35 years later. Science*, 1987. **237**(4819): p. 1154 - 1162.
181. Frossard N, F.V., Advenier C, *Nerve growth factor and its receptors in asthma and inflammation.* Eur J Pharmacol., 2004. **500**(1-3): p. 453-65.
182. Julio-Pieper M, L.H., Bravo JA, Romero C, *Effects of nerve growth factor (NGF) on blood vessels area and expression of the angiogenic factors VEGF and TGFbeta1 in the rat ovary.* Reprod Biol Endocrinol. , 2006. **4**: p. 57.

183. Pietrzak, A., A. Misiak-Tloczek, and E. Brzezinska-Blaszczyk, *Interleukin (IL)-10 inhibits RANTES-, tumour necrosis factor (TNF)- and nerve growth factor (NGF)-induced mast cell migratory response but is not a mast cell chemoattractant.* Immunol Lett, 2009. **123**(1): p. 46-51.
184. Lipnik-Stangelj, M. and M. Carman-Krzan, *Effects of histamine and IL-1beta on PKC-stimulated nerve growth factor secretion from glial cells.* Inflamm Res, 2006. **55 Suppl 1**: p. S34-5.
185. Lutz M, K.K., Schmitt S, ten Dijke P, Sebald W, Wizenmann A, Knaus P., *Nerve growth factor mediates activation of the Smad pathway in PC12 cells.* Eur J Biochem., 2004. **271**(5): p. 920-31.
186. Freund-Michel V, F.N., *The nerve growth factor and its receptors in airway inflammatory diseases.* Pharmacol Ther., 2008. **117**(1): p. 52-76.
187. Skaper, S.D., *The biology of neurotrophins, signalling pathways, and functional peptide mimetics of neurotrophins and their receptors.* CNS Neurol Disord Drug Targets, 2008. **7**(1): p. 46-62.
188. Nguyen, D.H., et al., *Growth factor and neurotrophic factor mRNA in human lacrimal gland.* Cornea, 1997. **16**(2): p. 192-9.
189. Lambiase A, M.L., Bonini S, Rama P, Micera A, Aloe L., *Nerve growth factor promotes corneal healing: structural, biochemical, and molecular analyses of rat and human corneas.* Invest Ophthalmol Vis Sci., 2000. **41**(5): p. 1063-9.
190. Micera A, L.A., Puxeddu I, Aloe L, Stampachiacchiere B, Levi-Schaffer F, Bonini S, Bonini S, *Nerve growth factor effect on human primary fibroblastic-keratocytes: possible mechanism during corneal healing.* Exp Eye Res., 2006. **83**(4): p. 747-57.
191. Ríos JD, G.E., Gu J, Hodges RR, Dartt DA, *Role of neurotrophins and neurotrophin receptors in rat conjunctival goblet cell secretion and proliferation.* . Invest Ophthalmol Vis Sci., 2007. **48**(4): p. 1543-51.
192. Woo, H.M., et al., *Nerve growth factor and corneal wound healing in dogs.* Exp Eye Res, 2005. **80**(5): p. 633-42.
193. Lambiase, A., et al., *Clinical application of nerve growth factor on human corneal ulcer.* Arch Ital Biol, 2003. **141**(2-3): p. 141-8.
194. Chang, E.J., et al., *The role of nerve growth factor in hyperosmolar stress induced apoptosis.* J Cell Physiol, 2008. **216**(1): p. 69-77.
195. Micera, A., et al., *Nerve growth factor modulates toll-like receptor (TLR) 4 and 9 expression in cultured primary VKC conjunctival epithelial cells.* Mol Vis, 2009. **15**: p. 2037-44.
196. R. Li, K.M., T. Lama, P. Jain, H.U. Saragovi, G. Cumberlidge, *An NGF Mimetic, MIM-D3, Demonstrates Therapeutic Efficacy in a Rat Model of Scopoloamine-Induced Dry Eye* ARVO abstrct, 2009. **#3661**.
197. Wang, Z.X. and X.G. Sun, *[The effect of nerve growth factor on proliferation and expression of mucin gene in human conjunctival goblet cells].* Zhonghua Yan Ke Za Zhi, 2007. **43**(10): p. 928-31.
198. *The definition and classification of dry eye disease: report of the Definition and Classification Subcommittee of the International Dry Eye WorkShop (2007).* Ocul Surf, 2007. **5**(2): p. 75-92.

199. Solomon R, D.E., Perry HD, *The effects of LASIK on the ocular surface.* Ocul Surf., 2006. **2**(1): p. 34-44.
200. Araki-Sasaki, K., et al., *An SV40-immortalized human corneal epithelial cell line and its characterization.* Invest Ophthalmol Vis Sci, 1995. **36**(3): p. 614-21.
201. Diebold, Y., et al., *Characterization of a spontaneously immortalized cell line (IOBA-NHC) from normal human conjunctiva.* Invest Ophthalmol Vis Sci, 2003. **44**(10): p. 4263-74.
202. McDermott, A.M., et al., *Defensin expression by the cornea: multiple signalling pathways mediate IL-1beta stimulation of hBD-2 expression by human corneal epithelial cells.* Invest Ophthalmol Vis Sci, 2003. **44**(5): p. 1859-65.
203. Narayanan S, M.J., Proske R, McDermott AM., *Effect of hyperosmolality on beta-defensin gene expression by human corneal epithelial cells.* Cornea, 2006. **25**(9): p. 1063-8.
204. Akdis, M., et al., *Immune responses in healthy and allergic individuals are characterized by a fine balance between allergen-specific T regulatory 1 and T helper 2 cells.* J Exp Med, 2004. **199**(11): p. 1567-75.
205. Blaschke, V., et al., *Rapid quantitation of proinflammatory and chemoattractant cytokine expression in small tissue samples and monocyte-derived dendritic cells: validation of a new real-time RT-PCR technology.* J Immunol Methods, 2000. **246**(1-2): p. 79-90.
206. Ueng, T.H., et al., *Induction of fibroblast growth factor-9 and interleukin-1alpha gene expression by motorcycle exhaust particulate extracts and benzo(a)pyrene in human lung adenocarcinoma cells.* Toxicol Sci, 2005. **87**(2): p. 483-96.
207. Curat, C.A., et al., *Macrophages in human visceral adipose tissue: increased accumulation in obesity and a source of resistin and visfatin.* Diabetologia, 2006. **49**(4): p. 744-7.
208. Torcia, M., et al., *Nerve growth factor is an autocrine survival factor for memory B lymphocytes.* Cell, 1996. **85**(3): p. 345-56.
209. Julio-Pieper M, L.H., Bravo JA, Romero C, *Effects of nerve growth factor (NGF) on blood vessels area and expression of the angiogenic factors VEGF and TGFbeta1 in the rat ovary.* Reprod Biol Endocrinol., 2006. **4**: p. 57.
210. Coassin, M., et al., *Nerve growth factor modulates in vitro the expression and release of TGF-beta1 by amniotic membrane.* Graefes Arch Clin Exp Ophthalmol, 2006. **244**(4): p. 485-91.
211. Frossard, N., et al., *Nerve growth factor is released by IL-1beta and induces hyperresponsiveness of the human isolated bronchus.* Eur Respir J, 2005. **26**(1): p. 15-20.
212. Aloe, L., et al., *Emotional stress induced by parachute jumping enhances blood nerve growth factor levels and the distribution of nerve growth factor receptors in lymphocytes.* Proc Natl Acad Sci U S A, 1994. **91**(22): p. 10440-4.
213. Bonini, S., et al., *Nerve growth factor: an important molecule in allergic inflammation and tissue remodelling.* Int Arch Allergy Immunol, 1999. **118**(2-4): p. 159-62.
214. Blais, D.R., et al., *LBP and CD14 secreted in tears by the lacrimal glands modulate the LPS response of corneal epithelial cells.* Invest Ophthalmol Vis Sci, 2005. **46**(11): p. 4235-44.

215. Nagelhout, T.J., et al., *Preservation of tear film integrity and inhibition of corneal injury by dexamethasone in a rabbit model of lacrimal gland inflammation-induced dry eye.* J Ocul Pharmacol Ther, 2005. **21**(2): p. 139-48.
216. Li, S., et al., *Small proline-rich protein 1B (SPRR1B) is a biomarker for squamous metaplasia in dry eye disease.* Invest Ophthalmol Vis Sci, 2008. **49**(1): p. 34-41.
217. Lam, H., et al., *Tear cytokine profiles in dysfunctional tear syndrome.* Am J Ophthalmol, 2009. **147**(2): p. 198-205 e1.
218. Marmorstein, A.D., et al., *Saturation of, and competition for entry into, the apical secretory pathway.* Proc Natl Acad Sci U S A, 2000. **97**(7): p. 3248-53.
219. Assoian, R.K., et al., *Transforming growth factor-beta in human platelets. Identification of a major storage site, purification, and characterization.* J Biol Chem, 1983. **258**(11): p. 7155-60.
220. Cao, X., et al., *Hydrogen peroxide-induced cellular apoptosis is mediated by TGF-beta2 signaling pathway in cultured human lens epithelial cells.* Int Ophthalmol, 2010. **30**(3): p. 229-37.
221. Erickson, R.P., I.J. Karolyi, and S.R. Diehl, *Correlation of susceptibility to 6-aminonicotinamide and hydrocortisone-induced cleft palate.* Life Sci, 2005. **76**(18): p. 2071-8.
222. Tong, L., et al., *Comparison of gene expression profiles of conjunctival cell lines with primary cultured conjunctival epithelial cells and human conjunctival tissue.* Gene Expr, 2009. **14**(5): p. 265-78.
223. Sornelli, F., et al., *NGF and NGF-receptor expression of cultured immortalized human corneal endothelial cells.* Mol Vis, 2010. **16**: p. 1439-47.
224. Strom, A., et al., *Mediation of NGF signaling by post-translational inhibition of HES-1, a basic helix-loop-helix repressor of neuronal differentiation.* Genes Dev, 1997. **11**(23): p. 3168-81.
225. Limpert, A.S., J.C. Karlo, and G.E. Landreth, *Nerve growth factor stimulates the concentration of TrkA within lipid rafts and extracellular signal-regulated kinase activation through c-Cbl-associated protein.* Mol Cell Biol, 2007. **27**(16): p. 5686-98.
226. Micera, A., et al., *Nerve growth factor and tissue repair remodeling: trkA(NGFR) and p75(NTR), two receptors one fate.* Cytokine Growth Factor Rev, 2007. **18**(3-4): p. 245-56.
227. Soilu-Hanninen, M., et al., *Nerve growth factor signaling through p75 induces apoptosis in Schwann cells via a Bcl-2-independent pathway.* J Neurosci, 1999. **19**(12): p. 4828-38.
228. Gong, X., et al., *Monocyte chemotactic protein-2 (MCP-2) uses CCR1 and CCR2B as its functional receptors.* J Biol Chem, 1997. **272**(18): p. 11682-5.
229. Kuziel, W.A., et al., *Severe reduction in leukocyte adhesion and monocyte extravasation in mice deficient in CC chemokine receptor 2.* Proc Natl Acad Sci U S A, 1997. **94**(22): p. 12053-8.
230. Leenen, P.J., et al., *Markers of mouse macrophage development detected by monoclonal antibodies.* J Immunol Methods, 1994. **174**(1-2): p. 5-19.
231. Asli, B., et al., *Roles of lymphoid cells in the differentiation of Langerhans dendritic cells in mice.* Immunobiology, 2004. **209**(1-2): p. 209-21.

232. Strauss-Ayali, D., S.M. Conrad, and D.M. Mosser, *Monocyte subpopulations and their differentiation patterns during infection.* J Leukoc Biol, 2007. **82**(2): p. 244-52.
233. Gautier, E.L., C. Jakubzick, and G.J. Randolph, *Regulation of the migration and survival of monocyte subsets by chemokine receptors and its relevance to atherosclerosis.* Arterioscler Thromb Vasc Biol, 2009. **29**(10): p. 1412-8.
234. Clanchy, F.I., et al., *Detection and properties of the human proliferative monocyte subpopulation.* J Leukoc Biol, 2006. **79**(4): p. 757-66.
235. Randolph, G.J., et al., *Differentiation of monocytes into dendritic cells in a model of transendothelial trafficking.* Science, 1998. **282**(5388): p. 480-3.
236. Liu, K., et al., *In vivo analysis of dendritic cell development and homeostasis.* Science, 2009. **324**(5925): p. 392-7.
237. Metcalf, D., *Murine hematopoietic stem cells committed to macrophage/dendritic cell formation: stimulation by Flk2-ligand with enhancement by regulators using the gp130 receptor chain.* Proc Natl Acad Sci U S A, 1997. **94**(21): p. 11552-6.
238. Bozic, C.R., et al., *Expression and biologic characterization of the murine chemokine KC.* J Immunol, 1995. **154**(11): p. 6048-57.
239. Scandella, E., et al., *Prostaglandin E2 is a key factor for CCR7 surface expression and migration of monocyte-derived dendritic cells.* Blood, 2002. **100**(4): p. 1354-61.
240. Caroleo, M.C., et al., *Human monocyte/macrophages activate by exposure to LPS overexpress NGF and NGF receptors.* J Neuroimmunol, 2001. **113**(2): p. 193-201.
241. Musson, R.A., *Human serum induces maturation of human monocytes in vitro. Changes in cytolytic activity, intracellular lysosomal enzymes, and nonspecific esterase activity.* Am J Pathol, 1983. **111**(3): p. 331-40.
242. Berryhill, B.L., et al., *Partial restoration of the keratocyte phenotype to bovine keratocytes made fibroblastic by serum.* Invest Ophthalmol Vis Sci, 2002. **43**(11): p. 3416-21.
243. Horwitz, D.A., et al., *Identification of human mononuclear leucocyte populations by esterase staining.* Clin Exp Immunol, 1977. **30**(2): p. 289-98.
244. Yamazaki, T., *Measurement of fitness at the esterase-5 locus in Drosophila pseudoobscura.* Genetics, 1971. **67**(4): p. 579-603.
245. Sunderkotter, C., et al., *Subpopulations of mouse blood monocytes differ in maturation stage and inflammatory response.* J Immunol, 2004. **172**(7): p. 4410-7.
246. Geissmann, F., et al., *Blood monocytes: distinct subsets, how they relate to dendritic cells, and their possible roles in the regulation of T-cell responses.* Immunol Cell Biol, 2008. **86**(5): p. 398-408.
247. Burn, T.C., et al., *Monocyte chemoattractant protein-1 gene is expressed in activated neutrophils and retinoic acid-induced human myeloid cell lines.* Blood, 1994. **84**(8): p. 2776-83.
248. Solovjov, D.A., E. Pluskota, and E.F. Plow, *Distinct roles for the alpha and beta subunits in the functions of integrin alphaMbeta2.* J Biol Chem, 2005. **280**(2): p. 1336-45.
249. Bruyere, F., et al., *Modeling lymphangiogenesis in a three-dimensional culture system.* Nat Methods, 2008. **5**(5): p. 431-7.

250. Xu, H., et al., *LYVE-1-positive macrophages are present in normal murine eyes.* Invest Ophthalmol Vis Sci, 2007. **48**(5): p. 2162-71.
251. Chen, L., et al., *Novel expression and characterization of lymphatic vessel endothelial hyaluronate receptor 1 (LYVE-1) by conjunctival cells.* Invest Ophthalmol Vis Sci, 2005. **46**(12): p. 4536-40.
252. Chinnery, H.R., et al., *Bone marrow chimeras and c-fms conditional ablation (Mafia) mice reveal an essential role for resident myeloid cells in lipopolysaccharide/TLR4-induced corneal inflammation.* J Immunol, 2009. **182**(5): p. 2738-44.
253. Sosnova, M., M. Bradl, and J.V. Forrester, *CD34+ corneal stromal cells are bone marrow-derived and express hemopoietic stem cell markers.* Stem Cells, 2005. **23**(4): p. 507-15.
254. Lambiase, A., et al., *In vitro evidence of nerve growth factor effects on human conjunctival epithelial cell differentiation and mucin gene expression.* Invest Ophthalmol Vis Sci, 2009. **50**(10): p. 4622-30.
255. Gong, N., et al., *Local overexpression of nerve growth factor in rat corneal transplants improves allograft survival.* Invest Ophthalmol Vis Sci, 2007. **48**(3): p. 1043-52.
256. Heerssen, H.M. and R.A. Segal, *Location, location, location: a spatial view of neurotrophin signal transduction.* Trends Neurosci, 2002. **25**(3): p. 160-5.
257. Lucidi-Phillipi, C.A., et al., *TrkA activation is sufficient to rescue axotomized cholinergic neurons.* Neuron, 1996. **16**(3): p. 653-63.
258. Riccio, A., et al., *An NGF-TrkA-mediated retrograde signal to transcription factor CREB in sympathetic neurons.* Science, 1997. **277**(5329): p. 1097-100.
259. Lindholm, D., et al., *Interleukin-1 regulates synthesis of nerve growth factor in non-neuronal cells of rat sciatic nerve.* Nature, 1987. **330**(6149): p. 658-9.
260. Jessen, K.R. and R. Mirsky, *Developmental regulation in the Schwann cell lineage.* Adv Exp Med Biol, 1999. **468**: p. 3-12.
261. Randolph, G.J., *The fate of monocytes in atherosclerosis.* J Thromb Haemost, 2009. **7 Suppl 1**: p. 28-30.
262. Lumeng, C.N., J.L. Bodzin, and A.R. Saltiel, *Obesity induces a phenotypic switch in adipose tissue macrophage polarization.* J Clin Invest, 2007. **117**(1): p. 175-84.
263. Van Krinks, C.H., M.K. Matyszak, and J.S. Gaston, *Characterization of plasmacytoid dendritic cells in inflammatory arthritis synovial fluid.* Rheumatology (Oxford), 2004. **43**(4): p. 453-60.